Title
Modulating Aging and Aging-related Symptoms Using Endogenous Small Molecules

Author
Chai, Min

Publication Date
2019

Peer reviewed|Thesis/dissertation

UNIVERSITY OF CALIFORNIA

Los Angeles

Modulating Aging and Aging-related Symptoms Using Endogenous Small Molecules

A dissertation submitted in partial satisfaction of the

requirements for the degree Doctor of Philosophy

in Molecular Biology

by

Min Chai

2019

ABSTRACT OF THE DISSERTATION

Modulating Aging and Aging-related Symptoms

Using Endogenous Small Molecules

by

Min Chai

Doctor of Philosophy in Molecular Biology

University of California, Los Angeles, 2019

Professor Jing Huang, Chair

Aging and aging related diseases are closely related to wellness and lifespan of aged population. Modulating aging can be achieved by specific gene mutations, intrinsic signaling regulation (e.g. by dietary restriction) and pharmacological perturbations. Recent studies on the role of metabolism and endogenous metabolites in aging process provided hope for new anti-aging approaches to counter aging and aging related diseases. Here we identified a novel anti-aging metabolite, α-ketobutyrate (α-KB), that extends the lifespan of adult *Caenorhabditis elegans* and aged mice. Utilizing drug affinity responsive target stability assay, *in-vitro* enzymatic kinetics analysis, and epistasis, we demonstrated

that α-KB depends on pyruvate dehydrogenase perturbation as a competitive alternative substrate to extend lifespan. Consistently, rewired pyruvate metabolism was detected in both α-KB treatment and genetic inhibition of pyruvate dehydrogenase in mammalian models. Furthermore, AMP-activated protein kinase (AMPK) pathway activation is required to induce longevity by α-KB. In an Alzheimer's disease *C. elegans* model, epistasis demonstrated that α-KB requires pyruvate dehydrogenase and AMPK to delay the age dependent paralysis progression. Besides lifespan extension, α-KB also improves fitness in aged mice, including maintaining healthy hair growth. In the search of its mechanism and additional hair regenerative compounds, we discovered the essential role of autophagy in hair growth cycle and potential application of autophagy activators in hair loss therapy. As a shared effector of anti-aging signaling pathways, including TOR and AMPK pathways, autophagy is successfully induced by known aging modulators, α-ketoglutarate, α-KB, rapamycin, and metformin in mouse skin and confers their hair regeneration effect. Co-treatment of specific autophagy inhibitors blocks the stimulation of hair regeneration, which further confirmed the requirement of autophagy activation by these agents. Consistently, dynamically regulated autophagy level is detected during hair cycle: upregulation from telogen throughout anagen phase and downregulation from catagen until telogen. Our finding that α-KB combats aging and aging related disorders in worms and mice has implications for human anti-aging remedies development.

The dissertation of Min Chai is approved.

Siavash K. Kurdistani

James A. Wohlschlegel

Karen Reue

Guoping Fan

Jing Huang, Committee Chair

University of California, Los Angeles

2019

To my family and friends, for always standing in my back through good and bad times.

Table of Contents

LIST OF FIGURES AND TABLES

For CHARPTER 2:

For CHAPTER 3:

ACKNOWLEDGEMENTS

First, I would like to thank my advisor, Prof. Jing Huang, for supporting me and leading me through my Ph.D. training. When I joined Jing's lab, she gave me all opportunities to learn from everyone and explore all possibilities in my future projects inside and outside of our lab. I benefited a lot from this comprehensive training ranging from cultured cells, *C. elegans* to mouse. Jing always guides me with her inspiring ideas and scientific attitude. She is the best scientist and mentor I could imagine as a graduate student. When I initiated my work with *C. elegans*, she brought up the idea of testing ketoacids and their combination in *C. elegans* lifespan and aging related disease models, which turned out to be a very exciting and fruitful project. I really appreciate all the support and guidance Jing gave to me during my Ph.D. study.

I would like to thank my committee members, Siavash K. Kurdistani, James A. Wohlschlegel, Karen Reue and Guoping Fan for their inspiring comments, valuable suggestions, professional expertise and generous technical help. I also want to thank Meisheng Jiang, Laurent Vergnes from Karen Reue lab and Stéphanie de Barros from Gay Crooks lab. They helped me a lot in technical training including mouse handling, Seahorse assay and RT-qPCR, without which my project would not move forward as planned. Additionally, I want to thank everyone from Jing Huang lab. Randall Chin taught me on lifespan assay using *C. elegans* and other *C. elegans* techniques. Xudong Fu guided me in western blot, metabolomics analysis and other biochemical assays using cultured cells. Brett Lomenick was always willing to discuss my project and helped to

solve my technical problems on daily basis. Heejun Hwang was the first one who lead me to start mouse experiment. Jessie Chu and Wilson Huang were the most helpful and intelligent undergraduate technicians I ever had. Xiang Yin and Chieh Chen discussed about science and graduate life with me. I cannot achieve what I presented here without their contribution.

For the study in CHAPTER 2, I would like to acknowledge contribution from: X. Fu, B. Lomenick, H. Hwang, L. Vergnes, K. Reue, D. Brass, Z. Quan, S.J. Bensinger, N.H. Kim, M.A. Teitell, M. Jiang, A.S. Divakaruni, and J. Huang. X. Fu performed assays in cultured cells, including western blot, *in-vitro* enzymatic kinetics assay and metabolomics. B. Lomenick and H. Hwang did DARTS, the target identification assay. L. Vergenes and K. Reue helped to set up mitochondrial respiration Seahorse assay in experimental design, sample processing and data analysis. D. Brass performed mass spectrometry on isolated metabolites prepared by X. Fu. J. Huang is the principle investigator, provided ideas and gave guidance in experimental design and data processing. J. Huang, X. Fu, and M. Chai wrote and revised the manuscript.

In CHAPTER 3, all the mouse experiments were done with the help from M. Jiang in mouse housing and monitoring. Besides, I would like to thank L. Vergnes, X. Fu, S. de Barros, J. Chu, W. Huang, J. Jiao, H. Herschman, G. Crooks, K. Reue and J. Huang. L. Vergnes and K. Reue helped with designing animal treatment protocol and RT-qPCR analysis. X. Fu contributed to animal tissue fixation and processing. S. de Barros and G. Crooks helped to obtain aged mice for our anti-aging analysis. J. Chu and W. Huang

helped with the *in-vitro* validation of compounds effect. J.Jiao and H. Herschman provided help with mouse tissue immunohistochemistry protocol design. I also thank the Translational Pathology Core Laboratory at UCLA for core services, H. Dang for expert help with skin tissue immunostaining, and H. Hwang, B. Lomenick for technical advice. J. Huang is the principle investigator, provided ideas in experimental design and data processing. J. Huang and M. Chai wrote, revised and submitted the manuscript, which has been accepted by *Cell reports* in May 2019.

VITA

EDUCATION BACKGROUND:

Sept. 2010 ~ Jul.2014:

University: University of Science and Technology of China (USTC)

Major: Biosciences (Bachelor of Science)

RESEARCH EXPERIENCE:

- Graduate student researcher in Molecular and Medical Pharmacology Department, UCLA, Los Angeles, USA

  April 2015-present: "Modulating aging using endogenous small molecules in *C.elegans* and mice"

  - Established small molecules screening for healthspan and lifespan extension in *C.elegans* and aged mice; Investigated and validated druggable targets required for longevity by small molecules.
  - Characterized effect of anti-aging small molecules in delaying neurodegenerative diseases using an Alzheimer's diseases *C.elegans* model.
  - Discovered the role of autophagy in hair follicle activation and hair regeneration; developed the application of anti-aging small molecules on hair growth stimulation.

Advisor: Prof. Jing Huang

- Undergraduate student researcher in Institute of Immunology, USTC, Hefei, P.R.China

Sept.2013-Jun.2014: “The influence of microRNA-9 on the expression of NKG2D on natural killer cells”

- Constructed dual-luciferase reporter vectors, overexpression vectors and RNA sponge; Identified the negative effect of microRNA-9 on NKG2D level and anti-tumor activity in natural killer cells.

Advisor: Prof. Zhigang Tian

TEACHING EXPERIENCE:

Jan-Mar 2016/Apr-Jun 2017: gave independent lectures, led discussions and held office hours for Molecular Biology.

PUBLICATIONS & PATENTS:

Chai, M., Jiang, M., Vergnes, L., Fu, X., de Barros, S.C., Doan, N.B., Huang, W., Chu, J., Jiao, J., Herschman, H.R., Crooks, G.M., Reue, K. and Huang, J. (2019). Stimulation of hair growth by small molecules that activate autophagy. *Cell Reports*, in press.

TALKS & POSTERS:

Chai, M., Hair regeneration by longevity metabolites and drugs that activate autophagy. Poster presentation for “Mitochondrial Biology & Selective Autophagy” Keystone Symposia, April 22-26, 2018, Kyoto, Japan.

Chai, M., Modulating Aging Using an Endogenous Small Molecule. Talk for Student Seminar in UCLA Molecular Biology Institute, May 2017 & May 2019.

CHAPTER 1

Introduction

Aging is an unavoidable process of living organisms, with accumulated functional declines in a time dependent manner. Hallmarks of aging include instability in genome (e.g. DNA double strand breaks), imbalance of cellular metabolism (e.g. NAD+ decrease), malfunction of mitochondria and dysfunction of proteostasis [1]. These physiological declines contribute to the high incidence of aging related diseases, such as cancer, heart disease, type 2 diabetes, arthritis, and kidney disease in aged population [2]. Additionally, there is a dramatically and continuously increased elderly population with the high demand of anti-aging research and human trial translation [3]. Therefore, it's important and urgent to better understand the biological mechanism of aging process and develop anti-aging remedies for aging and aging related diseases prevention in human.

In the past few decades, aging studies have identified the contribution of intrinsic signaling pathways, genetic regulation by transcriptional factors, and cellular metabolism homeostasis to aging [4]. Interestingly, the intrinsic signaling pathways, such as insulin/insulin like growth factor (IGF-1), the target of rapamycin (TOR), and AMP-activated protein kinase (AMPK) pathways, can act as nutrient sensors and/or stress response inducers and then rewire metabolism to fulfill nutrient and energy demand.

These highly conserved pathways are also demonstrated to be key anti-aging mediators and modulating them can achieve lifespan extension and aging related symptoms onset delay [4]. Here, we will discuss these key aging regulatory factors and how they interact with each other to exert anti-aging effects.

Insulin/IGF-1 pathway

The Insulin/IGF-1 (IIS) pathway was the very first metabolic pathway to be reported as an aging mediator. Daf-2 (insulin/IGF-1 receptor homologue in *C. elegans*) mutations were found to double the lifespan of *C. elegans*, a widely used longevity assay model with a short mean lifespan of 14-16 days [5]. Consistently, activating PTEN/DAF-18, an IIS pathway inhibitor, extends lifespan in *C. elegans* [6]. As a highly conserved pathway in multiple organisms, IIS pathway inhibition exhibits lifespan extension in animal models ranging from worms, flies to mice [5,7,8]. Recently, targeting IGF-1 receptor in female mice using antibodies has been shown to improve both healthspan and lifespan [9]. In *C. elegans*, epistasis analysis identified the anti-aging mechanisms by IIS pathway. The downstream effectors of IIS include phosphatidylinositol 3-kinase (PI3K), AKT, FOXO/DAF-16, heat-shock factor-1 (HSF-1) and Nrf2/SKN-1 [10]. PI3K and AKT respond to the signaling transduced from insulin/IGF-1 receptors, which prevents the translocation of FOXO/DAF-16 from cytoplasm to nucleus. As a transcriptional factor, FOXO/DAF-16 reduction results in decreased transcription of its target genes. By contraries, inhibiting IIS inducing signals leads to upregulated FOXO/DAF-16 translocation and therefore increased stress response related genes expression[4]. These stress induced response accounts for the anti-aging effects from IIS perturbation. Besides FOXO/DAF-16, other transcription

factors, like HSF-1 (in heat-stress response) and Nrf2/SKN-1(in oxidative stress response), also contribute to dampened IIS induced anti-aging effects [11,12]. Consistently, loss of function mutation of any of the mentioned transcription factors (FOXO/DAF-16, HSF-1, and Nrf2/SKN-1) partially or fully abolishes anti-aging effects of IIS inhibition [13,5,11,12]. Another essential anti-aging effector in *daf-2* mutant is autophagy [14,15]. In fact, autophagy is a shared longevity mediator in TOR inhibition, AMPK activation, and mitochondrial perturbation as well. Besides, dietary restriction (DR) model and *eat-2* mutant showed different synergy with IIS. For example, double mutations of *eat-2* and *daf-2* showed longer lifespan of each[5]. It may be mediated by FOXO/DAF-16 which is not required for *eat-2* mutants longevity but required by DR by bacterial dilution [16].

Dietary restriction

DR means decrease in food intake without inducing malnutrition. It was firstly described in 1935 that DR can extend both the mean and maximal lifespan of rats [17]. DR in multiple organisms, ranging from yeast, worms, flies, to mammalian systems, mice and primates, has be proven to conservatively induce lifespan extension [18-24]. Moreover, aging related diseases can also be alleviated by DR, as documented in human trial that DR can effectively prevent atherosclerosis and memory loss [25-29]. The mechanisms of longevity induced by DR have been well investigated in worms with genetic mutation in *eat-2* gene or diluted bacterial food source [5,16]. IIS, TOR, and AMPK signaling pathways have been demonstrated to conservatively contribute to the longevity in response to DR in worms, drosophila, and mice. Among these nutrient sensing pathways, TOR is the most investigated and validated signaling pathway mediating DR related anti-aging effects [30,13].

TOR pathway

TOR can sense changes in cellular energy status, nutrient (e.g. amino acid levels), mitogens, and signaling from the IIS and AMPK pathways [31]. There are two functional complexes in TOR kinase, TOR complex 1 (TORC1) and TOR complex 2 (TORC2) [32]. In the aging related studies, the contribution of TORC1 has been much more well investigated than TORC2. TORC1 can regulate gene transcription, synthesis of protein, nucleotide, and fatty acid, autophagy, and cell growth/division/division/motility in response to a variety of signal cues, including ADP/ATP status, amino acids, glucose, oxygen, and growth factors [33]. It is mainly achieved by inhibiting protein translation and activating autophagy through conserved S6 kinase (S6K)/ eukaryotic translation initiation factor 4E (eIF4E)-binding protein 1 (4E-BP1) and PHA-4/FOXA, respectively [34-36]. Phosphorylation of S6K and subsequent 4E-BP1 activation by TORC1 signaling increases ribosome and mRNA production and translation initiation and elongation efficiency [33]. Protein synthesis reduction has been shown to be sufficient for lifespan extension [36,37]. In addition, TORC1 signaling also depends on transcription factor PHA-4/FOXA mediated autophagy induction. unc-51-like kinase 1 (ULK1) is also a downstream regulator of autophagy by TOR [38]. TOR is a well-studied pharmacological target for lifespan extension and aging related diseases therapy. Mice lifespan and wellness can be improved by inhibition of TOR by rapamycin [39]. Recently, anti-aging endogenous metabolites have been identified as TOR modulators, such as α-ketoglutarate, 2-hydroxyglutarate, branch chain amino acids, and Δ7-dafachronic acid [40-43].

AMPK pathway

AMPK is responsive to intracellular AMP/ADP as well as calcium levels [44]. As a nutrition level sensor, it controls catabolism and anabolism by directly activating its substrates involved in glucose metabolism, lipid metabolism, cell proliferation, and autophagy [44]. AMPK is also involved in the regulation of other proteins activity and signaling pathways, including acetyl-CoA carboxylase (ACC), ULK1, DAF-16, HIF-1, SOD-3, SKN-1, and TOR pathway [45,20]. In *C.elegans*, overexpression of AAK-2 (AMPK homologue in *C. elegans*) is sufficient to extend lifespan [45-47]. Loss of function mutation of AAK-2 can abolish the longevity effect of multiple anti-aging remedies, which indicates that AMPK is necessary for longevity in some circumstances [48,49]. For example, metformin is found to extend *C. elegans* lifespan in an AMPK dependent manner [48]. Beneficial effect of metformin in mice has also be reported [50]. And the anti-aging study of metformin in human trial has been approved [51]. Another AMPK modulator for delaying aging is glucosamine, which is an endogenous glycolysis inhibitor. AMPK pathway and ROS induced stress response are required for its lifespan extension effect [52].

Autophagy

Autophagy is responsive to nutrient starvation and other stress clues by degrading and recycling protein and organelles via the lysosomal pathway [53-55]. This fundamental machinery can fulfill the increased nutrient demand and protect from stresses from the inducing signaling clues [56,54]. For example, toxic stress from proteostasis can induce autophagy to eliminate damaged proteins and organelles to achieve protein homeostasis. Autophagy declines with age. It may contribute to the higher prevalence of autophagy-related diseases, including neurodegenerative diseases and cancer in the elderly

population [14,57]. Conservatively, autophagy can be activated in three types in multiple organisms: macroautophagy, microautophagy, and chaperone-mediated autophagy. As a shared anti-aging machinery, macroautophagy is much more studied than the other two for longevity [58]. Macroautophagy requires the fusion of a double-membrane structure, called autophagosomes engulfing damaged cellular compartments to be degraded, and secondary lysosomes. Acidification of fused lysosomes will break down the content for recycling [59]. In the regulation of autophagy activation, ULK1 and transcription factor EF binding protein (TFEB), downstream of TORC1, play an essential role. ULK1 is a kinase that has been shown to be required for autophagy initiation. TFEB directly controls gene expression associated with fusion, autophagosome formation, lysosomal degradation, and cargo degradation. When TORC1 is activated under nutrient-rich conditions, both ULK1 and TFEB will be phosphorylated, resulted in suppressed ULK1 activity and decreased TFEB translocation into the nucleus, respectively [22]. Therefore, TORC1 signaling exerts inhibitory effects on autophagy induction. Generally, autophagy is blocked by TORC1 with abundant nutrient presence and activated during starvation to achieve nutrient recycling. Even autophagy has been demonstrated to be required for the lifespan extension by multiple longevity pathways and anti-aging drugs, including reduced IIS, inhibited TOR, restricted diet, and perturbed mitochondrial respiration [60,61,14,15], the underlying mechanisms and their crosstalk of longevity and autophagy is complex [54]. On one hand, in most of the anti-aging remedies, autophagy is demonstrated to be required for their longevity effects [62,57]. Overexpressing some autophagy associated genes, including TFEB or Atg5 [63,60], results in elevated autophagy level and extended lifespan. Lifespan and healthspan are also extended in transgenic mice with increased autophagy

activity [57]. On the other hand, deficiency in autophagy machinery doesn't necessarily cause lifespan decrease; autophagy alone may not be sufficient for lifespan increase [14,58].

Mitochondrial perturbation

Mitochondria are the main organelle for maintaining energy and redox potential levels, such as through ATP and NADH production. Moreover, mitochondria are also the organelle where tricarboxylic acid cycle (TCA cycle) coordinates cellular metabolism, including glucose, glutamate, and lipids metabolism. Aging and aging related diseases have been discovered to be associated with dampened mitochondrial function [64]. And the role of increased mitochondrial function in longevity by calorie restriction has been reported [65,66]. Therefore, modulating mitochondria function can affect lifespan by rewiring energy homeostasis and metabolism. Indeed, moderate disruption on mitochondrial electron transport chain (ETC) subunits can extend lifespan in multiple animal organisms, including yeast, *C.elegans* [67], *Drosophila*, and mouse [68-70]. On the other hand, extended lifespan can also be induced by elevated mitochondrial biogenesis or increased mitochondrial complex I expression [71-73]. The underlying mechanisms of mitochondria associated longevity have been widely explored but not fully uncovered. Genetic mutation, genetic knockdown through RNAi, or pharmacological treatment can be utilized to induce modest inhibition in mitochondrial ETC and longevity. Not only different pharmacological dosages can result in different extent of ETC dysfunction and lifespan extension, disruption on different ETC subunits and different disruption degree are also important for the mitochondria associated lifespan extension 74-77,64. One well studied mechanism for mitochondrial perturbation induced longevity is oxidative stress, including reactive

oxygen species (ROS) [77]. Another conserved mechanism involves mitochondrial unfolded protein response (UPR^{mt}) [78-80], which responds to mitochondrial imbalance, such as imbalance between mitochondrial proteins encoded by nuclear mitochondrial genes and mitochondrial perturbation through RNAi knockdown. Even UPR^{mt} can be activated by certain mitochondrial ETC knockdown, its contribution to lifespan extension effects is debatable [78-80]. As for the relationship between mitochondria induced longevity and conserved anti-aging pathways, mitochondrial perturbation is distinct from both the IIS and TOR pathways but requires some shared anti-aging effectors. For example, autophagy deficiency abolishes the lifespan extension effects by mitochondrial inhibition [61]. The fact that mitochondrial ETC RNAi extends lifespan in both *daf-16* and *daf-2* mutants indicates that mitochondrial perturbation induces longevity independently of IIS pathway [81]. Different mitochondrial ETC perturbation yielded different result in *eat-2* mutant animals. While mutation in complex I subunit gene *nuo-6* can further extend the lifespan of long-lived *eat-2* mutants but mutation in coenzyme Q synthesis related gene *clk-1* cannot [74,82].

In this dissertation, we discuss the longevity mechanism of α-ketobutyrate (α-KB) and its application in delaying aging related diseases in *C. elegans* and mice. Epistasis identified AMPK and downstream effectors, including DAF-16, SKN-1, and SIR-2.1, as required pathway for lifespan extension by α-KB. *In-vitro* and *in-vivo* mitochondrial respiration assay indicated the malfunction of mitochondrial complex I came from the decrease pyruvate oxidation, instead of dampened complex I activity by α-KB. An unbiased target identification method [83] confirmed the binding of α-KB on pyruvate oxidation enzyme,

pyruvate dehydrogenase. Moreover, we demonstrated that α-KB depends on pyruvate dehydrogenase perturbation to inhibit respiration, activate AMPK pathway, extend lifespan, and delay Alzheimer's diseases progression. Besides the reliable target validation and mechanism investigation, its beneficial effects in mice aging and aging related disorders imply the potential role α-KB in combating human aging.

References

1. López-Otín, C., Blasco, M. A., Partridge, L., Serrano, M., & Kroemer, G. (2013). The hallmarks of aging. *Cell*, *153*(6), 1194-1217.

2. Niccoli, T., & Partridge, L. (2012). Ageing as a risk factor for disease. *Current Biology*, *22*(17), R741-R752.

3. US Department of Health and Human Services (2008), A. o. A. Projected future growth of the older population, retrieved from http://www.aoa.gov/Aging_Statistics/future_growth/future_growth.aspx#age

4. Lapierre, L. R., & Hansen, M. (2012). Lessons from C. elegans: signaling pathways for longevity. *Trends in Endocrinology & Metabolism*, *23*(12), 637-644.

5. Kenyon, C., Chang, J., Gensch, E., Rudner, A., & Tabtiang, R. (1993). A C. elegans mutant that lives twice as long as wild type. *Nature*, *366*(6454), 461.

6. Mihaylova, V. T., Borland, C. Z., Manjarrez, L., Stern, M. J., & Sun, H. (1999). The PTEN tumor suppressor homolog in Caenorhabditis elegans regulates longevity and dauer formation in an insulin receptor-like signaling pathway. *Proceedings of the National Academy of Sciences*, *96*(13), 7427-7432.

7. Tatar, M., Kopelman, A., Epstein, D., Tu, M. P., Yin, C. M., & Garofalo, R. S. (2001). A mutant Drosophila insulin receptor homolog that extends life-span and impairs neuroendocrine function. *Science*, *292*(5514), 107-110.

8. Holzenberger, M., Dupont, J., Ducos, B., Leneuve, P., Géloën, A., Even, P. C., ... & Le Bouc, Y. (2003). IGF-1 receptor regulates lifespan and resistance to oxidative stress in mice. *Nature*, *421*(6919), 182.

9. Mao, K., Quipildor, G. F., Tabrizian, T., Novaj, A., Guan, F., Walters, R. O., ... & Li, P. (2018). Late-life targeting of the IGF-1 receptor improves healthspan and lifespan in female mice. *Nature communications*, *9*(1), 2394.

10. Wolff, S., & Dillin, A. (2006). The trifecta of aging in Caenorhabditis elegans. *Experimental gerontology*, *41*(10), 894-903.

11. Tullet, J. M., Hertweck, M., An, J. H., Baker, J., Hwang, J. Y., Liu, S., ... & Blackwell, T. K. (2008). Direct inhibition of the longevity-promoting factor SKN-1 by insulin-like signaling in C. elegans. *Cell*, *132*(6), 1025-1038.

12. Hsu, A. L., Murphy, C. T., & Kenyon, C. (2003). Regulation of aging and age-related disease by DAF-16 and heat-shock factor. *Science*, *300*(5622), 1142-1145.

13. Kenyon, C. J. (2010). The genetics of ageing. *Nature*, *464*(7288), 504.

14. Hansen, M., Chandra, A., Mitic, L. L., Onken, B., Driscoll, M., & Kenyon, C. (2008). A role for autophagy in the extension of lifespan by dietary restriction in C. elegans. *PLoS genetics*, *4*(2), e24.

15. Meléndez, A., Tallóczy, Z., Seaman, M., Eskelinen, E. L., Hall, D. H., & Levine, B. (2003). Autophagy genes are essential for dauer development and life-span extension in C. elegans. *Science*, *301*(5638), 1387-1391.

16. Greer, E. L., & Brunet, A. (2009). Different dietary restriction regimens extend lifespan by both independent and overlapping genetic pathways in C. elegans. *Aging cell*, *8*(2), 113-127.

17. McCay, C. M., Crowell, M. F., & Maynard, L. A. (1935). The effect of retarded growth upon the length of life span and upon the ultimate body size: one figure. *The journal of Nutrition*, *10*(1), 63-79.

18. Lin, S. J., Defossez, P. A., & Guarente, L. (2000). Requirement of NAD and SIR2 for life-span extension by calorie restriction in Saccharomyces cerevisiae. *Science*, *289*(5487), 2126-2128.

19. Lakowski, B., & Hekimi, S. (1998). The genetics of caloric restriction in Caenorhabditis elegans. *Proceedings of the National Academy of Sciences*, *95*(22), 13091-13096

20. Greer, E. L., Dowlatshahi, D., Banko, M. R., Villen, J., Hoang, K., Blanchard, D., ... & Brunet, A. (2007). An AMPK-FOXO pathway mediates longevity induced by a novel method of dietary restriction in C. elegans. *Current biology*, *17*(19), 1646-1656.

21. Colman, R. J., Anderson, R. M., Johnson, S. C., Kastman, E. K., Kosmatka, K. J., Beasley, T. M., ... & Weindruch, R. (2009). Caloric restriction delays disease onset and mortality in rhesus monkeys. *Science*, *325*(5937), 201-204.

22. Colman, R. J., Beasley, T. M., Kemnitz, J. W., Johnson, S. C., Weindruch, R., & Anderson, R. M. (2014). Caloric restriction reduces age-related and all-cause mortality in rhesus monkeys. *Nature communications*, *5*, 3557.

23. Weindruch, R., & Walford, R. L. (1982). Dietary restriction in mice beginning at 1 year of age: effect on life-span and spontaneous cancer incidence. *Science*, *215*(4538), 1415-1418.

24. Weindruch, R., Walford, R. L., Fligiel, S., & Guthrie, D. (1986). The retardation of aging in mice by dietary restriction: longevity, cancer, immunity and lifetime energy intake. *The Journal of nutrition*, *116*(4), 641-654.

25. Omodei, D., & Fontana, L. (2011). Calorie restriction and prevention of age-associated chronic disease. *FEBS letters*, *585*(11), 1537-1542.

26. Lane, M. A., Ingram, D. K., & Roth, G. S. (1999). Calorie restriction in nonhuman primates: effects on diabetes and cardiovascular disease risk. *Toxicological sciences: an official journal of the Society of Toxicology*, *52*(suppl_1), 41-48.

27. Mattson, M. P., & Wan, R. (2005). Beneficial effects of intermittent fasting and caloric restriction on the cardiovascular and cerebrovascular systems. *The Journal of nutritional biochemistry*, *16*(3), 129-137.

28. Fontana, L., Meyer, T. E., Klein, S., & Holloszy, J. O. (2004). Long-term calorie restriction is highly effective in reducing the risk for atherosclerosis in humans. *Proceedings of the national Academy of Sciences*, *101*(17), 6659-6663.

29. Witte, A. V., Fobker, M., Gellner, R., Knecht, S., & Flöel, A. (2009). Caloric restriction improves memory in elderly humans. *Proceedings of the National Academy of Sciences*, *106*(4), 1255-1260.

30. Fontana, L., Partridge, L., & Longo, V. D. (2010). Extending healthy life span—from yeast to humans. *science*, *328*(5976), 321-326.

31. Wullschleger, S., Loewith, R., & Hall, M. N. (2006). TOR signaling in growth and metabolism. *Cell*, *124*(3), 471-484.

32. Martin, D. E., & Hall, M. N. (2005). The expanding TOR signaling network. *Current opinion in cell biology*, *17*(2), 158-166.

33. Laplante, M., & Sabatini, D. M. (2012). mTOR signaling in growth control and disease. *cell*, *149*(2), 274-293.

34. Bonawitz, N. D., Chatenay-Lapointe, M., Pan, Y., & Shadel, G. S. (2007). Reduced TOR signaling extends chronological life span via increased respiration and upregulation of mitochondrial gene expression. *Cell metabolism*, *5*(4), 265-277.

35. Kapahi, P., Vijg, J., Vijg, J., Campisi, J., Selman, C., Tullet, J. M., ... & Harrison, D. E. (2009). Aging Lost in Translation?. *New England Journal of Medicine*, *31*(27), 2669.

36. Hansen, M., Taubert, S., Crawford, D., Libina, N., Lee, S. J., & Kenyon, C. (2007). Lifespan extension by conditions that inhibit translation in Caenorhabditis elegans. *Aging cell*, *6*(1), 95-110.

37. Pan, K. Z., Palter, J. E., Rogers, A. N., Olsen, A., Chen, D., Lithgow, G. J., & Kapahi, P. (2007). Inhibition of mRNA translation extends lifespan in Caenorhabditis elegans. *Aging cell*, *6*(1), 111-119.

38. Kim, J., Kundu, M., Viollet, B., & Guan, K. L. (2011). AMPK and mTOR regulate autophagy through direct phosphorylation of Ulk1. *Nature cell biology*, *13*(2), 132.

39. Harrison, D. E., Strong, R., Sharp, Z. D., Nelson, J. F., Astle, C. M., Flurkey, K., ... & Pahor, M. (2009). Rapamycin fed late in life extends lifespan in genetically heterogeneous mice. *nature*, *460*(7253), 392.

40. Chin, R. M., Fu, X., Pai, M. Y., Vergnes, L., Hwang, H., Deng, G., ... & Hu, E. (2014). The metabolite α-ketoglutarate extends lifespan by inhibiting ATP synthase and TOR. *Nature*, *510*(7505), 397.

41. Fu, X., Chin, R. M., Vergnes, L., Hwang, H., Deng, G., Xing, Y., ... & Chen, C. (2015). 2-Hydroxyglutarate inhibits ATP synthase and mTOR signaling. *Cell metabolism*, *22*(3), 508-515.

42. Thondamal, M., Witting, M., Schmitt-Kopplin, P., & Aguilaniu, H. (2014). Steroid hormone signalling links reproduction to lifespan in dietary-restricted Caenorhabditis elegans. *Nature communications*, *5*, 4879.

43. Solon-Biet, S. M., McMahon, A. C., Ballard, J. W. O., Ruohonen, K., Wu, L. E., Cogger, V. C., ... & Gokarn, R. (2014). The ratio of macronutrients, not caloric intake, dictates cardiometabolic health, aging, and longevity in ad libitum-fed mice. *Cell metabolism*, *19*(3), 418-430.

44. Mihaylova, M. M., & Shaw, R. J. (2011). The AMPK signalling pathway coordinates cell growth, autophagy and metabolism. *Nature cell biology*, *13*(9), 1016.

45. Apfeld, J., O'Connor, G., McDonagh, T., DiStefano, P. S., & Curtis, R. (2004). The AMP-activated protein kinase AAK-2 links energy levels and insulin-like signals to lifespan in C. elegans. *Genes & development*, *18*(24), 3004-3009.

46. Arad, M., Benson, D. W., Perez-Atayde, A. R., McKenna, W. J., Sparks, E. A., Kanter, R. J., ... & Seidman, C. E. (2002). Constitutively active AMP kinase mutations cause glycogen storage disease mimicking hypertrophic cardiomyopathy. *The Journal of clinical investigation*, *109*(3), 357-362.

47. Mair, W., Morantte, I., Rodrigues, A. P., Manning, G., Montminy, M., Shaw, R. J., & Dillin, A. (2011). Lifespan extension induced by AMPK and calcineurin is mediated by CRTC-1 and CREB. *Nature*, *470*(7334), 404.

48. Cabreiro, F., Au, C., Leung, K. Y., Vergara-Irigaray, N., Cochemé, H. M., Noori, T., ... & Gems, D. (2013). Metformin retards aging in C. elegans by altering microbial folate and methionine metabolism. *Cell*, *153*(1), 228-239.

49. Price, N. L., Gomes, A. P., Ling, A. J., Duarte, F. V., Martin-Montalvo, A., North, B. J., ... & Hubbard, B. P. (2012). SIRT1 is required for AMPK activation and the

beneficial effects of resveratrol on mitochondrial function. *Cell metabolism*, *15*(5), 675-690.

50. Martin-Montalvo, A., Mercken, E. M., Mitchell, S. J., Palacios, H. H., Mote, P. L., Scheibye-Knudsen, M., ... & Schwab, M. (2013). Metformin improves healthspan and lifespan in mice. *Nature communications*, *4*, 2192.

51. Albert Einstein College of Medicine. Metformin in Longevity Study (MILES). (MILES) (Clinicaltrials.gov Identifier NCT02432287) (2015). Retrieved from https://clinicaltrials.gov/ct2/show/study/NCT02432287

52. Weimer, S., Priebs, J., Kuhlow, D., Groth, M., Priebe, S., Mansfeld, J., ... & Schulz, T. J. (2014). D-Glucosamine supplementation extends life span of nematodes and of ageing mice. *Nature communications*, *5*, 3563.

53. Ohsumi, Y. (2014). Historical landmarks of autophagy research. *Cell research*, *24*(1), 9.

54. Galluzzi, L., Pietrocola, F., Levine, B., & Kroemer, G. (2014). Metabolic control of autophagy. *Cell*, *159*(6), 1263-1276.

55. Mizushima, N., Levine, B., Cuervo, A. M., & Klionsky, D. J. (2008). Autophagy fights disease through cellular self-digestion. *nature*, *451*(7182), 1069.

56. Tang, A. H., & Rando, T. A. (2014). Induction of autophagy supports the bioenergetic demands of quiescent muscle stem cell activation. *The EMBO journal*, *33*(23), 2782-2797.

57. Fernández, Á. F., Sebti, S., Wei, Y., Zou, Z., Shi, M., McMillan, K. L., ... & Marciano, D. K. (2018). Disruption of the beclin 1–BCL2 autophagy regulatory complex promotes longevity in mice. *Nature*, *558*(7708), 136.

58. Carew, J., & Phillips, J. G. (2018). *U.S. Patent No. 9,926,326*. Washington, DC: U.S. Patent and Trademark Office.

59. Klionsky, D. J., & Emr, S. D. (2000). Autophagy as a regulated pathway of cellular degradation. *Science*, *290*(5497), 1717-1721.

60. Pyo, J. O., Yoo, S. M., Ahn, H. H., Nah, J., Hong, S. H., Kam, T. I., ... & Jung, Y. K. (2013). Overexpression of Atg5 in mice activates autophagy and extends lifespan. *Nature communications*, *4*, 2300.

61. Tóth, M. L., Sigmond, T., Borsos, É., Barna, J., Erdélyi, P., Takács-Vellai, K., ... & Vellai, T. (2008). Longevity pathways converge on autophagy genes to regulate life span in Caenorhabditis elegans. *Autophagy*, *4*(3), 330-338.

62. Jia, K., & Levine, B. (2007). Autophagy is required for dietary restriction-mediated life span extension in C. elegans. *Autophagy*, *3*(6), 597-599.

63. Lapierre, L. R., De Magalhaes Filho, C. D., McQuary, P. R., Chu, C. C., Visvikis, O., Chang, J. T., ... & Dillin, A. (2013). The TFEB orthologue HLH-30 regulates autophagy and modulates longevity in Caenorhabditis elegans. *Nature communications*, *4*, 2267.

64. Lin, M. T., & Beal, M. F. (2006). Mitochondrial dysfunction and oxidative stress in neurodegenerative diseases. *Nature*, *443*(7113), 787.

65. Guarente, L. (2008). Mitochondria—a nexus for aging, calorie restriction, and sirtuins?. *Cell*, *132*(2), 171-176.

66. Civitarese, A. E., Carling, S., Heilbronn, L. K., Hulver, M. H., Ukropcova, B., Deutsch, W. A., ... & Ravussin, E. (2007). Calorie restriction increases muscle mitochondrial biogenesis in healthy humans. *PLoS medicine*, *4*(3), e76.

67. Robida-Stubbs, S., Glover-Cutter, K., Lamming, D. W., Mizunuma, M., Narasimhan, S. D., Neumann-Haefelin, E., ... & Blackwell, T. K. (2012). TOR signaling and rapamycin influence longevity by regulating SKN-1/Nrf and DAF-16/FoxO. *Cell metabolism*, *15*(5), 713-724.

68. Liu, X., Jiang, N., Hughes, B., Bigras, E., Shoubridge, E., & Hekimi, S. (2005). Evolutionary conservation of the clk-1-dependent mechanism of longevity: loss of mclk1 increases cellular fitness and lifespan in mice. *Genes & development*, *19*(20), 2424-2434.

69. Copeland, J. M., Cho, J., Lo Jr, T., Hur, J. H., Bahadorani, S., Arabyan, T., ... & Walker, D. W. (2009). Extension of Drosophila life span by RNAi of the mitochondrial respiratory chain. *Current Biology*, *19*(19), 1591-1598.

70. Kirchman, P. A., Kim, S., Lai, C. Y., & Jazwinski, S. M. (1999). Interorganelle signaling is a determinant of longevity in Saccharomyces cerevisiae. *Genetics*, *152*(1), 179-190.

71. Rera, M., Bahadorani, S., Cho, J., Koehler, C. L., Ulgherait, M., Hur, J. H., ... & Walker, D. W. (2011). Modulation of longevity and tissue homeostasis by the Drosophila PGC-1 homolog. *Cell metabolism*, *14*(5), 623-634.

72. Bahadorani, S., Cho, J., Lo, T., Contreras, H., Lawal, H. O., Krantz, D. E., ... & Walker, D. W. (2010). Neuronal expression of a single-subunit yeast NADH–ubiquinone oxidoreductase (Ndi1) extends Drosophila lifespan. *Aging cell*, *9*(2), 191-202.

73. Hur, J. H., Bahadorani, S., Graniel, J., Koehler, C. L., Ulgherait, M., Rera, M., ... & Walker, D. W. (2013). Increased longevity mediated by yeast NDI1 expression in Drosophila intestinal stem and progenitor cells. *Aging (Albany NY)*, *5*(9), 662.

74. Yang, W., & Hekimi, S. (2010). Two modes of mitochondrial dysfunction lead independently to lifespan extension in Caenorhabditis elegans. *Aging cell*, *9*(3), 433-447.

75. Rea, S. L., Ventura, N., & Johnson, T. E. (2007). Relationship between mitochondrial electron transport chain dysfunction, development, and life extension in Caenorhabditis elegans. *PLoS biology*, *5*(10), e259.

76. Schapira, A. H. (2006). Mitochondrial disease. *The Lancet*, *368*(9529), 70-82.

77. Lee, S. J., Hwang, A. B., & Kenyon, C. (2010). Inhibition of respiration extends C. elegans life span via reactive oxygen species that increase HIF-1 activity. *Current Biology*, *20*(23), 2131-2136.

78. Durieux, J., Wolff, S., & Dillin, A. (2011). The cell-non-autonomous nature of electron transport chain-mediated longevity. *Cell*, *144*(1), 79-91.

79. Houtkooper, R. H., Mouchiroud, L., Ryu, D., Moullan, N., Katsyuba, E., Knott, G., ... & Auwerx, J. (2013). Mitonuclear protein imbalance as a conserved longevity mechanism. *Nature*, *497*(7450), 451.

80. Bennett, C. F., Vander Wende, H., Simko, M., Klum, S., Barfield, S., Choi, H., ... & Kaeberlein, M. (2014). Activation of the mitochondrial unfolded protein response does not predict longevity in Caenorhabditis elegans. *Nature communications*, *5*, 3483.

81. Dillin, A., Hsu, A. L., Arantes-Oliveira, N., Lehrer-Graiwer, J., Hsin, H., Fraser, A. G., ... & Kenyon, C. (2002). Rates of behavior and aging specified by mitochondrial function during development. *Science*, *298*(5602), 2398-2401.

82. Lakowski, B., & Hekimi, S. (1996). Determination of life-span in Caenorhabditis elegans by four clock genes. *science*, *272*(5264), 1010-1013.

83. Lomenick, B., Hao, R., Jonai, N., Chin, R. M., Aghajan, M., Warburton, S., ... & Wohlschlegel, J. A. (2009). Target identification using drug affinity responsive target stability (DARTS). *Proceedings of the National Academy of Sciences*, *106*(51), 21984-21989.

CHAPTER 2

The metabolite α-ketobutyrate promotes longevity by perturbing pyruvate oxidation and activating AMPK

Abstract

Aging is a complex process that is directly related to human health and disease. The extraordinary finding that aging is malleable, as shown in model organisms whose life and health spans are extended by specific gene mutations, dietary restriction, or pharmacological perturbations, has offered enormous hope for transforming our understanding and treatment of aging and age-related diseases[1,2]. Here we show that an unfamiliar endogenous metabolite, α-ketobutyrate (α-KB), increases the lifespan of adult *Caenorhabditis elegans* (*C. elegans*) and aged mice, and that α-KB supplementation confers robust protection against an Alzheimer's disease model in *C. elegans*. We find that α-KB perturbs pyruvate oxidation by acting as a competitive alternative substrate of pyruvate dehydrogenase (PDH), rewiring mitochondrial metabolism and activating AMP-activated protein kinase (AMPK). Furthermore, the *C. elegans* lifespan increase by α-KB requires PDH and AMPK, which are highly conserved throughout evolution. Our findings

suggest that human aging and related degeneration may be remedied by α-KB or α-KB like drugs.

Introduction

Metabolism plays an important role in aging and disease. Increasing evidence has shown that endogenous metabolites, as basic as α-ketoglutarate (α-KG) and nicotinamide adenine dinucleotide (NAD+), can delay the aging process and increase healthy lifespan[3-5]. Identifying such longevity metabolites and understanding their mechanisms not only can illuminate the biological regulation of aging, but also provide new interventions for aging-related diseases. Alpha-keto acids are important intermediates in metabolic pathways. Familiar examples include α-KG in the tricarboxylic acid (TCA) cycle, pyruvate as the end product of glycolysis, and branch chain α-keto acids (including α-ketoisovalerate (KIV), α-ketoisocaproate (KIC) and α-keto-β- methylvalerate (KMV) – which are α-keto acid analogues of the branch chain amino acids valine, leucine and isoleucine, respectively) associated with the metabolic disorder maple syrup urine disease. We previously discovered that α-KG extends the lifespan of adult *C. elegans* and identified the highly conserved ATP synthase as a novel target of α-KG in longevity[3]. The unexpected findings suggest that the regulatory networks acted on by metabolites are more complex than currently appreciated. Here we identify a new longevity-promoting α-keto acid, α- ketobutyrate (α-KB), and seek to understand the basis of its mechanism in lifespan regulation.

Results and Discussion

α-KB increases the lifespan of adult *C. elegans*

α-KB (Figure 1A) is a short-chain α-keto acid found in all cells. It is a metabolite in the catabolism of methionine, threonine, and homocysteine. α-KB is formed by cystathionine gamma-lyase from cystathionine, which is generated from homocysteine and serine by cystathionine beta synthase. Transamination of α-KB produces α-aminobutyric acid, a component of the non-ribosomal tripeptide ophthalmic acid first found in calf lens. Unlike pyruvate, α-KG, or branched-chain α-keto acids, there is no specific enzyme for α-KB oxidation. Instead, α-KB can be consumed by the branched-chain α-keto acid dehydrogenase complex (BCKDC) or the pyruvate dehydrogenase complex (PDC)[6]. Additionally, when respiration is inhibited, α-KB can serve as an electron acceptor and be converted to (*R*)-2-hydroxybutyrate (2- HB) by lactate dehydrogenase (LDH)[7]. Although the metabolism of α-KB has been well characterized, its biological function remains poorly understood.

We discovered that α-KB increases the lifespan of adult *C. elegans* by up to ~60% (Figure 1B). α-KB extended the lifespan of wild-type N2 worms in a concentration-dependent manner, with 4 mM α-KB yielding the largest lifespan extension (Figure 1C); 4 mM was the concentration used in all subsequent *C. elegans* experiments unless otherwise stated. α-KB not only extends lifespan, but also delays age-related phenotypes, such as the decline in rapid, coordinated body movement (video not shown). The dilution of the *C.*

elegans bacterial food source has been shown to extend worm lifespan[8]. However, α-KB does not inhibit bacterial proliferation (Figure S1A), and there is no significant change in pharyngeal pumping rates or foraging behavior in α-KB treated animals (Figure S1B-D).

AMPK is required for lifespan increase by α-KB

AMPK is an energy sensor for AMP/ADP and regulates glucose metabolism, lipid metabolism, cell growth and autophagy[9,10]. Loss of function mutation of AAK-2 (AMPK homologue in *C. elegans*) can abolish the longevity effect of multiple anti-aging remedies, which indicates the essential role of AMPK in longevity[11,12]. Similarly, we found that α-KB does not extend the lifespan of *aak-2* mutant worms (Figure 2A), supporting the involvement of AMPK in α-KB induced longevity. Meanwhile, another two anti-aging pathways, TOR and insulin/IGF-1 pathways, are not required for the longevity effect of α-KB (Figure 2B-C), evidenced by the further lifespan extension in *eat-2* and *daf-2* worms by α-KB. Importantly, phosphorylated AMPK (encoded by the *C. elegans* orthologue aak-2) is increased in α-KB treated worms (Figure 2D) as well as in H9C2 cells (Figure 2E), consistent with α-KB acting upstream of AMPK in longevity signaling.

Lifespan increase by α-KB also requires DAF-16, SKN-1, and SIR-2.1 (Figure 2F, H, I), which act downstream of AMPK pathway in longevity regulation[13]; α-KB can protect worms from heat stress under 35.5^{o}C (Figure 2G), which indicates the upregulation of

heat resistance genes by DAF-16. These epistasis data further support that α-KB extends lifespan in an AMPK-dependent manner.

α-KB inhibits pyruvate-driven mitochondrial complex I respiration

We previously found that α-KG increases longevity by inhibiting mitochondrial complex V[3]. Given the similarities in structure and lifespan effects of α-KB and α-KG, we asked whether α-KB may also affect the electron transport chain (ETC) by measuring mitochondrial respiration[14]. Interestingly, we found that when respiration is driven by the complex I substrates pyruvate and malate, there is a significant decrease in basal (ADP-induced, state 3) and maximal (FCCP-induced, state 3u) respiration in isolated mitochondria upon α-KB treatment (Figure 3A-B). However, when glutamate and malate are used as complex I substrates or when the complex II substrate succinate is provided, respiration is unaffected by α-KB (Figure 3A-B). These results show the specificity of α-KB in inhibiting pyruvate-driven complex I respiration, rather than directly interfering with complex I or other ETC complex activity.

α-KB reduces pyruvate oxidation by acting as a competitive alternative substrate of the PDC

The rate of pyruvate oxidation in isolated mitochondria is controlled by the mitochondrial pyruvate carrier (MPC) and PDC[15]. It has been shown that unlike pyruvate, α-KB is able to cross the mitochondrial inner membrane rapidly as a free acid[16]. Given that in our experimental conditions with the concentration of α-KB (500 μM) being 20-fold lower compared to pyruvate (10 mM), any effect of α-KB on pyruvate import by MPC should be negligible, and therefore any inhibitory effect on pyruvate oxidation by α-KB should be attributable to PDC inhibition by α-KB. To test this idea, we utilized methyl pyruvate, which freely diffuses into the mitochondrion without requiring transportation by MPC. As shown in Figure 3A-B, α-KB still inhibits pyruvate oxidation using methyl pyruvate as a respiratory substrate, indicating a direct inhibition of PDC by α-KB and ruling out any potential inhibitory effect on mitochondrial substrate import as rate limiting in the respiration inhibition by α-KB. Consistently, α-KB also inhibits respiration when methyl pyruvate is provided together with glutamate and malate as complex I substrates (Figure 3A-B). These findings further support the model in which α-KB indirectly inhibits complex I respiration via disruption of pyruvate oxidation. Indeed, using the DARTS (drug affinity responsive target stability) assay[17], we showed that α-KB directly binds to PDC but not to mitochondrial complex I (Figures 3C). In concordance, α-KB decreases pyruvate oxidation by PDC using purified enzyme (Figure 3D), but does not directly inhibit the activity of complex I in vitro (Figure S2A).

PDC is a large nuclear-encoded mitochondrial multienzyme complex consisting of pyruvate dehydrogenase (PDH, E1), dihydrolipoamide S-acetyltransferase (DLAT, E2), and dihydrolipoamide dehydrogenase (DLD, E3). The E3 subunit of PDC is shared with

branch chain keto acid dehydrogenase complex (BCKDC) and α-ketoglutarate dehydrogenase complex. PDC mainly catalyzes the oxidation of pyruvate to acetyl-CoA and CO_2, linking glycolysis and the TCA cycle. The E1 enzyme is a heterotetramer of two alpha and two beta subunits. E1 α1 subunit encoded by the *PDHA1* gene contains the E1 active site, and plays a key role in the function of the PDC. Mutations in *PDHA1* are associated with pyruvate dehydrogenase E1-α deficiency and X-linked Leigh syndrome. Mutations in other PDC subunits are also disease associated, including pyruvate dehydrogenase deficiency, primary lactic acidosis and maple syrup urine disease in infancy and early childhood. PDC activity is regulated by product inhibition by NADH, which competes with NAD+ for E3 binding; and by acetyl CoA, which competes with CoA for E2 binding. Several analogues of pyruvate, including fluoropyruvate and bromopyruvate, have been reported to inhibit PDC. However, these molecules also inhibit other pyruvate related enzymes such as pyruvate carboxylase (PC) and LDH and/or glycolytic enzymes (including GAPDH and hexokinase). No specific small molecule inhibitor of PDC has been described.

It has been reported that PDC can use α-KB as an alternative substrate[18]. We confirmed the direct binding of α-KB to PDC using DARTS (Figure 3C). To investigate the mechanism by which α-KB perturbs pyruvate oxidation as an alternative substrate, we performed PDC enzyme kinetics analysis. In contrast to pyruvate, which exhibits non-Michaelis-Menten kinetics (Hill coefficient $h = 1.48 \pm 0.096$) – similar to the *E. coli* enzyme as reported[19] – α-KB shows little cooperativity ($h = 1.05 \pm 0.084$) with similar apparent K_m but decreased V_{max} (Figure 3E). Presence of an excess of α-KB results in decreased

pyruvate oxidation by PDC (Figure 3D) and loss of cooperativity (Figure 3F). However, inhibition by α-KB is abrogated and rate of pyruvate oxidation is restored when pyruvate is provided in high concentrations. This is consistent with the model in which α-KB perturbs pyruvate oxidation as a competitive alternative substrate for PDC (Figure 3F). In contrast, α-KB does not detectably inhibit the reduction of pyruvate by LDH (Figure S2B-C) for which α-KB is also a substrate (Figure S2D). The *K*m of LDH for α-KB (3.92 mM) is ~50x higher than that for pyruvate (0.076 mM) (Figure S2E), supporting that pyruvate exhibits significantly higher affinity on LDH than α-KB. Additionally, α-KB does not protect PC from protease digestion in DARTS assay, suggesting that PC does not use α-KB as a substrate in vivo (Figure S2F). These results indicate that α-KB does not broadly affect all pyruvate-dependent reactions but only selectively inhibits pyruvate oxidation through PDC. In addition to PDC, BCKDC is able to oxidize α-KB[6]. However, α-KB does not alter BCKDC-driven respiration, as when individual branched-chain alpha-keto acids are offered as a substrate, mitochondrial respiration is not inhibited by α-KB (Figure S2G).

In eukaryotes, PDH is tightly regulated by pyruvate dehydrogenase kinase (PDK) and pyruvate dehydrogenase phosphatase, which inactivates and activates the enzyme, respectively[20]. Interestingly, phosphorylation of PDH is decreased upon α-KB treatment (Figure S2H), indicating that more PDH is in its unphosphorylated, active form. This would be expected based on the negative feedback on PDK as α-KB treatment decreases pyruvate oxidation and results in reduced acetyl-CoA production, which is an allosteric activator of PDK. Importantly, this suggests that the inhibition of pyruvate oxidation by α-

KB occurs independently of PDH phosphorylation and supports the mechanism of α-KB as a competitive alternative substrate of the PDH.

α-KB rewires mitochondrial substrate utilization through interruption of pyruvate oxidation

The mitochondrion is a pivotal organelle for core metabolic pathways, including TCA cycle, ETC, and lipid metabolism. Various substrates, including pyruvate, glutamine, and lipids, can be utilized for mitochondrial metabolism. Upon nutrient or pathological stress, such as dietary restriction or cancer, substrate utilization by the mitochondria can be drastically altered[21]. PDC is the gatekeeper enzyme controlling pyruvate entry into the TCA cycle. Upon disruption of pyruvate oxidation, cells would be expected to utilize less glucose and increase utilization of alternative substrates for mitochondrial metabolism, such as glutamine and fatty acids. In addition to PDC, MPC also regulates pyruvate oxidation by controlling substrate import. To confirm the effects of α-KB on pyruvate oxidation in cells, we performed metabolomics analysis. As would be expected of PDC inhibition, the abundance of acetyl-CoA and citrate was significantly decreased in α-KB treated cells (Figure 4A). Furthermore, metabolomics flux analysis using [U-$^{13}C_6$]glucose shows a significant decrease in glucose-derived citrate and other TCA cycle intermediates in α-KB treated cells (Figure 4B-C), supporting an inhibitory effect of α-KB on the oxidation of glucose-derived pyruvate. Meanwhile, the abundance of glucose-derived (M3) lactate was not altered by α-KB treatment, whereas the abundance of glucose-derived (M3)

alanine and serine was significantly increased (Figure S3A). The overall level of alanine also increased significantly upon α-KB treatment (Figure S3B). This increase in alanine and serine may at least partially contribute to the increase in α-KG, as the reactions that generate alanine and serine simultaneously converts glutamate to α-KG (Figure S3B). In contrast, the amount of leucine/isoleucine and valine was not changed upon α-KB treatment, suggesting that the oxidation of branch-chain alpha-keto acids is not affected (Figure S3B). Together the data indicate that α-KB treatment prevents the entry of glucose-derived pyruvate into the TCA cycle without affecting the conversion of pyruvate into lactate, increases transaminase conversion of pyruvate to alanine, and increases glucose flux into serine synthesis. This further supports that α-KB specifically interrupts PDH as an alternative substrate, but not LDH or alanine transaminase (ALT). By comparison, when pyruvate transportation into the mitochondria is abolished upon MPC inhibition, both total and glucose-derived alanine decreases (Figure S3A and S3C)[22], indicating that α-KB induces distinct metabolic states from MPC disruption.

To further confirm that the metabolic alterations upon α-KB treatment are primarily due to disruption of pyruvate oxidation, we knocked down DLAT, the E2 subunit of PDC, and found that both the total and glucose-derived citrate was decreased, similar to α-KB treatment (Figures 4D and S3D). Notably, both total and glucose-derived alanine was increased upon DLAT knockdown (Figure S3D-E), again consistent with α-KB treatment and different from MPC inhibition.

It is well documented that disruption of PDC induces distinct changes in glutamine metabolism compared to MPC perturbation by using [U-$^{13}C_5$]glutamine tracer[22]. [U-$^{13}C_5$]glutamine can be converted to M5 citrate through reductive carboxylation or to M4 citrate through oxidation. Additionally, [U-$^{13}C_5$]glutamine is oxidized and converted back to pyruvate through the malic enzyme reaction. The pyruvate derived from [U-$^{13}C_5$]glutamine can further go through PDC and generate labeled acetyl-CoA, which then combines with oxaloacetate to form M6 citrate. Alternatively, the glutamine-derived pyruvate can be converted to M3 lactate or alanine. M6 citrate is the most significantly increased isotopomer of citrate in MPC-knockdown cells, whereas M5 citrate is the most significantly increased species upon PDC inhibition. Our metabolomics analysis with [U-$^{13}C_5$]glutamine supports the hypothesis that PDC is the main target underlying α-KB's inhibition of pyruvate oxidation. Both M5 and M6 citrate increased significantly upon α-KB treatment (Figure 4E). Notably, the increase of M5 citrate is significantly higher than that of M6 citrate, suggesting that α-KB treatment, like hypoxia associated PDC inhibition, majorly increases reductive carboxylation in the TCA cycle[23,24]. On the contrary, M6 citrate is the major increase in UK5099-treated cells (Figure 4E), which is consistent with the previous report[22]. This further supports that PDC is the primary target for α-KB in mammalian cells. The abundance of fully labeled succinate, fumarate, α-KG, and malate increased significantly in α-KB-treated cells (Figure 4F), suggesting TCA cycle anaplerosis from increased glutaminolysis in α-KB treated cells. Additionally, M3 alanine is increased upon α-KB treatment (Figure S3F), indicating a higher flux of glutamine oxidation and conversion back to pyruvate through the malic enzyme.

Consistent with glucose and glutamine tracer results, we showed that glutamine contribution to lipogenic acetyl-CoA pool was significantly increased while the contribution from glucose was largely decreased. This further supports that pyruvate oxidation is disrupted by α-KB treatment (Figure 4G). Our metabolomics analysis indicates that α-KB treatment causes an increased flux of glutamine into the TCA cycle. A prediction of this finding is that the decreased pyruvate oxidation by α-KB would result in an increased reliance on glutamine in α-KB treated cells. Indeed, combined treatment with α-KB and BPTES, a known glutaminase inhibitor[25], synergistically inhibits cell growth (Figure S3G). In addition to glycolysis, β-oxidation provides acetyl-CoA to fuel into TCA cycle. To investigate whether β-oxidation serves as an compensatory pathway for TCA cycle upon disruption of pyruvate oxidation, we analyzed β-oxidation in α-KB-treated cells by utilizing the [U-$^{13}C_{16}$]palmitate tracer. α-KB treatment increases β-oxidation flux into the TCA cycle, as evidenced by the significant increase in M2 citrate as well as increased label incorporation into other TCA cycle intermediates (Figure 4H-I).

α-KB activates AMPK by disruption of pyruvate oxidation to extend lifespan in *C. elegans*

To assess the functional significance of α-KB on pyruvate oxidation in intact cells and *C. elegans*, we measured respiration levels in both cultured cells and live *C. elegans*. α-KB treatment partially but significantly decreases ATP-linked and maximal respiration in intact cells, whereas the complex I inhibitor rotenone completely abolishes respiration

(Figure 5A). This partial inhibition by α-KB is expected since α-KB does not directly inhibit complex I, and only specifically decreases pyruvate oxidation while sparing other NADH-generating enzymes such as α-KG dehydrogenase. Furthermore, knockdown of PDC subunits DLAT (E2) or PDHB (E1 component subunit beta) each activates AMPK and abolishes further AMPK activation by α-KB (Figure 5B), whereas AMPK activation by α-KB is normal in LDH or PC knockdown cells (Figure S4A-B). In agreement with the inhibitory effect of α-KB on cellular respiration, we found that α-KB treatment decreased the respiration of *C. elegans* as well, similar to the scenario with PDH knockdown (Figure 5C), but cannot further decrease respiration of PDH knockdown in *C. elegans*. Plus, AMPK is activated in PDH RNAi *C. elegans* (Figure 5D). Taken together, our results support the model in which α-KB activates AMPK through inhibition of pyruvate oxidation.

To determine the significance of pyruvate oxidation to the longevity by α-KB, we measured the lifespan of PDH RNAi adult *C. elegans* given α-KB. PDH RNAi animals live longer than control RNAi animals (Figure 5E), and α-KB does not further extend the lifespan of PDH RNAi worms (Figure 5E), consistent with the longevity effect of α-KB being dependent on pyruvate oxidation. Furthermore, the extended lifespan by PDH RNAi is abolished by AMPK pathway dysfunction in *aak-2* worms (Figure 5F). It indicates that α-KB depends on AMPK activation from pyruvate oxidation disruption to extend lifespan in *C. elegans*.

AMPK activation has been reported to be beneficial in various disease models, including Alzheimer's disease[26]. Therefore, we asked whether α-KB could relieve the proteotoxic

stress in a *C. elegans* Alzheimer's disease model wherein amyloid-beta toxicity causes progressive, age-dependent paralysis[27]. Remarkably, α-KB supplementation delays amyloid-beta induced paralysis (Figure 5G); importantly, α-KB does not protect PDH or AAK-2 knockdown *C. elegans* in this model (Figure 5G-H), consistent with the mechanism involving pyruvate oxidation and subsequent AMPK activation. The results suggest that α-KB induces AMPK activation in *C. elegans* and could be exploited for aging-related disease intervention.

Since induction of the mitochondrial unfolded protein response (UPR^{mt}) has recently been implicated in the longevity associated with mitochondrial perturbations[5,28,29], we tested whether the longevity effect of α-KB may involve UPR^{mt}. α-KB does not induce the UPR^{mt} marker HSP60 (Figure S4C), and α-KB extends the lifespan of *C. elegans* with knockdown of UBL-5 (Figure S4D), which is required for induction of the UPR^{mt}, suggesting that UPR^{mt} is not required for the longevity effect of α-KB. This is consistent with the idea that UPR^{mt} acts independently of AMPK in longevity[29].

SUMMARY

We show that an unfamiliar metabolite, α-KB, extends lifespan of adult *C. elegans*. This extension is likely through a direct inhibitory effect of α-KB on pyruvate oxidation and consequent activation of AMPK. Although it has been suggested that α-KB disturbs pyruvate oxidation in vitro[18,30], the physiological and biological significance of this effect

on pyruvate metabolism has not been studied. Our report shows that α-KB treatment increases lifespan expectancy by acting as a competitive alternative substrate of PDC. The inhibitory effect of α-KB on pyruvate oxidation is specific, as our results suggest that pyruvate reactions through LDH, PC, and ALT are not inhibited by α-KB treatment. Through its inhibition of PDH, α-KB treatment rewires mitochondrial substrate utilization. The entry of glucose-derived pyruvate into TCA cycle is perturbed upon α-KB treatment while increased glutamine and lipid are utilized by the mitochondria. Altered mitochondrial substrate utilization is associated with numerous pathological conditions, including obesity and diabetes[31,32]. Our finding that α-KB alters mitochondrial metabolism provides novel direction for the treatment of mitochondrial metabolism diseases.

Our results indicate that α-KB exhibits a comparable affinity as pyruvate to PDC, and this suggests the possibility for α-KB to be utilized as a major endogenous PDH substrate. Moreover, when PDC switches to use α-KB as its major substrate, due to the lower efficacy of α-KB, the overall activity of PDC is limited, mitochondrial metabolism is rewired, and AMPK is activated. This points to the possibility that alternative endogenous substrates for pivotal metabolic enzymes, such as PDC, are able to determine the activity of these enzymes and yield profound effects on the endogenous regulatory systems of signaling and aging. In addition, it is possible that these alternative substrates are employed by the organism under stress, and further studies on alternative substrates may shed light on novel anti-aging interventions. Perhaps reminiscent of the dual effects of mitochondrial ETC inhibition in longevity and disease, although severe PDC deficiency has been linked to neuronal degeneration, cancer, and glucose intolerance[33], moderate

inhibition of PDC can bestow health benefits without adversely affecting normal organismal function.

Energy metabolism and AMPK are intimately connected with both aging and health. Metformin, the plant-derived, most widely used anti-diabetic biguanide whose mechanisms include inhibition of mitochondrial complex I and activation of AMPK, has been shown to exhibit beneficial effects against aging and cancer. Our study demonstrates that an endogenous longevity small molecule can also successfully relieve aging-dependent degenerations through AMPK activation, further supporting the idea that aging-related diseases can be countered by regulation of longevity pathways.

Figure Legends

Figure 1. α-KB increases the lifespan of adult *C. elegans*.

(A) Structure of α-KB.

(B) α-KB extends the lifespan of adult worms, mean lifespan (days of adulthood) with vehicle treatment (m_{veh}) = 14.1 (n = 111 animals tested), $m_{\alpha\text{-KB}}$ = 22.4 (n = 66), $P < 0.0001$ (log-rank test).

(C) Dose–response curve of the α-KB effect on longevity.

Figure 2. α-KB extends lifespan through AMPK.

(A) α-KB does not extend (and, in fact, slightly reduces) the lifespan of *aak-2(gt33)* adult worms, m_{veh} = 15.9 (n = 120), $m_{\alpha\text{-KB}}$ = 15.1 (n = 138), P = 0.0029 (log-rank test).

(B) α-KB further extends the lifespan of *eat-2(ad1116)* adult worms, m_{veh} = 20.4 (n = 99), $m_{\alpha\text{-KB}}$ = 23.0 (n = 116), P = 0.0054 (log-rank test).

(C) α-KB further extends the lifespan of *daf-2(e1370)* adult worms, m_{veh} = 37.0 (n = 100), $m_{\alpha\text{-KB}}$ = 47.0 (n = 95), $P < 0.0001$ (log-rank test).

(D) α-KB increases phosphorylated AMPK in adult *C. elegans*.

(E) AMPK signaling is activated in α-KB-treated cells. Similar results were obtained in multiple cell lines, including H9C2 (shown), U87 and HAP1 cells (not shown).

(F) α-KB does not extend the lifespan of *daf-16(mu86)* adult worms, m_{veh} = 15.5 (n = 97), $m_{\alpha\text{-KB}}$ = 16.0 (n = 99), P = 0.1482 (log-rank test).

(G) α-KB increases heat resistance of adult *C. elegans*.

(H) α-KB does not extend the lifespan of *skn-1(zu67)* adult worms, m_{veh} = 12.0 (n = 60), $m_{\alpha\text{-KB}}$ = 13.0 (n = 46), P = 0.0475 (log-rank test).

(I) α-KB does not extend the lifespan of *sir-2.1(ok434)* adult worms, m_{veh} = 17.7 (n = 94), $m_{\alpha\text{-KB}}$ = 18.4 (n = 39), P = 0.2739 (log-rank test).

Figure 3. α-KB perturbs pyruvate oxidation.

(A-B) Isolated mitochondria from mouse liver are offered with different respiratory substrates. Upon α-KB treatment (500 μM), both state 3 **(A)** and state 3u **(B)** respiration is decreased when pyruvate (Pyr) and methyl pyruvate (Me-pyr) are utilized as substrates (**P < 0.01, *** P < 0.001). Unpaired t test, two-tailed, two-sample unequal variance is used. Mean ± s.d. is plotted.

(C) DARTS identifies PDH as an α-KB-binding protein complex. α-KB does not bind to ETC complex I; NQO1 and NDUFB8 are subunits of complex I. U87 cell lysates were used. Similar results were obtained with HEK293 cells (data not shown).

(D) Inhibition of PDC activity by α-KB. Pyruvate (1 mM) is provided as substrate.

(E) Allosteric sigmoidal kinetics of pyruvate and α-KB on PDC, by nonlinear regression least-squares fit. The V_{max} and K_m values for pyruvate vs. α-KB are 0.004 vs. 0.001 and 54.05 vs. 56.13, respectively.

(F) α-KB acts as a competitive alternative substrate to perturb pyruvate oxidation and decrease NADH generation. PDC activity is measured based on the synthesis rate of NADH.

Figure 4. α-KB treatment alters mitochondrial substrate utilization.

(A) Relative abundance of citrate of acetyl-CoA.

(B) Citrate mass isotopomer distribution (MID) upon α-KB treatment resulting from culture with [U-$^{13}C_6$]glucose (UGlc).

(C) Percentage of fully labeled metabolites derived from [U-$^{13}C_6$]glucose (UGlc).

(D) Citrate MID upon DLAT knockdown resulting from culture with [U-$^{13}C_6$]glucose (UGlc).

(E) Citrate mass isotopomer distribution (MID) upon α-KB or UK5099 (10 μM) treatment resulting from culture with [U-$^{13}C_5$]glutamine (UGln).

(F) Percentage of fully labeled metabolites derived from [U-$^{13}C_5$]glutamine (UGln).

(G) Contribution of UGln and UGlc to lipogenic AcCoA as determined by isotopomer enrichment modeling.

(H) Relative abundance of M2 citrate upon α-KB treatment resulting from culture with [U-$^{13}C_{16}$]palmitate conjugated to BSA (UPalm).

(I) Percentage of fully labeled metabolites derived from [U-$^{13}C_{16}$]palmitate conjugated to BSA (UPalm).

Unpaired t test, two-tailed, two-sample unequal variance was used for **(A)**-**(I)** (∗∗∗∗P < 0.0001, ∗∗∗ P < 0.001, ∗∗ P < 0.01, ∗ P < 0.05). Mean ± s.d. is plotted. 3.2 mM α-KB was used in **(A)**-**(I)**.

Figure 5. α-KB extends lifespan and ameliorate aging-dependent symptoms through disruption of pyruvate oxidation.

(**A**) Basal respiration, ATP-linked respiration (oligomycin-insensitive respiration) and maximum respiration (FCCP-induced respiration) upon α-KB (5 mM) or rotenone (1 μM) treatment; ∗∗∗∗ P < 0.0001, ∗∗ P < 0.01, ∗ P < 0.05. Unpaired t test, two-tailed, two-sample unequal variance was used.

(**B**) α-KB treatment does not further activate AMPK in PDC-knockdown H9C2 cells.

(**C**) Decreased oxygen consumption rate (OCR) in α-KB-treated or PDHB-1 knockdown worms (P < 0.05; by t-test, two-tailed, two-sample unequal variance) for the entire time.

(**D**) PDHB-1 knockdown increases phosphorylated AMPK in adult *C. elegans*.

(**E**) α-KB cannot extend the lifespan of PDHB-1 knockdown worms. Control, m_{veh} = 19.5 (n = 94), $m_{\alpha\text{-KB}}$ = 21.8 (n = 88), P < 0.0001 (log-rank test); *pdhb-1* RNAi, m_{veh} = 22.5 (n = 81), $m_{\alpha\text{-KB}}$ = 19.8 (n = 84), P < 0.0001 (log-rank test).

(**F**) α-KB or PDHB-1 knockdown does not extend the lifespan of *aak-2(gt33)* adult worms. Control, m_{veh} = 12.6 (n = 132), $m_{\alpha\text{-KB}}$ = 11.5 (n = 123), P = 0.0007 (log-rank test); *pdhb-1* RNAi, m_{veh} = 12.1 (n = 139), P = 0.1298 (log-rank test).

(**G**) α-KB delays paralysis in the $A\beta_{1\text{-}42}$ expressing GMC101 worms, but does not reduce amyloid-beta toxicity in PDHB-1 knockdown animals. Control, m_{veh} = 2.5 (n = 177), $m_{\alpha\text{-KB}}$ = 3.1 (n = 161), P < 0.0001 (log-rank test); *pdhb-1* RNAi, m_{veh} = 2.3 (n = 205), $m_{\alpha\text{-KB}}$ = 2.3 (n = 234), P = 0.4345 (log-rank test).

(**H**) α-KB delays paralysis in the $A\beta_{1\text{-}42}$ expressing GMC101 worms, but not in AAK-2 knockdown animals. Control, m_{veh} = 2.5 (n = 248), $m_{\alpha\text{-KB}}$ = 3.5 (n = 150), P < 0.0001 (log-rank test); *aak-2* RNAi, m_{veh} = 2.6 (n = 281), $m_{\alpha\text{-KB}}$ = 2.7 (n = 231), P = 0.7106 (log-rank test).

References

1. Longo, V. D., Antebi, A., Bartke, A., Barzilai, N., Brown-Borg, H. M., Caruso, C., ... & Ingram, D. K. (2015). Interventions to slow aging in humans: are we ready? *Aging cell*, *14*(4), 497-510.

2. López-Otín, C., Galluzzi, L., Freije, J. M., Madeo, F., & Kroemer, G. (2016). Metabolic control of longevity. *Cell*, *166*(4), 802-821.

3. Chin, R. M., Fu, X., Pai, M. Y., Vergnes, L., Hwang, H., Deng, G., ... & Hu, E. (2014). The metabolite α-ketoglutarate extends lifespan by inhibiting ATP synthase and TOR. *Nature*, *510*(7505), 397.

4. Zhang, H., Ryu, D., Wu, Y., Gariani, K., Wang, X., Luan, P., ... & Schoonjans, K. (2016). NAD+ repletion improves mitochondrial and stem cell function and enhances life span in mice. *Science*, *352*(6292), 1436-1443.

5. Mouchiroud, L., Houtkooper, R. H., Moullan, N., Katsyuba, E., Ryu, D., Cantó, C., ... & Guarente, L. (2013). The NAD+/sirtuin pathway modulates longevity through activation of mitochondrial UPR and FOXO signaling. *Cell*, *154*(2), 430-441.

6. Paxton, R., Scislowski, P. W., Davis, E. J., & Harris, R. A. (1986). Role of branched-chain 2-oxo acid dehydrogenase and pyruvate dehydrogenase in 2-oxobutyrate metabolism. *Biochemical Journal*, *234*(2), 295-303.

7. Sullivan, L. B., Gui, D. Y., Hosios, A. M., Bush, L. N., Freinkman, E., & Vander Heiden, M. G. (2015). Supporting aspartate biosynthesis is an essential function of respiration in proliferating cells. *Cell*, *162*(3), 552-563.

8. Cabreiro, F., & Gems, D. (2013). Worms need microbes too: microbiota, health and aging in Caenorhabditis elegans. *EMBO molecular medicine*, *5*(9), 1300-1310.

9. Mihaylova, M. M., & Shaw, R. J. (2011). The AMPK signalling pathway coordinates cell growth, autophagy and metabolism. *Nature cell biology*, *13*(9), 1016.

10. Hardie, D. G., Ross, F. A., & Hawley, S. A. (2012). AMPK: a nutrient and energy sensor that maintains energy homeostasis. *Nature reviews Molecular cell biology*, *13*(4), 251.

11. Cabreiro, F., Au, C., Leung, K. Y., Vergara-Irigaray, N., Cochemé, H. M., Noori, T., ... & Gems, D. (2013). Metformin retards aging in C. elegans by altering microbial folate and methionine metabolism. *Cell*, *153*(1), 228-239.

12. Weimer, S., Priebs, J., Kuhlow, D., Groth, M., Priebe, S., Mansfeld, J., ... & Schulz, T. J. (2014). D-Glucosamine supplementation extends life span of nematodes and of ageing mice. *Nature communications*, *5*, 3563.

13. Greer, E. L., Banko, M. R., & Brunet, A. (2009). AMP-activated Protein Kinase and FoxO Transcription Factors in Dietary Restriction–induced Longevity. *Annals of the New York Academy of Sciences*, *1170*(1), 688-692.

14. Brand, M. D., & Nicholls, D. G. (2011). Assessing mitochondrial dysfunction in cells. *Biochemical Journal*, *435*(2), 297-312.

15. Bricker, D. K., Taylor, E. B., Schell, J. C., Orsak, T., Boutron, A., Chen, Y. C., ... & Redin, C. (2012). A mitochondrial pyruvate carrier required for pyruvate uptake in yeast, Drosophila, and humans. *Science*, *337*(6090), 96-100.

16. Halestrap, A. P. (1975). The mitochondrial pyruvate carrier. Kinetics and specificity for substrates and inhibitors. *Biochemical Journal*, *148*(1), 85-96.

17. Lomenick, B., Hao, R., Jonai, N., Chin, R. M., Aghajan, M., Warburton, S., ... & Wohlschlegel, J. A. (2009). Target identification using drug affinity responsive target stability (DARTS). *Proceedings of the National Academy of Sciences*, *106*(51), 21984-21989.

18. Kanzaki, T., Hayakawa, T., Hamada, M., Fukuyoshi, Y., & Koike, M. (1969). Mammalian α-keto acid dehydrogenase complexes IV. Substrate specificities and kinetic properties of the pig heart pyruvate and 2-oxoglutarate dehydrogenase complexes. *Journal of Biological Chemistry*, *244*(5), 1183-1187.

19. Bisswanger, H., & Henning, U. (1971). Regulatory Properties of the Pyruvate-Dehydrogenase Complex from Escherichia coli: Positive and Negative Cooperativity. *European journal of biochemistry*, *24*(2), 376-384.

20. Linn, T. C., Pettit, F. H., Hucho, F., & Reed, L. J. (1969). α-Keto acid dehydrogenase complexes, XI. Comparative studies of regulatory properties of the pyruvate dehydrogenase complexes from kidney, heart, and liver mitochondria. *Proceedings of the National Academy of Sciences*, *64*(1), 227-234.

21. Peters, S. J., & LeBlanc, P. J. (2004). Metabolic aspects of low carbohydrate diets and exercise. *Nutrition & metabolism*, *1*(1), 7.

22. Vacanti, N. M., Divakaruni, A. S., Green, C. R., Parker, S. J., Henry, R. R., Ciaraldi, T. P., ... & Metallo, C. M. (2014). Regulation of substrate utilization by the mitochondrial pyruvate carrier. *Molecular cell*, *56*(3), 425-435.

23. Kim, J. W., Tchernyshyov, I., Semenza, G. L., & Dang, C. V. (2006). HIF-1-mediated expression of pyruvate dehydrogenase kinase: a metabolic switch required for cellular adaptation to hypoxia. *Cell metabolism*, *3*(3), 177-185.

24. Papandreou, I., Cairns, R. A., Fontana, L., Lim, A. L., & Denko, N. C. (2006). HIF-1 mediates adaptation to hypoxia by actively downregulating mitochondrial oxygen consumption. *Cell metabolism*, *3*(3), 187-197.

25. Robinson, M. M., Mcbryant, S. J., Tsukamoto, T., Rojas, C., Ferraris, D. V., Hamilton, S. K., ... & Curthoys, N. P. (2007). Novel mechanism of inhibition of rat kidney-type glutaminase by bis-2-(5-phenylacetamido-1, 2, 4-thiadiazol-2-yl) ethyl sulfide (BPTES). *Biochemical Journal*, *406*(3), 407-414.

26. Vingtdeux, V., Giliberto, L., Zhao, H., Chandakkar, P., Wu, Q., Simon, J. E., ... & Marambaud, P. (2010). AMP-activated protein kinase signaling activation by resveratrol modulates amyloid-β peptide metabolism. *Journal of Biological Chemistry*, *285*(12), 9100-9113.

27. McColl, G., Roberts, B. R., Pukala, T. L., Kenche, V. B., Roberts, C. M., Link, C. D., ... & Cherny, R. A. (2012). Utility of an improved model of amyloid-beta (Aβ 1-42) toxicity in Caenorhabditis elegans for drug screening for Alzheimer's disease. *Molecular neurodegeneration*, *7*(1), 57.

28. Durieux, J., Wolff, S., & Dillin, A. (2011). The cell-non-autonomous nature of electron transport chain-mediated longevity. *Cell*, *144*(1), 79-91.

29. Houtkooper, R. H., Mouchiroud, L., Ryu, D., Moullan, N., Katsyuba, E., Knott, G., ... & Auwerx, J. (2013). Mitonuclear protein imbalance as a conserved longevity mechanism. *Nature*, *497*(7450), 451.

30. Jones, S. M., & Yeaman, S. J. (1986). Oxidative decarboxylation of 4-methylthio-2-oxobutyrate by branched-chain 2-oxo acid dehydrogenase complex. *Biochemical Journal*, *237*(2), 621-623.

31. Gaster, M., Rustan, A. C., Aas, V., & Beck-Nielsen, H. (2004). Reduced lipid oxidation in skeletal muscle from type 2 diabetic subjects may be of genetic origin: evidence from cultured myotubes. *Diabetes*, *53*(3), 542-548.

32. Kim, J. Y., Hickner, R. C., Cortright, R. L., Dohm, G. L., & Houmard, J. A. (2000). Lipid oxidation is reduced in obese human skeletal muscle. *American Journal of Physiology-Endocrinology And Metabolism*, *279*(5), E1039-E1044.

33. Stacpoole, P. W. (2012). The pyruvate dehydrogenase complex as a therapeutic target for age-related diseases. *Aging cell*, *11*(3), 371-377.

Figure 1

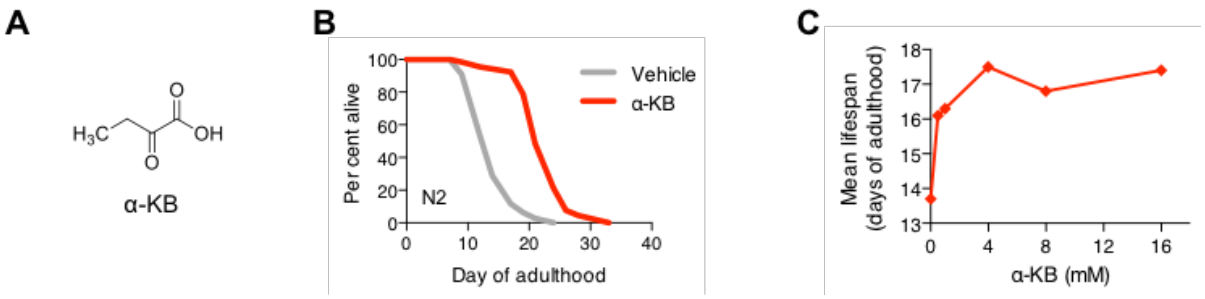
A
O
H3C
OH
O
α-KB
B
100
80
60
40
20
0
Per cent alive
N2
Vehicle
α-KB
0
10
20
30
40
Day of adulthood
C
18
17
16
15
14
13
Mean lifespan
(days of adulthood)
0
4
8
12
16
α-KB (mM)

Figure 2

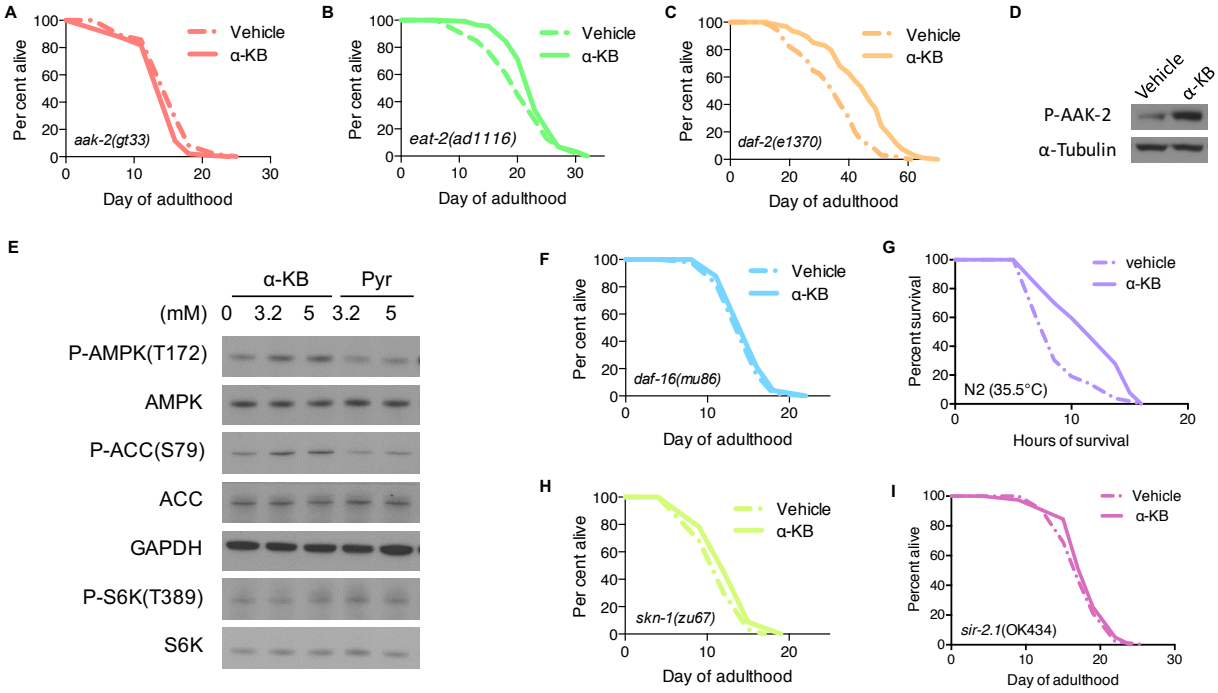
A
Per cent alive
Vehicle
α-KB
aak-2(gt33)
Day of adulthood
B
eat-2(ad1116)
C
daf-2(e1370)
D
Vehicle
α-KB
P-AAK-2
α-Tubulin
E
α-KB
Pyr
(mM) 0 3.2 5 3.2 5
P-AMPK(T172)
AMPK
P-ACC(S79)
ACC
GAPDH
P-S6K(T389)
S6K
F
daf-16(mu86)
G
vehicle
Percent survival
N2 (35.5°C)
Hours of survival
H
skn-1(zu67)
I
sir-2.1(OK434)

Figure 3

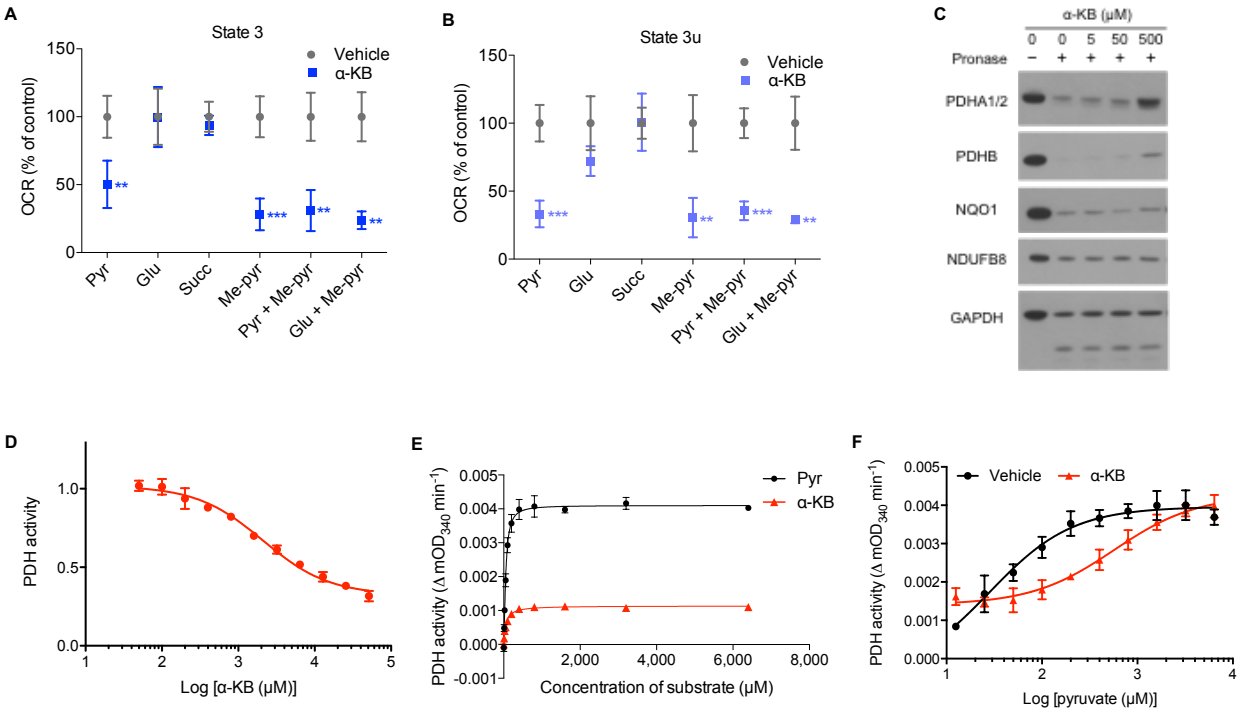
A
State 3
Vehicle
α-KB
OCR (% of control)
150
100
50
0
Pyr
Glu
Succ
Me-pyr
Pyr + Me-pyr
Glu + Me-pyr
B
State 3u
Vehicle
α-KB
OCR (% of control)
C
α-KB (μM)
0 0 5 50 500
Pronase
− + + + +
PDHA1/2
PDHB
NQO1
NDUFB8
GAPDH
D
PDH activity
Log [α-KB (μM)]
E
Pyr
α-KB
PDH activity (Δ mOD340 min−1)
Concentration of substrate (μM)
F
Vehicle
α-KB
PDH activity (Δ mOD340 min−1)
Log [pyruvate (μM)]

Figure 4

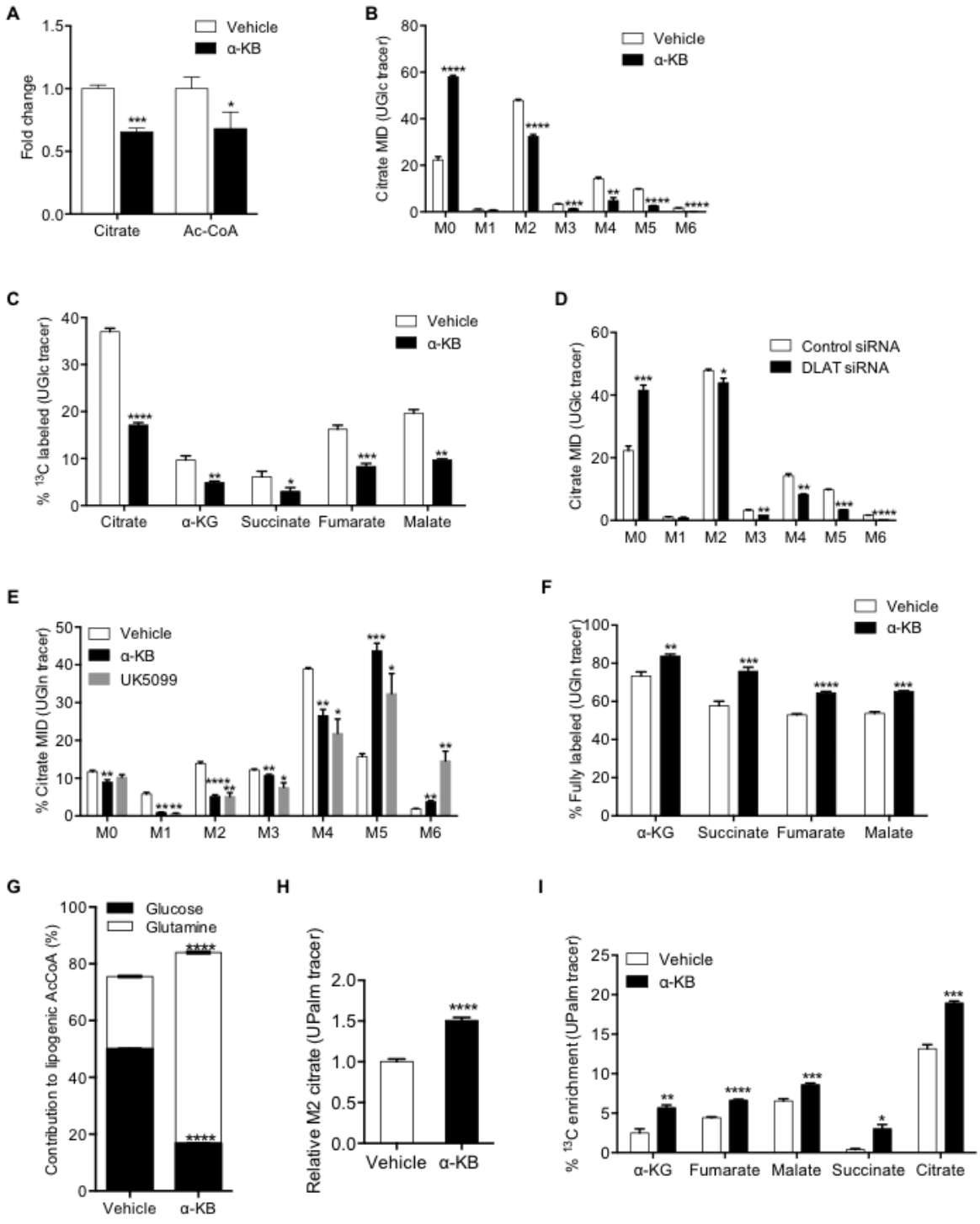
A
Vehicle
α-KB
Fold change
Citrate
Ac-CoA
B
Vehicle
α-KB
Citrate MID (UGlc tracer)
M0 M1 M2 M3 M4 M5 M6
C
Vehicle
α-KB
% 13C labeled (UGlc tracer)
Citrate α-KG Succinate Fumarate Malate
D
Control siRNA
DLAT siRNA
Citrate MID (UGlc tracer)
M0 M1 M2 M3 M4 M5 M6
E
Vehicle
α-KB
UK5099
% Citrate MID (UGln tracer)
M0 M1 M2 M3 M4 M5 M6
F
Vehicle
α-KB
% Fully labeled (UGln tracer)
α-KG Succinate Fumarate Malate
G
Glucose
Glutamine
Contribution to lipogenic AcCoA (%)
Vehicle α-KB
H
Relative M2 citrate (UPalm tracer)
Vehicle α-KB
I
Vehicle
α-KB
% 13C enrichment (UPalm tracer)
α-KG Fumarate Malate Succinate Citrate

Figure 5

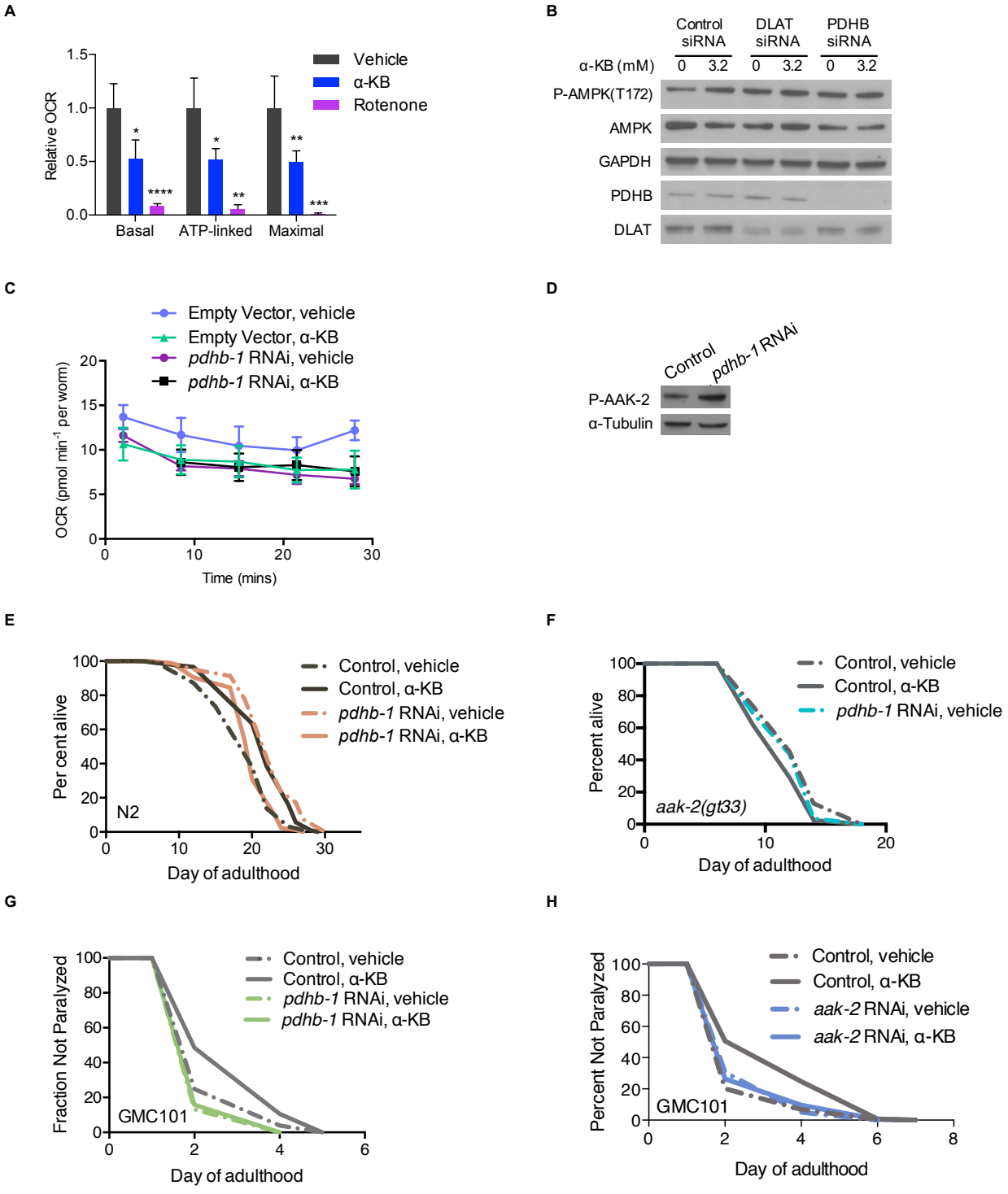
A
Relative OCR
Vehicle
α-KB
Rotenone
Basal
ATP-linked
Maximal
B
Control siRNA
DLAT siRNA
PDHB siRNA
α-KB (mM)
0 3.2 0 3.2 0 3.2
P-AMPK(T172)
AMPK
GAPDH
PDHB
DLAT
C
Empty Vector, vehicle
Empty Vector, α-KB
pdhb-1 RNAi, vehicle
pdhb-1 RNAi, α-KB
OCR (pmol min-1 per worm)
Time (mins)
D
Control
pdhb-1 RNAi
P-AAK-2
α-Tubulin
E
Control, vehicle
Control, α-KB
pdhb-1 RNAi, vehicle
pdhb-1 RNAi, α-KB
Per cent alive
N2
Day of adulthood
F
Control, vehicle
Control, α-KB
pdhb-1 RNAi, vehicle
Percent alive
aak-2(gt33)
Day of adulthood
G
Control, vehicle
Control, α-KB
pdhb-1 RNAi, vehicle
pdhb-1 RNAi, α-KB
Fraction Not Paralyzed
GMC101
Day of adulthood
H
Control, vehicle
Control, α-KB
aak-2 RNAi, vehicle
aak-2 RNAi, α-KB
Percent Not Paralyzed
GMC101
Day of adulthood

Supplemental figures

Figure S1

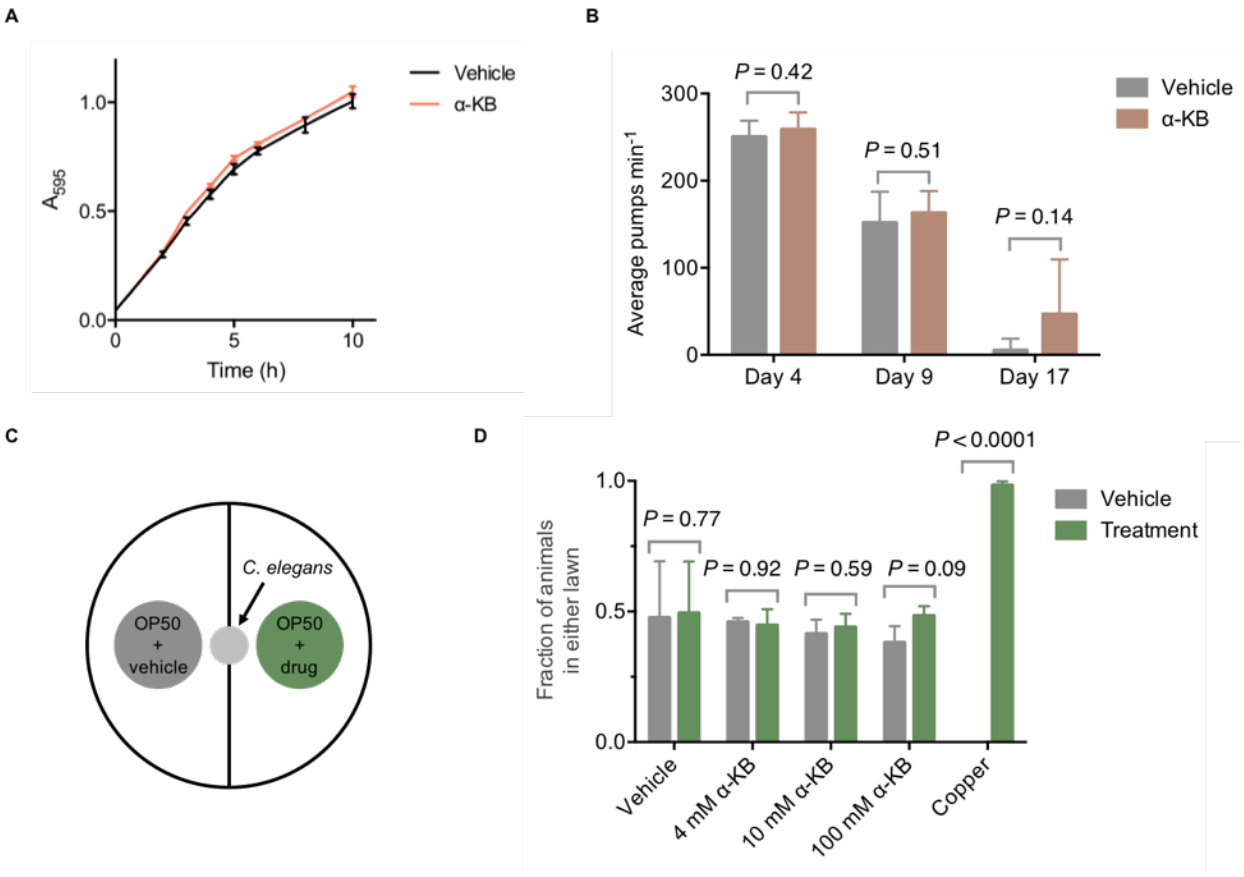

Figure S1, related to Figure 1. α-KB increases the lifespan of adult *C. elegans*.

(A) α-KB does not alter the growth rate of the OP50 *E. coli.* OP50 is the standard laboratory food source for nematodes. α-KB (4 mM) or vehicle (H_2O) was added to standard LB media and the pH was adjusted to 6.6 by the addition of NaOH. Bacterial cells from the same overnight OP50 culture were added to the LB/α-KB mixture at a 1:40 dilution, and then placed in the 37 ^{o}C incubator shaker at 300 r.p.m. The absorbance at 595 nm was read at 1 h time intervals to generate the growth curve.

(B) Pharyngeal pumping rate of *C. elegans* on 4 mM α-KB is not significantly altered (by t-test, two-tailed, two-sample unequal variance).

(C) Schematic representation of food preference assay.

(D) N2 worms show no preference between OP50 *E. coli* food treated with vehicle or α-KB (by t-test, two-tailed, two-sample unequal variance).

Figure S2

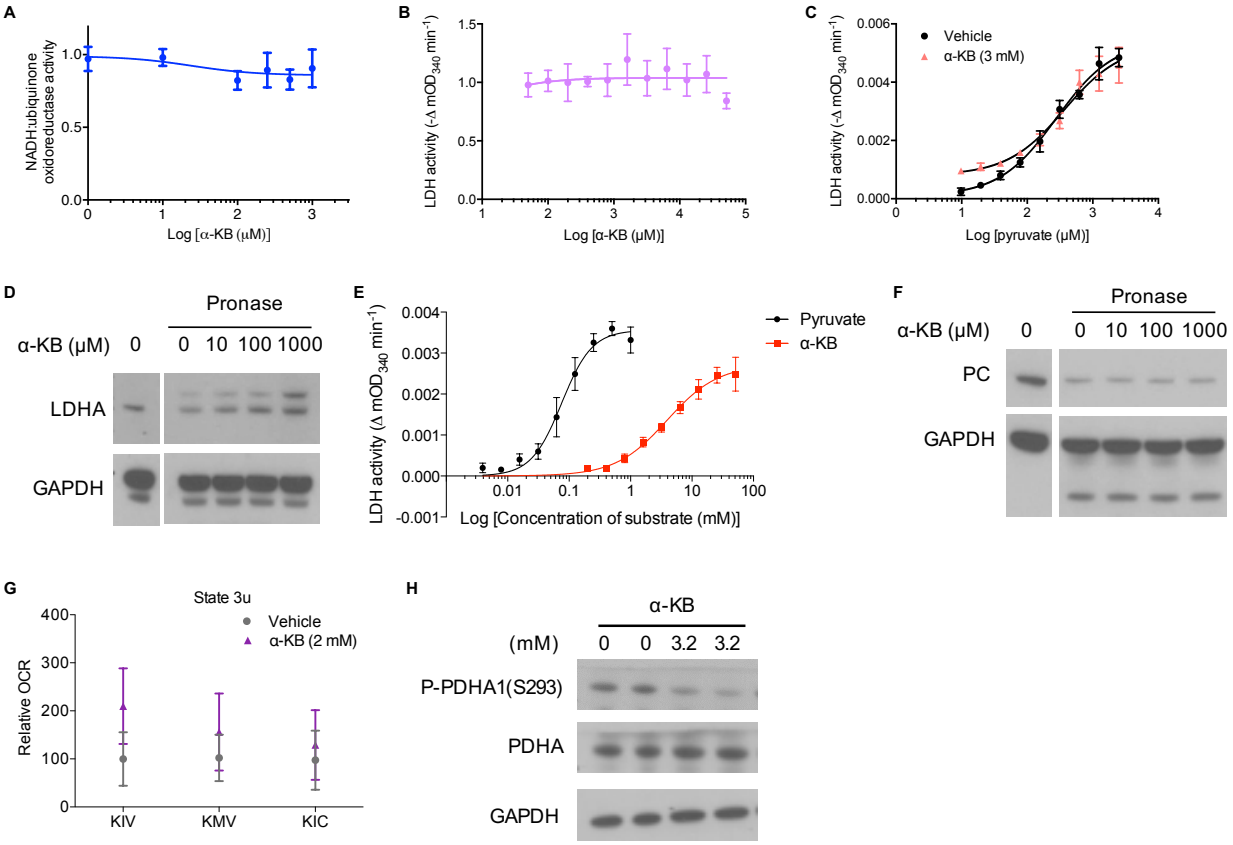

Figure S2, related to Figure 3. α-KB perturbs pyruvate oxidation.

(A) α-KB does not inhibit complex I activity.

(B) α-KB does not decrease LDH activity in converting pyruvate to lactate. Pyruvate (1 mM) is provided as substrate.

(C) α-KB does not act as a competitive alternative substrate for pyruvate on LDH and does not decrease NADH consumption rate. LDH activity is measured based on the consumption rate of NADH.

(D) DARTS showing α-KB binding to LDH.

(E) Allosteric sigmoidal curves of pyruvate vs. α-KB on LDH, by nonlinear regression least- squares fit. The Vmax and Km values for pyruvate vs. α-KB are 0.0036 vs. 0.0027

and 0.076 vs. 3.92, respectively. LDH activity is measured based on the consumption rate of NADH. Mean ± s.d. is plotted.

(F) DARTS showing α-KB does not bind to PC.

(G) Isolated mitochondria from mouse liver are offered with different respiratory substrates. Upon α-KB, states 3u mitochondrial respiration is not inhibited when 5 mM KIC, 10 mM KIV, or 10 mM KMV is utilized as substrates together with 10 mM malate.

(H) The level of phosphor-PDHA1 is decreased upon α-KB treatment in H9C2 cells. Mean ± s.d. is plotted.

Figure S3

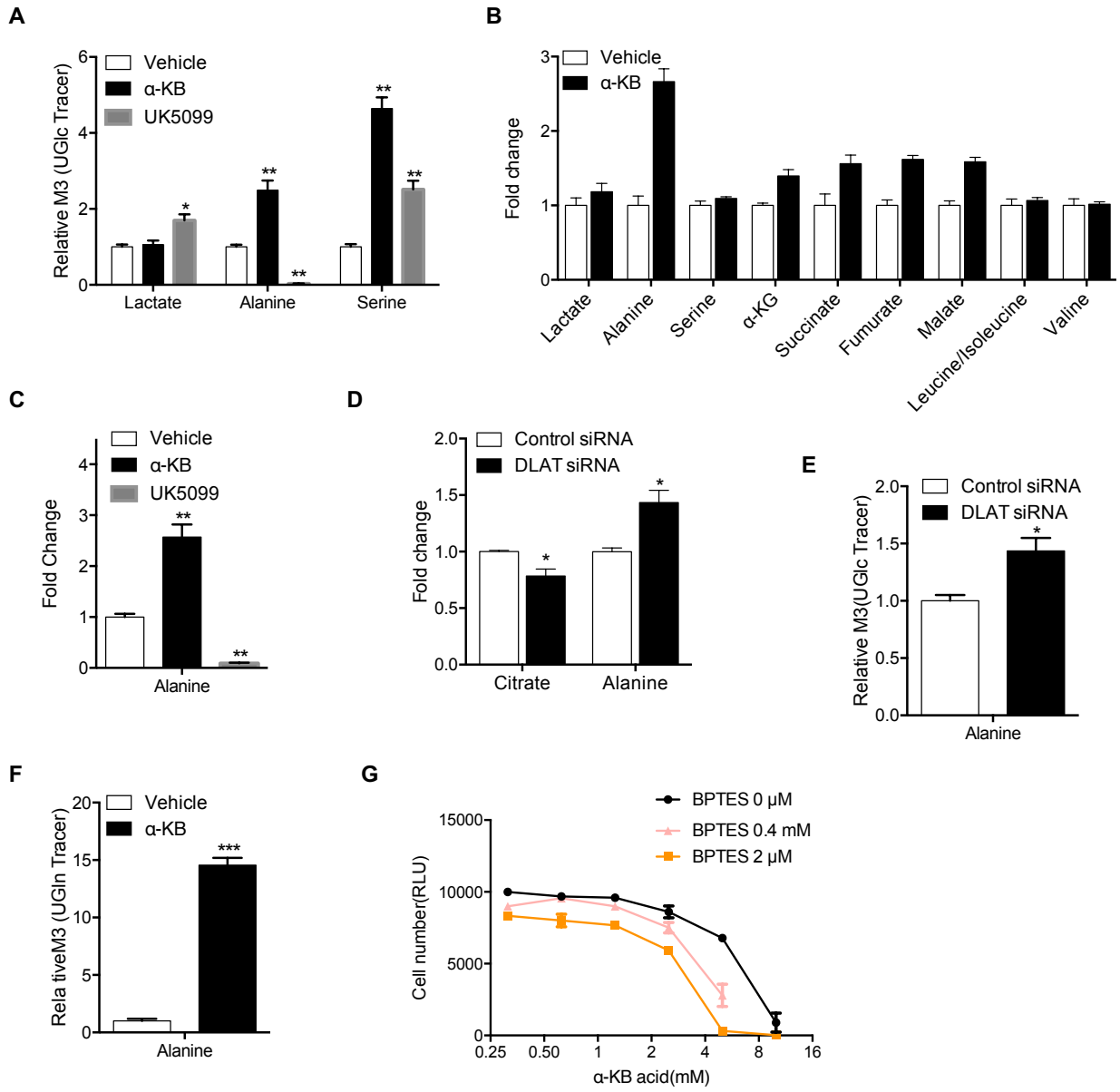

Figure S3, related to Figure 4. α-KB treatment alters mitochondrial substrate utilization.

(A) Relative abundance of M3 lactate, alanine, and serine in cells with α-KB or UK5099 (10 μM) treatment resulting from culture with UGlc.

(B) Relative abundance of lactate, alanine, and serine in cells with α-KB treatment.

(C) Relative abundance of alanine in cells with α-KB or UK5099 (10 μM) treatment resulting from culture with UGlc.

(D) DLAT-knockdown cells exhibit decreased citrate and increased alanine.

(E) Relative abundance of M3 alanine in DLAT-knockdown cells resulting from culture with UGlc.

(F) Relative abundance of M3 alanine in cells treated with α-KB resulting from culture with UGln.

(G) α-KB synergistically inhibits cell growth with BPTES.

Unpaired t test, two-tailed, two-sample unequal variance was used for **(A)**-**(F)** (∗∗∗∗P < 0.0001, ∗∗∗ P < 0.001, ∗∗ P < 0.01, ∗ P < 0.05). Mean ± s.d. is plotted. 3.2 mM α-KB was used in **(A)**-**(G)**.

Figure S4

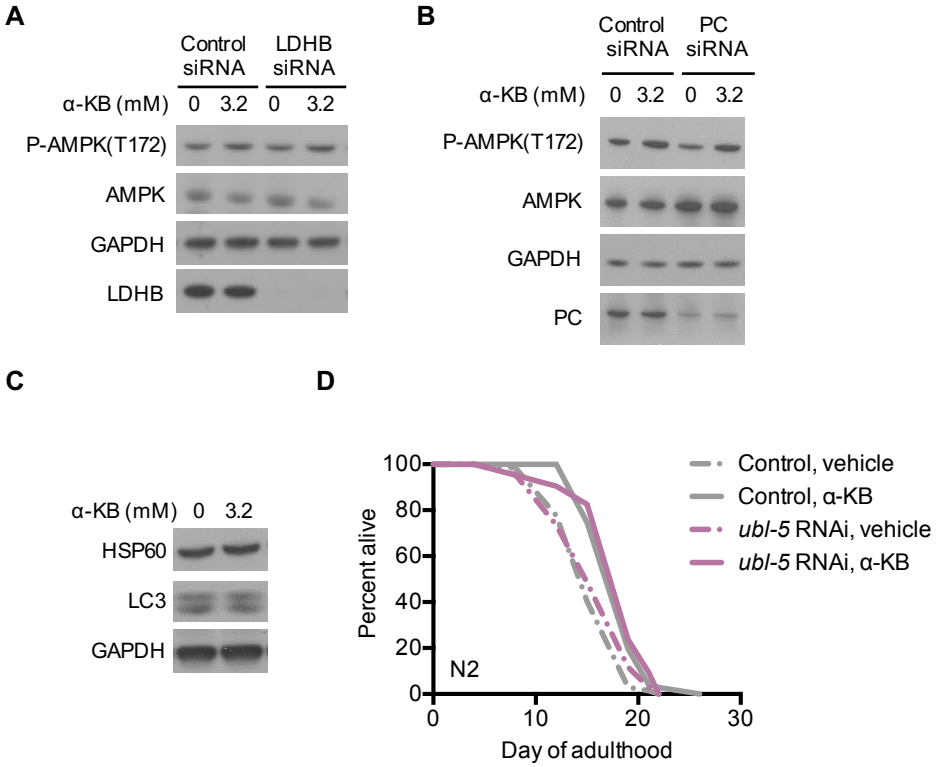

Figure S4, related to Figure 5. α-KB extends lifespan and ameliorate aging-dependent symptoms through AMPK and disruption of pyruvate oxidation.

(**A**) LDHB (lactate dehydrogenase B chain) knockdown does not abolish α-KB activation of AMPK. H9C2 cells were used.

(**B**) PC knockdown does not abolish α-KB activation of AMPK. H9C2 cells were used. (**C**) α-KB does not modulate HSP60 or LC3.

(**D**) α-KB extends the lifespan of adult worms with UBL-5 knockdown. Control, m_{veh} = 16.0 (n = 67), $m_{\alpha\text{-KB}}$ = 18.5 (n = 71), P < 0.0001 (log-rank test); *ubl-5* RNAi, m_{veh} = 16.2 (n = 68), $m_{\alpha\text{-KB}}$ = 18.4 (n = 63), P < 0.0001 (log-rank test).

Supplemental Experimental Procedures

Nematode strains

The following strains were used (strain, genotype): Bristol N2, wild type; TG38*, aak-2(gt33)X*; DA1116, *eat-2(ad1116)II*; CB1370, *daf-2(e1370)III*; CF1038, *daf-16(mu86)*; *skn-1(zu67)*. All strains were obtained from the Caenorhabditis Genetics Center (CGC).

C. elegans Lifespan analysis

Lifespan assays were conducted as described[1] at 20 °C on solid nematode growth media (NGM) using standard protocols and were replicated in at least two independent experiments. The sample size was chosen on the basis of standards done in the field in published manuscripts. No statistical method was used to predetermine the sample size. Animals were assigned randomly to the experimental groups. Worms that ruptured, bagged (that is, exhibited internal progeny hatching), or crawled off the plates were censored. Lifespan data were analyzed using GraphPad Prism; P values were calculated using the log-rank (Mantel–Cox) test.

Statistical analyses

All experiments were repeated at least two times with identical or similar results. Data represent biological replicates. Appropriate statistical tests were used for every figure. Data meet the assumptions of the statistical tests described for each figure. Mean ± s.d. is plotted in all figures unless stated otherwise.

Assay for *C. elegans* paralysis in Alzheimer's disease model

The GMC101 *C. elegans* strain[2] expresses the full length human amyloid-beta 1-42 protein in the body wall muscle cells, leading to a fully-penetrant age-progressive paralysis. Worms were age-synchronized by performing a timed egg lay for 3 h with ~100 gravid adults and the eggs placed in a 20 °C incubator. Once the eggs had developed to the L4 stage at 42 h post egg lay, they were picked onto NGM treatment plates containing 49.5 μM 5-fluoro-2'-deoxyuridine (FUDR, Sigma F0503) to prevent progeny production and either α-KB (2 mM) or vehicle (water) control. Worms were then shifted to 30°C to induce amyloid-beta aggregation and paralysis. Worms were assessed for paralysis daily, beginning on the second day of treatment, by the failure to perform whole body bends and to significantly move forward and backward upon gentle prodding with a platinum wire. Most paralyzed worms could still move their heads and part of their body. All worms were transferred to fresh treatment plates on day 4.

Pharyngeal pumping rates of *C. elegans* treated with 4 mM α-KB.

The pharyngeal pumping rates of 7 wild-type N2 worms per condition were assessed. Pharyngeal contractions were recorded and counted for 1 min using a Zeiss M2 BioDiscovery microscope and an attached Sony NDR-XR500V video camera at 12-fold optical zoom. Statistical analysis was performed using GraphPad Prism (t-test, two-tailed, two-sample unequal variance).

Food preference assay.

Protocol adapted from Abada et al.[3]. A 10 cm NGM plate was seeded with two spots of OP50 as shown in Supplemental Figure 1C. After letting the OP50 lawns dry over 2 days at room temperature, vehicle (H_2O), α-KB (4 mM, 10 mM, 100 mM), or copper was added to the top of the lawn and allowed to dry over 2 days at room temperature. Approximately 40–60 synchronized adult day 1 worms were placed onto the center of the plate and their preference for either bacterial lawn was recorded after 3 h at room temperature. Three plates per condition were assessed. Statistical analysis was performed using GraphPad Prism (t-test, two-tailed, two-sample unequal variance).

Measurement of mitochondrial respiration

Mitochondria were isolated from mouse liver as described[1]. The final mitochondrial pellet was resuspended in 30 µl of MAS buffer (70 mM sucrose, 220 mM mannitol, 10 mM KH_2PO_4, 5 mM $MgCl_2$, 2 mM HEPES, 1 mM EGTA, and 0.2% fatty acid free BSA, pH 7.2). Mitochondrial respiration was measured by running coupling and electron flow assays. For the coupling assay, MAS buffer supplemented with10 mM succinate and 2 µM rotenone, or 10 mM pyruvate and 2 mM malate (with or without 20 mM methyl pyruvate), or 10 mM glutamate and 10 mM malate (with or without 20 mM methyl pyruvate), or 10 mM methyl pyruvate and 2mM malate. Mitochondria in complete MAS buffer were seeded into a XF24 Seahorse plate by centrifugation at 2,000g for 20 min at 4 °C. Just before the assay, the mitochondria were supplemented with complete MAS buffer for a total of 500 µl (with Vehicle or α-KB), and warmed at 37 °C for 30 min before starting the OCR measurements. Mitochondrial respiration begins in a coupled state 2; state 3 is initiated by 2 mM ADP; state 4o (oligomycin insensitive, that is, complex V independent) is induced

by 2.5 μM oligomycin; and state 3u (FCCP-uncoupled maximal respiratory capacity) by 4 μM FCCP. Finally, 1.5 μg/mL antimycin A was injected at the end of the assay. For the electron flow assay, the MAS buffer was supplemented with 10 mM sodium pyruvate, 2 mM malate and 4 μM FCCP, and the mitochondria are seeded the same way as described for the coupling assay. After basal readings, the sequential injections were as follows: 2 μM rotenone (complex I inhibitor), 10 mM succinate (complex II substrate), 4 μM antimycin A (complex III inhibitor), and 10 mM/100 μM ascorbate/ tetramethylphenylenediamine (TMPD, complex IV substrate).

Measurement of oxygen consumption rates (OCR)

OCR measurements were made using a Seahorse XF-24 analyzer (Seahorse Bioscience). H9C2 Cells were seeded in Seahorse XF-24 cell culture microplates in DMEM media supplemented with 10% FBS and 10 mM glucose, and incubated at 37 °C and 5% CO2 overnight. Treatment with designated compounds was for 2 h. Cells were washed in unbuffered DMEM medium (pH 7.4, 10 mM glucose) just before measurements, and maintained in this buffer with indicated concentrations of α-KB. OCR was measured three times under basal conditions and normalized to protein concentration per well. Measurement of OCR in living *C. elegans* was carried out as follows. Wild-type day 1 adult N2 worms were placed on NGM plates containing 4 mM α-KB or H_2O (vehicle control). OCR was assessed on day 2 of adulthood. On day 2 of adulthood, worms were collected and washed four times with M9 to rid the samples of bacteria, and then the animals were in Seahorse XF-24 cell culture microplates (Seahorse Bioscience, V7-PS) in 200 μl M9 at ~100 worms per well. Oxygen consumption rates were measured seven

times under basal conditions and normalized to the number of worms counted per well. The experiment was repeated twice. Statistical analysis was performed using Microsoft Excel (t-test, two-tailed, two-sample unequal variance).

Complex I (NADH:ubiquinone oxidoreductase) assay

NADH:ubiquinone oxidoreductase activity was measured using MitoToxTM Complex I OXPHOS Activity Microplate Assay (Abcam, ab109903) according to manufacturer's instructions. Pyruvate dehydrogenase (PDH) and lactate dehydrogenase (LDH) enzyme activity assays. The enzyme activities were measured as described [4,5] using purified porcine heart PDH (Sigma, P7032-25UN) and purified rabbit LDH (Promega, G9071). 10 mM NaF is included to exclude the effect of enzyme phosphorylation for PDH assay.

Metabolic profile analysis

Cells were cultured for 24 h, rinsed with PBS, and medium containing [U-$^{13}C_6$]glucose, [U-$^{13}C_5$]glutamine, or [U-$^{13}C_{16}$]palmitate added. After 24 h culture, cells were rinsed with ice-cold 150 mM NH_4AcO (pH 7.3) followed by addition of 400 µL cold methanol and 400 µL cold water. Cells were scraped off, transferred to an Eppendorf tube, and 10 nmol norvaline as well as 400 µL chloroform added to each sample. For the metabolite extraction, samples were vortexed for 5 min on ice, spun down, and the aqueous layer transferred into a glass vial and dried. Metabolites were resuspended in 70% ACN, and 5 µL sample loaded onto a Phenomenex Luna 3u NH2 100A (150 x 2.0 mm) column. The chromatographic separation was performed on an UltiMate 3000RSLC (Thermo Scientific) with mobile phases A (5 mM NH_4AcO, pH 9.9) and B (ACN) and a flow rate of 300 µL/

min. The gradient ran from 15% A to 95% A over 18 min, 9 min isocratic at 95% A, and re-equilibration for 7 min. Metabolite detection was achieved with a Thermo Scientific Q Exactive mass spectrometer run in polarity switching mode (+3.0 kV / −2.25 kV). TraceFinder 3.1 (Thermo Scientific) was used to quantify metabolites as area under the curve using retention time and accurate mass measurements (⩽ 3 ppm). Relative amounts of metabolites were calculated by summing up all isotopomers of a given metabolite and were normalized to internal standard and cell number. Natural occurring ^{13}C was accounted for as described[6].

Cell Culture

H9C2 cells were cultured in glucose-free DMEM (Life technologies, 11966-025) supplemented with 10% fetal bovine serum (FBS) and 10 mM glucose. H9C2 cells were cultured at 37°C and 5% CO_2. Cells were transfected with indicated siRNA using DharmaFECT 1 Transfection Reagent by following the manufacturer's instructions. Knockdown efficiency was confirmed by Western blotting.

RNAi in *C. elegans*

RNAi in *C. elegans* was accomplished by feeding worms HT115 (DE3) bacteria expressing target-gene double-stranded RNA (dsRNA) from the pL4440 vector. dsRNA production was induced overnight on plates containing 1 mM isopropyl-b-D-thiogalactoside (IPTG). All RNAi feeding clones were obtained from the *C. elegans* ORF-RNAi Library (Thermo Scientific/Open Biosystems) unless otherwise stated. In lifespan experiments, we used RNAi to inactivate AAK- 2, UBL-5 and PDHB-1 in mature animals

in the presence or absence of exogenous α-KB. The concentration of α-KB used in these experiments (4 mM) was empirically determined to be most beneficial for wild-type animals (Figure 1C).

Assay for AMPK pathway activity in *C. elegans*

Wild-type N2 were grown at 20 °C from the L1 stage until L4. L4 worms were transferred onto NGM plates (55-mm diameter) with vehicle (water), 4mM α-KB, *pdhb-1* RANi bacteria. After one-day treatment, adult worms were washed from three plates using M9 buffer, followed by centrifuging at 1400 rpm for 1 min. After removing the supernatant, the worms were frozen in ~ 25 µl M9 buffer quickly in liquid nitrogen. Then the worm samples were stored at -80 °C. Before western blotting analysis, worms were thaw on ice and mixed with 2× sample loading buffer (50 mM Tris-Cl, pH 6.8, 2 mM EDTA, 4% glycerol, 4% SDS, bromophenol blue, 1X PIC) and sonicated at 50 sonics at 40 °C for 3 min and then boiled at 95 °C for 6 min. Cool samples on ice before load in 4-12% Bis-Tris gel. AMPK pathway activity in *C. elegans* treated with α-KB or *pdhb-1* knockdown was determined by the levels of phosphorylation of AMPK (T172) 6. Specific antibodies used: P-AMPKα T172 (Cell Signaling, 2535S), α-Tubulin (Sigma, T6199).

Assay for AMPK and mammalian TOR (mTOR) pathway activity

AMPK and mTOR pathway activity in cells treated with α-KB was determined by the levels of phosphorylation of AMPK (T172), AAC (S79), and S6K (T389). Specific antibodies used: phospho (P)-S6K T389 (Cell Signaling, 9234), S6K (Cell Signaling, 9202S), P-AMPKα T172 (Cell Signaling, 2535S), AMPKα (Cell Signaling, 2532S), P-ACC S79 (Cell

Signaling, 3661S), ACC (Cell Signaling, 3662S), GAPDH (Santa Cruz Biotechnology, 25778), DLAT (Thermofisher, PA5-29043), DLD (Thermofisher, PA5-27364), P-PDHA (Novus, NB110-93479), LDHA (Cell Signaling, 2012S), LDHB (Abcam, ab53292), PC(Abcam, ab126707), PKM1/2 (Cell Signaling, 3186s), and PDHA (Cell Signaling, 2784S).

Assay for cellular growth

H9C2 cells were seeded in 96-well plates at 2 x 10^3 cells per well and treated with indicated compound for 2 days. Cell number was measured using the CellTiter-Glo luminescent ATP assay (Promega, G7572); luminescence was read using Analyst HT (Molecular Devices).

Assay for NAD+/NADH

NAD+/NADH level is measured by NAD/NADH-GloTM Assay (Promega, G9071) with adapted protocol as described[5].

Isotopomer enrichment modeling

Isotopomer enrichment modeling was performed as described[7].

Supplemental References

1. Chin, R. M. et al. The metabolite alpha-ketoglutarate extends lifespan by inhibiting ATP synthase and TOR. Nature 510, 397-401, doi:10.1038/nature13264 (2014).

2. McColl, G. et al. Utility of an improved model of amyloid-beta (Abeta(1)(-)(4)(2)) toxicity in Caenorhabditis elegans for drug screening for Alzheimer's disease. Mol Neurodegener 7, 57, doi:10.1186/1750-1326-7-57 (2012).

3. Abada, E. A. et al. C. elegans behavior of preference choice on bacterial food. Mol. Cells 28, 209–213 (2009).

4. Supporting Aspartate Biosynthesis Is an Essential Function of Respiration in Proliferating Cells. Cell 162, 552-563, doi:10.1016/j.cell.2015.07.017 (2015).

5. Hinman, L. M. & Blass, J. P. An NADH-linked spectrophotometric assay for pyruvate dehydrogenase complex in crude tissue homogenates. J Biol Chem 256, 6583-6586 (1981).

6. Yuan, Jie, Bryson D. Bennett, and Joshua D. Rabinowitz. "Kinetic flux profiling for quantitation of cellular metabolic fluxes." Nature protocols 3.8 (2008): 1328.

7. Williams, K. J. et al. An essential requirement for the SCAP/SREBP signaling axis to protect cancer cells from lipotoxicity. Cancer Res 73, 2850-2862, doi:10.1158/0008-5472. CAN-13-0382-T (2013).

CHAPTER 3

Stimulation of hair regeneration by small molecules that activate autophagy

Abstract

Hair plays important roles, ranging from the conservation of body heat to the preservation of psychological well-being. Hair loss or alopecia affects millions worldwide, but methods that can be used to regrow hair are lacking. We report that quiescent (telogen) hair follicles can be stimulated to initiate anagen and hair growth by small molecules that activate autophagy, including the metabolites α-ketoglutarate (α-KG) and α-ketobutyrate (α-KB), and the prescription drugs rapamycin and metformin which impinge on mTOR and AMPK signaling. Stimulation of hair growth by these agents is blocked by specific autophagy inhibitors, suggesting a mechanistic link between autophagy and hair regeneration. Consistently, increased autophagy is detected upon anagen entry during the natural hair follicle cycle, and oral α-KB prevents hair loss in aged mice. Our finding, that anagen can be pharmacologically activated in telogen skin when natural anagen-inducing signal(s) are absent, has implications for the treatment of hair loss patients.

Introduction

The biological and psychological importance of hair is well recognized. Hair loss affects millions worldwide and can occur because of aging, hormonal dysfunction, autoimmunity, or as a side effect of cancer treatment. Mammalian hair growth consists of cyclic repetitions of telogen (quiescence), anagen (regeneration) and catagen (degeneration) phases of the hair follicle [1,2]. This hair follicle cycle is regulated by both intrinsic and extrinsic signals which control quiescence and activation of hair follicle stem cells (HFSC). Inadequate HFSC activation and proliferation underlie alopecia in numerous biological and pathological conditions, including aging [3,4,5,6]. Molecules that can promote HFSC activation and anagen initiation have been intensely searched for, as they may both help reveal how hair regeneration is regulated and provide therapeutic and cosmetic interventions. Here, we postulate that telogen hair follicles may be induced to enter anagen by pharmacologically triggering autophagy.

As a fundamental process for degrading and recycling cellular components, autophagy is critical for adaptation to nutrient starvation and other adverse environmental conditions as well as it is regulated by such signals [7,8]. Autophagy is also important for quality control of proteostasis through the elimination of misfolded or damaged proteins and damaged organelles. The loss of autophagy may be causally related to neurodegeneration and other diseases [9]. Autophagy declines with age [10,11], likely contributing to the higher prevalence of autophagy-related diseases (e.g., cancer and neurodegenerative diseases) in the elderly. Autophagic clearing of active, healthy mitochondria in hematopoietic stem

cells is required to maintain quiescence and stemness [12], and autophagy fulfills the nutrient demand of quiescent muscle stem cell activation [13].

In the skin, autophagy is required for self-renewal and differentiation of epidermal and dermal stem [14,15,16], but its role in hair follicle stem cells has remained controversial. On one hand, autophagy may be required for hair growth as skin grafts from the autophagy-related gene 7 (Atg7)-deficient mice exhibit abnormal hair growth [17]. On the other hand, Atg7-deficiency in epithelial cells of the skin and hair was reported to be compatible with growth of hair, although sebaceous glands were affected and male mutant mice developed an oily coat when they aged [18]. It was reported that psychological stress induced autophagy and delay of hair cycle [19].

Previously, alterations in intrinsic signaling, gene expression, and circadian function were implicated to prevent anagen entry in aged HFSC and result in alopecia [20,5,21]. The unforeseen finding that supplementation of a metabolite α-ketobutyrate (α-KB) in old mice can increase longevity and prevent alopecia [22] suggests that rejuvenating aging or aging associated deficiencies may restore HFSC function and hair growth in skin. We report herein that autophagy is increased during anagen phase of the natural hair follicle cycle and demonstrate that specific small molecules that induce autophagy can be used to promote anagen entry and hair growth from quiescent telogen phase.

Results

Induction of autophagy is mediated by some of the same cellular energy metabolism regulators which have been linked to or implicated in the effect of dietary restriction (DR) on longevity. We previously showed that the metabolite α-ketoglutarate (α-KG) is induced upon DR and mediates its longevity effect in *C. elegans*. α-KG also increases autophagy in both worms and cultured mammalian cells [23]. Here we tested whether α-KG can increase hair regeneration, using a commonly used in vivo C57BL/6J mouse dorsal skin model. We mainly tested topical treatment method as it is most easily translated to human patients. Minoxidil, a vasodilator used to treat pattern hair loss [24], was included for comparison as it has typically been used as a positive control in many papers on hair research (Figure S1A). Male mice at 6.5 weeks of age (postnatal day 44) were shaved on the back, when dorsal skin hair follicles are in telogen [1]. α-KG or vehicle control treatment was applied topically every other day. α-KG treatment drastically enhances hair regeneration (Figure 1A-B). Anagen in black mice is macroscopically recognizable by the melanin pigment visible through the skin, as the melanogenic activity of follicular melanocytes is strictly coupled to the anagen stage of the hair cycle [25]. In the experiment shown in Figure 1B, skin pigmentation was visible by day 12 post-treatment with α-KG (Figure 1C). In contrast, in vehicle-treated control mice no pigmentation or only a few scattered pigmented spots were apparent at least until day 39, when animals were sacrificed for histological and biochemical analyses. Hair grew from the pigmented skin area of α-KG treated mice within 5~7 days, and by day 39 post-treatment α-KG treated mice exhibited robust hair growth; in contrast, control mice showed little or no hair growth overall (Figure 1B). The effects of α-KG on anagen initiation and hair regeneration were even more dramatic when mice were treated later in telogen at 8 weeks of age (Figure

S1B-C). α-KG stimulation of hair growth is gender-independent; α-KG exhibited similar hair stimulating effects in female mice (Figure S1D).

Formation and differentiation of hair follicles in α-KG treated mice were correspondingly demonstrated by histological analyses (Figure 1D). More follicles and high proliferation marker Ki-67 expression were observed in α-KG treatment group, showing anagen phase induction (Figure 1D). In telogen skin, α-KG initiated new anagen waves as early as day 7 post-treatment. Since inflammation and wound repair are known to stimulate tissue, including hair regeneration [26], our study only focused on molecules that do not cause skin damage or other abnormal skin conditions. There was no evidence of skin irritation or inflammation by α-KG or other small molecule treatments described in this study (unless otherwise indicated) as per visual inspection and confirmed by IL-6 and F4/80 staining (Figure 1D and Figure S1E).

Mice of the same age as those used for regeneration experiments were also acutely treated and analyzed for early biochemical changes. Increased autophagy induction in the α-KG treated mouse skin was supported by western blot analysis of LC3 [27], both at 24 h and 5 days post-treatment (Figure 1E). Expression of the autophagy substrate p62/SQSTM1, which is widely used as an indicator of autophagic degradation, was also increased with autophagy induction by α-KG in the mouse skin (Figure 1E) as well as by rapamycin induced autophagy (see below). This is likely due to compensation through upregulation of p62 transcription (Figure S1F), as was reported for p62 during prolonged starvation [28].

Longevity increase by α-KG was found to be mediated, at the molecular level, through direct inhibition of the highly conserved mitochondrial ATP synthase/ATPase (complex V) and subsequent decrease of target of rapamycin (TOR) activity downstream [23]. We tested whether hair regeneration by α-KG may also be mediated by ATP synthase inhibition. Consistent with this mechanism, topical treatment with the complex V inhibitor oligomycin similarly promoted hair regeneration in both male (Figure 2A-D) and female (Figure S1D) mice. Also, like α-KG, oligomycin treatment results in TOR inhibition and autophagy activation [23]. Here we also detected increased autophagy in topical oligomycin treated mouse skin as indicated by LC3 expression (Figure 2E).

The target of rapamycin (TOR) protein is a main mediator of the effect of DR in longevity. Inhibition of TOR, e.g., by rapamycin, elicits autophagy. We therefore asked whether rapamycin may also increase hair regeneration. As shown in Figure 2F-I and Figure S2, topical rapamycin treatment accelerated hair regeneration, both visually and histologically. Autophagic LC3, p62, and mTOR-dependent phosphorylated Beclin 1 S14 [29,30] were increased in rapamycin treated mouse telogen skin (Figure 2E). Consistently, Beclin 1 S14 phosphorylation was also increased in mouse skin by day 5 post-treatment with α-KG (Figure 1E) and oligomycin (Figure 2E). Together, these results show that hair regeneration can be accelerated by either indirect or direct inhibition of TOR pathway activity and induction of autophagy.

AMP-activated protein kinase (AMPK) is another common downstream effector of α-KG and oligomycin [23]. AMPK, a key cellular energy sensor, is activated by decreases in

cellular energy charge, e.g., upon glucose starvation and many other cellular stress conditions [31,32]. AMPK also elevates autophagy [8]. Consistent with this understanding, AMPK-dependent Beclin 1 phosphorylation on S91 [33] was increased in mouse skin treated with α-KG and oligomycin (Figures 1E and 2E). Further, as shown in Figure 3A-D, anagen induction and hair regeneration were also stimulated by topical treatment with the AMPK activator, 5-aminoimidazole-4-carboxamide ribonucleotide (AICAR), an AMP analog. Metformin, another agonist of AMPK [34], has been widely used as a diabetes drug and was the first drug approved for human anti-aging studies [35,36]. Here we show that topical metformin similarly induced autophagy and hair regeneration (Figure 3E-H). Interestingly, although metformin has not been used to study hair growth or treat hair loss, decreased hair loss in polycystic ovary syndrome patients treated with metformin tablets has been documented [37,38].

Mechanistically, metformin has been shown to inhibit mitochondrial complex I in the electron transport chain [39,40]. Interestingly, long-lived *C. elegans* mitochondrial mutants accumulate various alpha-keto acid metabolites in the exometabolome [41]. We previously found that one of these compounds, α-ketobutyrate (α-KB), extends the lifespan and alleviates many aging-related symptoms in the aged mice [22]. α-KB supplementation in drinking water over 30 weeks greatly improved hair coating in old mice (Figure 3I-J). However, in pilot experiments testing topical treatments on aged mice, topical α-KB treatment only moderately promoted hair growth in shaved aged animals, whereas topical α-KG or rapamycin did not visibly increase (or even slightly decreased, if it changed at all) hair regeneration (data not shown). In contrast, in young mice, like α-KG and rapamycin

treatments, topical α-KB treatment substantially induced skin pigmentation and hair regeneration (Figure 3K-M). Autophagy was also induced, as indicated by elevated LC3 and phosphorylated Beclin 1 in the treated skin (Figure 3N).

mTOR has previously been reported to be required for HFSC activation and anagen entry [20,42,43]. However, our results above indicate that moderate inhibition of mTOR by rapamycin accompanied by autophagy induction stimulates hair regeneration. Such a dichotomy may also exist for mitochondrial regulation. Mitochondrial respiration is required for HFSC cycle and yet genetic perturbation of mitochondrial function abolishes hair regeneration [44,45,46]. Our finding that the well-established complex V inhibitor oligomycin in fact promotes hair regeneration suggested that possibly, as in lifespan regulation, mild mitochondrial inhibition may prove to be beneficial. Since mitochondrial complex V acts upstream of TOR from *C. elegans* to Drosophila and humans [23,47,48], and autophagy is induced both by mitochondrial complex V inhibition and by TOR inhibition (Figure 2E), we decided to determine if autophagy induction alone may be sufficient to elicit hair regeneration.

We took advantage of a TOR-independent autophagy inducing small molecule, SMER28 [49], to test our hypothesis that autophagy induction alone would elicit hair regeneration. Topical SMER28 administration increased autophagic induction of LC3 and p62 in mouse dorsal skin (Figure 4A-B, and Figure S1F). The level of Beclin 1 Ser14 phosphorylation, which depends on mTOR [29], was not increased in SMER28-treated skin (Figure 4B), indicating an mTOR-independent autophagy-inducing effect by SMER28. Additionally,

SMER28 did not appear to induce autophagy by impinging on AMPK, as Beclin 1 S91 phosphorylation was also not increased in SMER28-treated skin (Figure 4B). Strikingly, SMER28 also greatly induced hair regeneration (Figure 4C). These findings strongly support the role of autophagy in promoting hair regeneration. To examine whether autophagy is necessary for SMER28-stimulated hair regeneration, we employed autophinib, which inhibits VPS34 and autophagosome formation [50]. Co-treatment with autophinib prevented hair regeneration by SMER28 (Figure 4D), indicating a critical role of autophagy in hair regeneration. Likewise, autophagy is also necessary for the stimulation of hair regeneration by α-KG (Figure S3) as shown by co-treatments with autophinib, as well as with bafilomycin A1, which disrupts autophagic flux by inhibiting vacuolar H(+)-ATPase (V-ATPase)-dependent acidification and Ca-P60A/SERCA-dependent autophagosome-lysosome fusion [51].

In summary, we showed that inducing autophagy is necessary and sufficient to initiate hair follicle activation and hair regeneration. To understand whether autophagy may be integral to the natural hair follicle cycle, we followed autophagy over different hair follicle stages. We discovered that indeed autophagy is elevated as hair follicle progresses naturally through anagen; autophagy decreases in catagen and remains low in telogen (Figure 5). These data indicate a biological role of autophagy in normal hair growth initiation and elongation. Consistent with this idea, autophagy has been implicated in maintaining anagen, as autophagy inhibition by knocking down ATG5 in ex vivo human anagen hair follicles prematurely induces catagen [52]. It remains open which cells are critical for the stimulating effects of the hair regeneration agents. In anagen, hair matrix

keratinocytes of organ-cultured human hair follicles exhibit an active autophagic flux [52]. As it was postulated that human dermal adipocytes adjacent to catagen hair follicles undergo autophagic degradation of intracellular lipid droplets, communication between hair follicles and dermal white adipose tissue may also be important for hair regeneration[53].

Discussion

The regulation of hair regeneration by microenvironment, including Wnt, BMP, JAK-STAT, Treg, interleukin-2 receptor signaling, has been widely studied, but little is known about its regulation by intracellular metabolic signals [26,54,6]. Previously cellular redox [44], mitochondrial integrity and energy production [45,46] have been shown to be involved in HFSC activation during normal hair growth cycles which are impaired or dysregulated during aging. Here we have shown that simply treating telogen skin with specific autophagy-inducing small molecules is sufficient to establish anagen and promote hair regeneration.

Rapid anagen entry on whole dorsal telogen skin was observed from time to time among mice treated with α-KG, oligomycin, rapamycin, and SMER28, but never in α-KB, metformin, or AICAR-treated mice, nor in vehicle control mice. Temporally, pigmentation (anagen entry) induction by α-KB, AICAR, or metformin takes much longer, e.g., on a time scale of 12~18 days, as compared to 5~14 days by α-KG, oligomycin, or rapamycin.

It is possible that this may reflect a differential effect by mTOR inhibition and by AMPK activation on the regulation of autophagy; these possibilities remain to be examined. The crosstalk between metabolism and autophagy is complex [8]. Autophagy is generally induced by limitations in ATP availability or a lack of essential nutrients, including glucose and amino acids, yet ATP is required for autophagy. Starvation and ensuing decreased energy charge and increased ROS levels are potent activators of autophagy. Recently it was reported that calorie restriction also promotes hair follicle growth and retention in mice [55] but the underlying mechanism was unclear. It is tempting to speculate that this effect of calorie restriction on hair growth may also be mediated through autophagy activation. In line with this idea, it is conceivable that molecules like α-KG, rapamycin and metformin – which may function as calorie restriction (or dietary restriction) mimetics – decrease energy metabolism, reducing skin temperature and inducing hair growth as a defense mechanism against heat loss.

Autophagy has been linked to longevity, but the underlying mechanisms are unclear. Although autophagy alone may not be sufficient for lifespan increase, many longevity pathways at least partially depend on induction of autophagy to increase lifespan [56,57] and life- and health-span extension in mice with increased basal autophagy was recently reported [58]. Disrupted autophagy has been linked to neurodegenerative diseases, cancer, and other age-related disorders. Given the conservation in energy metabolism and autophagy machinery, induction of hair regeneration by autophagy activation discovered in mice herein should translate to humans. Although it has not been tested in human hair

regeneration studies, autophagy has been shown to be essential to maintaining growth of an ex vivo human scalp hair follicle organ culture [59].

It also remains to be studied whether the same autophagy modulators could be useful for treating hair loss patients. Our data show stimulation of hair regeneration in the telogen phase, but have not been tested for hair regeneration in alopecia. Although our study did not use a model for alopecia, the findings are relevant to hair loss in the following way. First, hair regeneration, which occurs cyclically under normal conditions but fails in alopecia, would require reactivation of dormant hair follicle stem cells. In our experiments, because mice were shaved in telogen, all hair follicles from the previous cycle were in a resting phase. We find that pharmacological induction of autophagy is sufficient to activate these quiescent telogen hair follicles – when natural anagen-inducing signal(s) are absent – and initiate new anagen and hair regeneration. This suggests that hair loss, e.g., due to lengthened telogen phase, shortened anagen phase, and/or hampered anagen induction, may also be rescued by pharmacologically activating autophagy. Further consistent with this idea, increased autophagy is detected upon anagen entry during the natural hair follicle cycle and aged mice fed the autophagy- and anagen-inducing metabolite α-KB are protected from hair loss.

Figure Legends

Figure 1. Hair regeneration is induced by topical treatment with α-KG. See also Figure S1.

(**A**) Structure of α-KG.

(**B**) α-KG induces hair regeneration. Male mice were shaved on postnatal day 44 (telogen) and topically treated with vehicle control (DMSO in ~250 μL PLO Base) or α-KG (dissolved in DMSO and then added to ~250 μL PLO Base at 32 mM final) every other day over 39 days. Melanin pigmentation in the skin of α-KG treated animals, indicative of anagen induction by the treatment, became visible as early as on day 12; vehicle-treated mice did not show significant pigmentation for at least 39 days. Hair growth from the pigmented skin areas of α-KG treated mice was visible within 5~7 days. Photographs shown were taken on day 39 post-treatment, by which time mice treated with α-KG exhibited overall hair growth whereas control mice still had no hair generally except for random hair patches on some animals. Total number of animals: control (26), α-KG (28). Similar effects by α-KG were seen in female mice (shown in Figure S1D).

(**C**) Quantification for appearance of melanin pigmentation (indicating onset of anagen) in mouse skin treated with α-KG vs. control. Pigmentation scoring is described in Methods. Number of animals shown in (A): control (4), α-KG (4). Data are represented as mean ± standard deviation (s.d.).

(**D**) Microphotographs of hematoxylin and eosin (H&E) stained skin tissue sections from mice treated with 32 mM α-KG, showing new hair follicles and enlarged bulbs, elongated hair shafts, and thickened dermal layers. Hematoxylin is a basic dye that stains nucleic acids purplish blue; eosin is an acidic dye that stains cytoplasm and extracellular matrix (e.g., collagen) pink. Immunohistochemistry for Ki-67, a marker for cell proliferation [57], further demonstrated the formation of new hair follicles. IL-6 and F4/80 are inflammatory cytokine and macrophage markers, respectively [60,61]. Controls for IL-6 and F4/80 positive

inflammatory skin are shown in Figure S1E. Scale bars for H&E, 1 mm; Ki-67, IL-6 and F4/80, 400 μm.

(**E**) Induction of autophagy associated markers, including LC3, p62, and phosphorylated Beclin 1, in telogen skin of mice treated with α-KG for 6 h, 24 h, and 5 days. Skin remained in telogen during the treatment period as confirmed by the lack of skin pigmentation. Each lane is from a different animal. Number of animals: 4 for each treatment.

Figure 2. Hair regeneration is induced by topical treatment with oligomycin and rapamycin. See also Figure S2.

(**A**) Structure of oligomycin.

(**B**) Oligomycin (100 μM) induces hair regeneration. Male mice were shaved on postnatal day 44 and topically treated every other day. Photographs shown were taken on day 23 post-treatment. Number of animals: control (23), oligomycin (23). Similar effects by oligomycin were seen in female mice (Figure S1D).

(**C**) Quantification for appearance of melanin pigmentation in mouse skin treated with oligomycin vs. control. Number of animals: control (3), oligomycin (3). Data are represented as mean ± s.d..

(**D**) Microphotographs of H&E and Ki-67 stained skin tissue section from mice treated with 100 μM oligomycin. Scale bars for H&E, 1 mm; Ki-67, 400 μm.

(**E**) Western blot analysis of autophagy related markers in telogen skin of mice treated 5 days with indicated compounds. Ctrl, control; Oligo, oligomycin; Rapa, rapamycin.

(**F**) Structure of rapamycin.

(**G**) Rapamycin (1.6 μM) induces hair regeneration. Male mice were shaved on postnatal day 43 and treated topically every other day. Photographs were taken on day 37 post-treatment. Number of animals: control (18), rapamycin (17). Rapamycin at 100 nM gave similar results as 1.6 μM (Figure S2). Similar effects by rapamycin were seen in female mice (Figure S2B). Rapamycin at 16 μM, however, resulted in hair loss and open wounds (data not shown), consistent with a previous vascular grafts study in rats receiving high dose rapamycin [62]; this may be due to more severe inhibition of mTOR which was reported to be required for HFSC activation [20,42,43].

(**H**) Quantification for appearance of melanin pigmentation in mouse skin treated with rapamycin (1.6 μM) vs. control. Number of animals: control (3), rapamycin (3). Data are represented as mean ± s.d..

(**I**) Microphotographs of H&E and Ki-67 stained skin tissue section from mice shown in (G). Scale bars for H&E, 1 mm; Ki-67, 400 μm.

Figure 3. Hair regeneration is induced by AICAR, metformin and α-KB.

(**A**) Structure of AICAR.

(**B**) AICAR (16 mM) induces hair regeneration. Male mice were shaved on postnatal day 44 and treated topically every other day. Photographs were taken on day 41 post-treatment. Number of animals: control (11), AICAR (9). Similar effects in females (not shown).

(**C**) Quantification for skin pigmentation in mice from (B). Number of animals: control (3), AICAR (3). Data are represented as means ± s.d..

(**D**) H&E and Ki-67 stained skin tissue section from mice treated with 16 mM AICAR. Scale bars for H&E, 1 mm; Ki-67, 400 μm.

(**E**) Structure of metformin.

(**F**) Metformin (160 mM) induces hair regeneration. Male mice were shaved on postnatal day 43 and treated topically every other day with metformin or vehicle control (H_2O in this experiment). Photographs were taken on day 48 post-treatment. Number of animals: control (13), metformin (12). Similar effects in females (not shown).

(**G**) Quantification for skin pigmentation in mice from (F). Number of animals: control (3), metformin (3). Data are represented as means ± s.d..

(**H**) H&E and Ki-67 stained skin tissue section from mice shown in (F). Scale bars for H&E, 1 mm; Ki-67, 400 μm.

(**I**) Structure of α-KB.

(**J**) Oral α-KB (8 mM in drinking water) treatment negates hair loss in aged female mice. Photo was taken at 131 weeks of age. Number of animals: control (5), α-KB (5).

(**K**) Topical α-KB (32 mM) induces hair regeneration in young male mice. Mice were shaved on postnatal day 44 and treated topically every other day. Photographs were taken on day 39 post-treatment. Number of animals: control (18), α-KB (18). Similar effects in females (not shown).

(**L**) Quantification for skin pigmentation in mice from (K). Number of animals: control (4), α-KB (4). Data are represented as means ± s.d..

(**M**) H&E and Ki-67 stained skin tissue section from mice treated with 32 mM α-KB. Scale bars for H&E, 1 mm; Ki-67, 400 μm.

(**N**) Western blot analysis of autophagy related markers in telogen skin of mice treated 5 days with indicated compounds.

Figure 4. SMER28 induces hair regeneration in an autophagy-dependent manner. See also Figure S3.

(**A**) Structure of SMER28.

(**B**) Western blot analysis of autophagy related markers in telogen skin of mice treated 5 days with 1 mM SMER28. Each lane is from a separate mouse.

(**C**) Male mice were shaved on postnatal day 45 and treated daily with 1 mM SMER28; photographs were taken on day 23 post-treatment. Every other day treatment demonstrated similar results (not shown). Number of animals: control (6), SMER28 (6). Similar effects were observed in females (not shown).

(**D**) SMER28 (2 mM) induced hair regeneration is inhibited by co-treatment with autophinib (4 mM). Mice were shaved on postnatal day 51 and topically treated every other day. Photographs were taken on day 20 post-treatment; histology of corresponding skin tissue section was shown. Scale bars for H&E, 1 mm; Ki-67, 400 μm. Number of animals: control (20), SMER28 (16), SMER28 + autophinib (7), autophinib (7).

Figure 5. Autophagy levels are indicative of hair follicle cycle stages, increased upon anagen induction.

Mice were shaved on postnatal day 93 for males and on postnatal day 92 for females and monitored for hair cycle progression. Mice at each indicated stage were sacrificed for Western blot analysis of autophagy markers. T, telogen; A, anagen; C, catagen.

References

1. Muller-Rover, S., *et al.* (2001). "A comprehensive guide for the accurate classification of murine hair follicles in distinct hair cycle stages." *J Invest Dermatol* 117(1): 3-15.

2. Schneider, M. R., *et al.* (2009). "The hair follicle as a dynamic miniorgan." *Curr Biol* 19(3): R132-142.

3. Gilhar, A., *et al.* (2012). "Alopecia areata." *N Engl J Med* 366(16): 1515-1525.

4. Petukhova, L., *et al.* (2010). "Genome-wide association study in alopecia areata implicates both innate and adaptive immunity." *Nature* 466(7302): 113-117.

5. Keyes, B. E., *et al.* (2013). "Nfatc1 orchestrates aging in hair follicle stem cells." *Proc Natl Acad Sci* U S A 110(51): E4950-4959.

6. Chueh, S. C., *et al.* (2013). "Therapeutic strategy for hair regeneration: hair cycle activation, niche environment modulation, wound-induced follicle neogenesis, and stem cell engineering." *Expert Opin Biol Ther* 13(3): 377-391.

7. Ohsumi, Y. (2014). "Historical landmarks of autophagy research." *Cell Res* 24(1): 9-23.

8. Galluzzi, L., *et al.* (2014). "Metabolic control of autophagy." *Cell* 159(6): 1263-1276.

9. Mizushima, N., *et al.* (2008). "Autophagy fights disease through cellular self-digestion." *Nature* 451(7182): 1069-1075.

10. Cuervo, A. M. and J. F. Dice (2000). "Age-related decline in chaperone-mediated autophagy." *J Biol Chem* 275(40): 31505-31513.

11. Levine, B. and G. Kroemer (2008). "Autophagy in the pathogenesis of disease." *Cell* 132(1): 27-42.

12. Ho, T. T., *et al.* (2017). "Autophagy maintains the metabolism and function of young and old stem cells." *Nature* 543(7644): 205-210.

13. Tang, A. H. and T. A. Rando (2014). "Induction of autophagy supports the bioenergetic demands of quiescent muscle stem cell activation." *Embo Journal* 33(23): 2782-2797.

14. Salemi, S., *et al.* (2012). "Autophagy is required for self-renewal and differentiation of adult human stem cells." *Cell Res* 22(2): 432-435.

15. Belleudi, F., *et al.* (2014). "FGF7/KGF regulates autophagy in keratinocytes: A novel dual role in the induction of both assembly and turnover of autophagosomes." *Autophagy* 10(5): 803-821.

16. Chikh, A., *et al.* (2014). "iASPP is a novel autophagy inhibitor in keratinocytes." *J Cell Sci* 127(Pt 14): 3079-3093.

17. Yoshihara, N., *et al.* (2015). "The significant role of autophagy in the granular layer in normal skin differentiation and hair growth." *Arch Dermatol Res* 307(2): 159-169.

18. Rossiter, H., *et al*. (2018). "Inactivation of autophagy leads to changes in sebaceous gland morphology and function." *Exp Dermatol* 27(10): 1142-1151.

19. Wang, L., *et al.* (2015). "Oxidative stress and substance P mediate psychological stress-induced autophagy and delay of hair growth in mice." *Arch Dermatol Res* 307(2): 171-181.

20. Castilho, R. M., *et al.* (2009). "mTOR mediates Wnt-induced epidermal stem cell exhaustion and aging." *Cell Stem Cell* 5(3): 279-289.

21. Solanas, G., *et al.* (2017). "Aged Stem Cells Reprogram Their Daily Rhythmic Functions to Adapt to Stress." *Cell* 170(4): 678-692 e620.

22. Huang, J., *et al.* (2016). Ketobutyrate compounds and compositions for treating age-related symptoms and diseases. Google Patents, Google Patents.

23. Chin, R. M., *et al.* (2014). "The metabolite alpha-ketoglutarate extends lifespan by inhibiting ATP synthase and TOR." *Nature* 509(7505): 397-401.

24. Messenger, A. G. and J. Rundegren (2004). "Minoxidil: mechanisms of action on hair growth." *Br J Dermatol* 150(2): 186-194.

25. Slominski, A. and R. Paus (1993). "Melanogenesis is coupled to murine anagen: toward new concepts for the role of melanocytes and the regulation of melanogenesis in hair growth." *J Invest Dermatol* 101(1 Suppl): 90S-97S.

26. Ito, M., *et al.* (2007). "Wnt-dependent de novo hair follicle regeneration in adult mouse skin after wounding." *Nature* 447(7142): 316-320.

27. Kabeya, Y., *et al.* (2000). "LC3, a mammalian homologue of yeast Apg8p, is localized in autophagosome membranes after processing." *EMBO J* 19(21): 5720-5728.

28. Sahani, M. H., *et al.* (2014). "Expression of the autophagy substrate SQSTM1/p62 is restored during prolonged starvation depending on transcriptional upregulation and autophagy-derived amino acids." *Autophagy* 10(3): 431-441.

29. Russell, R. C., *et al.* (2013). "ULK1 induces autophagy by phosphorylating Beclin-1 and activating VPS34 lipid kinase." *Nat Cell Biol* 15(7): 741-750.

30. Liang, X. H., *et al.* (1999). "Induction of autophagy and inhibition of tumorigenesis by beclin 1." *Nature* 402(6762): 672-676.

31. Hardie, D. G., *et al.* (2012). "AMPK: a nutrient and energy sensor that maintains energy homeostasis." *Nat Rev Mol Cell Biol* 13(4): 251-262.

32. Zhang, C. S., *et al.* (2017). "Fructose-1,6-bisphosphate and aldolase mediate glucose sensing by AMPK." *Nature* 548(7665): 112-116.

33. Kim, J., *et al.* (2013). "Differential regulation of distinct Vps34 complexes by AMPK in nutrient stress and autophagy." *Cell* 152(1-2): 290-303.

34. Burkewitz, K., *et al.* (2014). "AMPK at the nexus of energetics and aging." *Cell Metab* 20(1): 10-25.

35. Knowler, W. C., *et al.* (2002). "Reduction in the incidence of type 2 diabetes with lifestyle intervention or metformin." *N Engl J Med* 346(6): 393-403.

36. Barzilai, N., *et al.* (2016). "Metformin as a Tool to Target Aging." *Cell Metab* 23(6): 1060-1065.

37. Ou, H. T., *et al.* (2016). "Metformin improved health-related quality of life in ethnic Chinese women with polycystic ovary syndrome." *Health Qual Life Outcomes* 14(1): 119.

38. Shahebrahimi, K., *et al.* (2016). "Comparison clinical and metabolic effects of metformin and pioglitazone in polycystic ovary syndrome." *Indian J Endocrinol Metab* 20(6): 805-809.

39. Owen, M. R., *et al.* (2000). "Evidence that metformin exerts its anti-diabetic effects through inhibition of complex 1 of the mitochondrial respiratory chain." *Biochem J* 348 Pt 3: 607-614.

40. Wheaton, W. W., *et al.* (2014). "Metformin inhibits mitochondrial complex I of cancer cells to reduce tumorigenesis." *Elife* 3: e02242.

41. Butler, J. A., *et al.* (2010). "Long-lived mitochondrial (Mit) mutants of Caenorhabditis elegans utilize a novel metabolism." *FASEB J* 24(12): 4977-4988.

42. Kellenberger, A. J. and M. Tauchi (2013). "Mammalian target of rapamycin complex 1 (mTORC1) may modulate the timing of anagen entry in mouse hair follicles." *Exp Dermatol* 22(1): 77-80.

43. Deng, Z., *et al.* (2015). "mTOR signaling promotes stem cell activation via counterbalancing BMP-mediated suppression during hair regeneration." *J Mol Cell Biol* 7(1): 62-72.

44. Hamanaka, R. B., *et al.* (2013). "Mitochondrial reactive oxygen species promote epidermal differentiation and hair follicle development." *Sci Signal* 6(261): ra8.

45. Shyh-Chang, N., *et al.* (2013). "Lin28 enhances tissue repair by reprogramming cellular metabolism." *Cell* 155(4): 778-792.

46. Kloepper, J. E., *et al.* (2015). "Mitochondrial function in murine skin epithelium is crucial for hair follicle morphogenesis and epithelial-mesenchymal interactions." *J Invest Dermatol* 135(3): 679-689.

47. Sun, X., *et al.* (2014). "A mitochondrial ATP synthase subunit interacts with TOR signaling to modulate protein homeostasis and lifespan in Drosophila." *Cell Rep* 8(6): 1781-1792.

48. Fu, X., *et al.* (2015). "2-Hydroxyglutarate Inhibits ATP Synthase and mTOR Signaling." *Cell Metab* 22(3): 508-515.

49. Sarkar, S., *et al.* (2007). "Small molecules enhance autophagy and reduce toxicity in Huntington's disease models." *Nat Chem Biol* 3(6): 331-338.

50. Robke, L., *et al.* (2017). "Phenotypic Identification of a Novel Autophagy Inhibitor Chemotype Targeting Lipid Kinase VPS34." *Angew Chem Int Ed Engl* 56(28): 8153-8157.

51. Mauvezin, C. and T. P. Neufeld (2015). "Bafilomycin A1 disrupts autophagic flux by inhibiting both V-ATPase-dependent acidification and Ca-P60A/SERCA-dependent autophagosome-lysosome fusion." *Autophagy* 11(8): 1437-1438.

52. Parodi, C., *et al.* (2018). "Autophagy is essential for maintaining the growth of a human (mini-)organ: Evidence from scalp hair follicle organ culture." *PLoS Biol* 16(3): e2002864.

53. Nicu, C., *et al.* (2019). "Do human dermal adipocytes switch from lipogenesis in anagen to lipophagy and lipolysis during catagen in the human hair cycle?" *Exp Dermatol* **28**(4): 432-435.

54. Harel, S., *et al.* (2015). "Pharmacologic inhibition of JAK-STAT signaling promotes hair growth." *Sci Adv* 1(9): e1500973.

55. Forni, M. F., *et al.* (2017). "Caloric Restriction Promotes Structural and Metabolic Changes in the Skin." *Cell Rep* 20(11): 2678-2692.

56. Jia, K. and B. Levine (2007). "Autophagy is required for dietary restriction-mediated life span extension in C. elegans." *Autophagy* 3(6): 597-599.

57. Hansen, M., *et al.* (2008). "A role for autophagy in the extension of lifespan by dietary restriction in C. elegans." *PLoS Genet* 4(2): e24.

58. Fernandez, A. F., *et al.* (2018). "Disruption of the beclin 1-BCL2 autophagy regulatory complex promotes longevity in mice." *Nature* 558(7708): 136-140.

59. Magerl, M., *et al.* (2001). "Patterns of proliferation and apoptosis during murine hair follicle morphogenesis." *J Invest Dermatol* 116(6): 947-955.

60. Hirano, T., *et al.* (1990). "Biological and clinical aspects of interleukin 6." *Immunol Today* 11(12): 443-449.

61. Wang, H., *et al.* (2006). "Activated macrophages are essential in a murine model for T cell-mediated chronic psoriasiform skin inflammation." *J Clin Invest* 116(8): 2105-2114.

62. Walpoth, B. H., *et al.* (2001). "Prevention of neointimal proliferation by immunosuppression in synthetic vascular grafts." *Eur J Cardiothorac Surg* 19(4): 487-492.

Figure 1

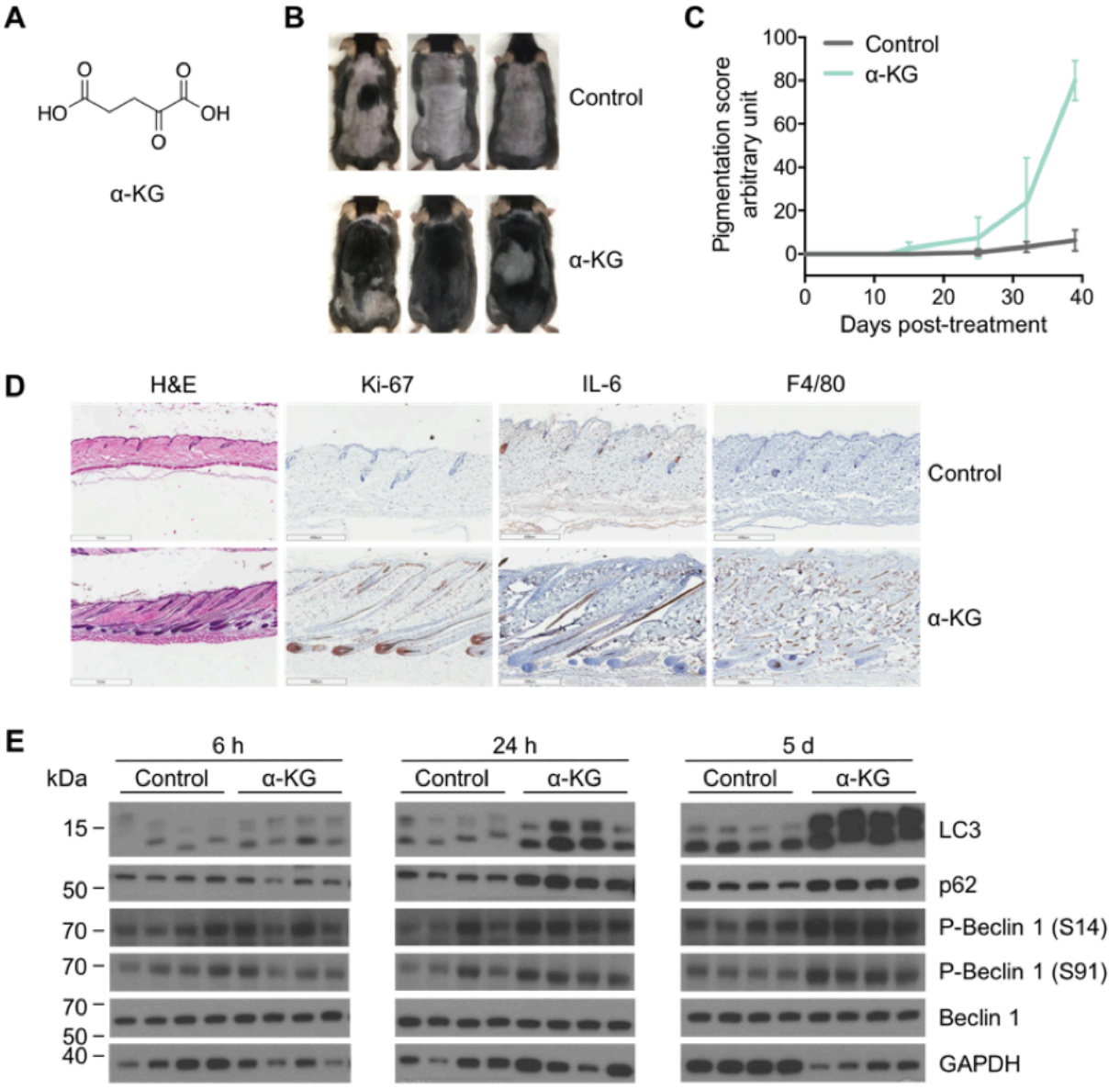
A
HO
O
O
O
OH
O
α-KG
B
Control
α-KG
C
Control
α-KG
Pigmentation score
arbitrary unit
100
80
60
40
20
0
0
10
20
30
40
Days post-treatment
D
H&E
Ki-67
IL-6
F4/80
Control
α-KG
E
6 h
24 h
5 d
kDa
Control
α-KG
Control
α-KG
Control
α-KG
15
50
70
70
70
50
40
LC3
p62
P-Beclin 1 (S14)
P-Beclin 1 (S91)
Beclin 1
GAPDH

Figure 2

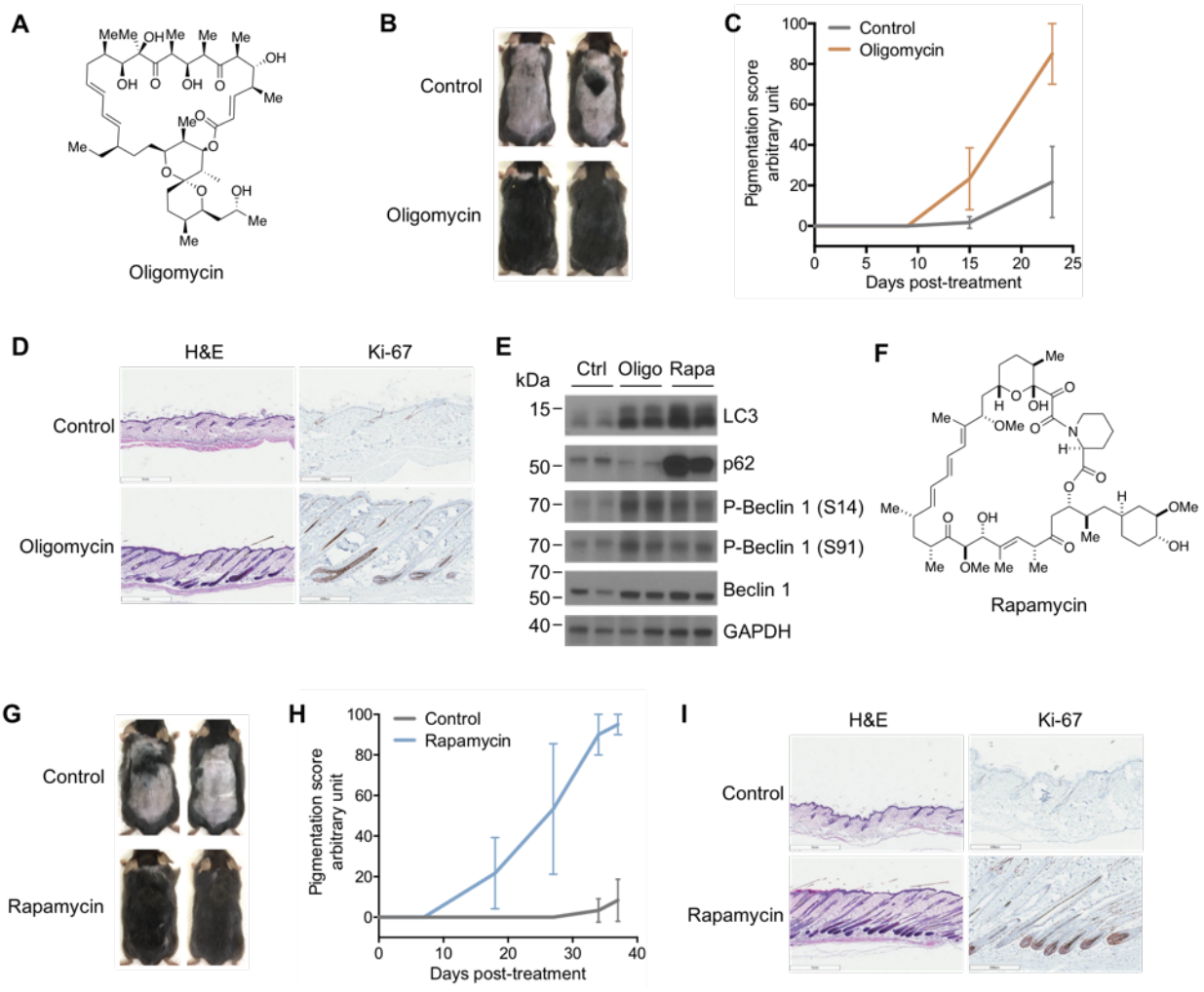
A
Oligomycin
B
Control
Oligomycin
C
Control
Oligomycin
Pigmentation score arbitrary unit
Days post-treatment
D
H&E
Ki-67
Control
Oligomycin
E
kDa
Ctrl Oligo Rapa
LC3
p62
P-Beclin 1 (S14)
P-Beclin 1 (S91)
Beclin 1
GAPDH
F
Rapamycin
G
Control
Rapamycin
H
Control
Rapamycin
Pigmentation score arbitrary unit
Days post-treatment
I
H&E
Ki-67
Control
Rapamycin

Figure 3

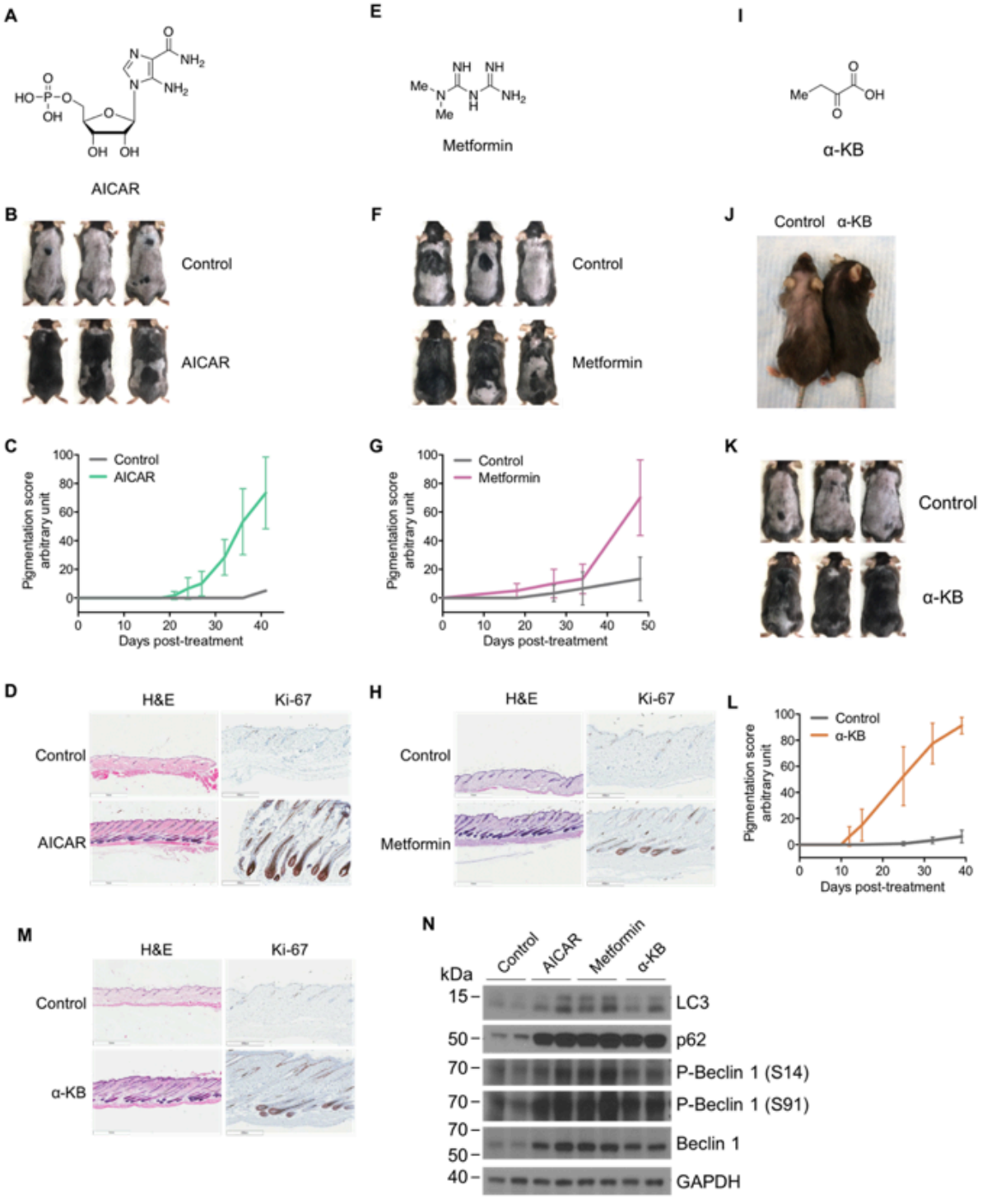
A
AICAR
E
Metformin
I
α-KB
B
Control
AICAR
F
Control
Metformin
J
Control α-KB
C
Control
AICAR
Pigmentation score arbitrary unit
Days post-treatment
G
Control
Metformin
Pigmentation score arbitrary unit
Days post-treatment
K
Control
α-KB
D
H&E
Ki-67
Control
AICAR
H
H&E
Ki-67
Control
Metformin
L
Control
α-KB
Pigmentation score arbitrary unit
Days post-treatment
M
H&E
Ki-67
Control
α-KB
N
kDa
Control
AICAR
Metformin
α-KB
15
LC3
50
p62
70
P-Beclin 1 (S14)
70
P-Beclin 1 (S91)
70
50
Beclin 1
40
GAPDH

Figure 4

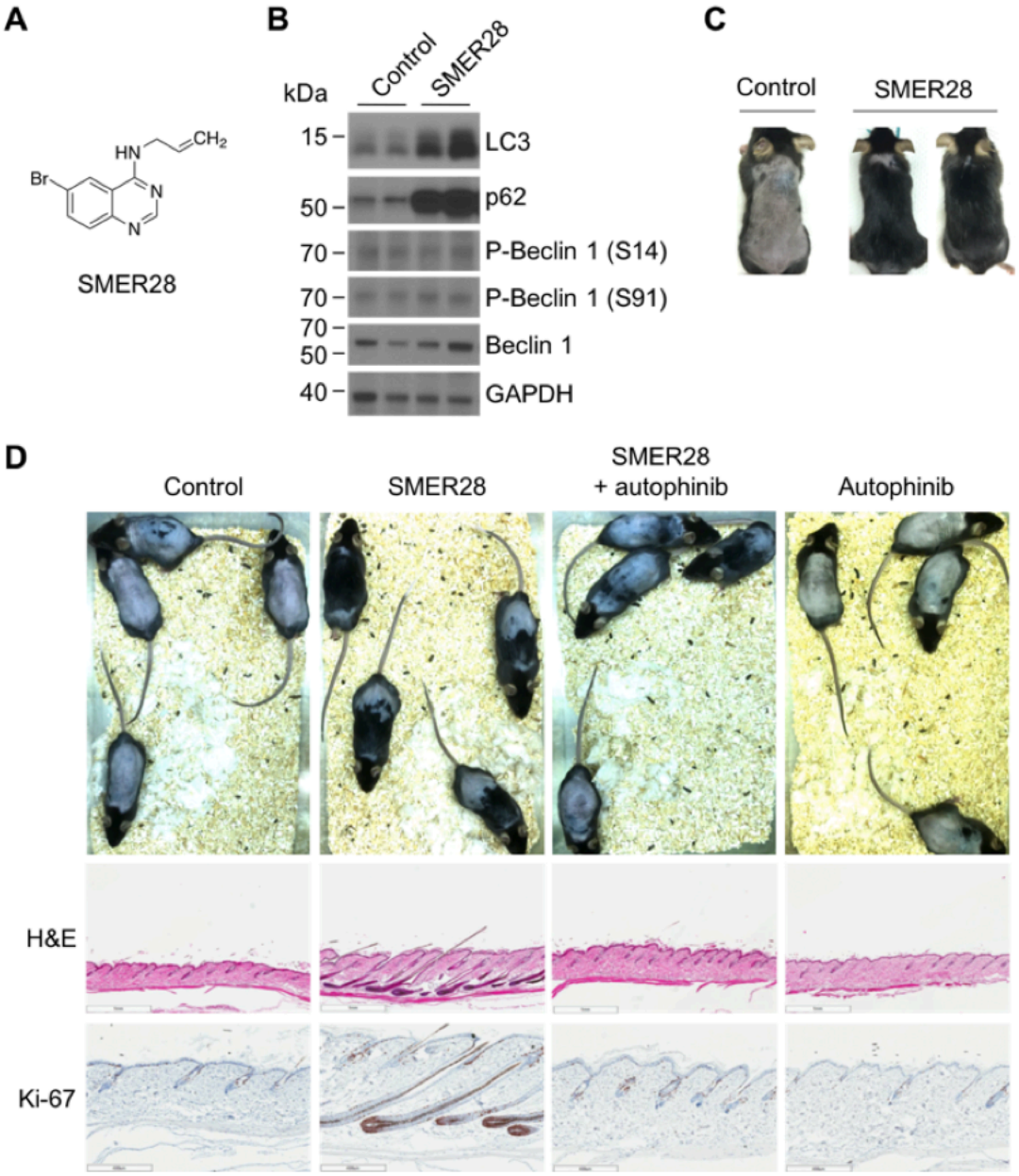
A
HN
CH2
Br
N
N
SMER28
B
kDa
Control
SMER28
15
LC3
50
p62
70
P-Beclin 1 (S14)
70
P-Beclin 1 (S91)
70
50
Beclin 1
40
GAPDH
C
Control
SMER28
D
Control
SMER28
SMER28
+ autophinib
Autophinib
H&E
Ki-67

Figure 5

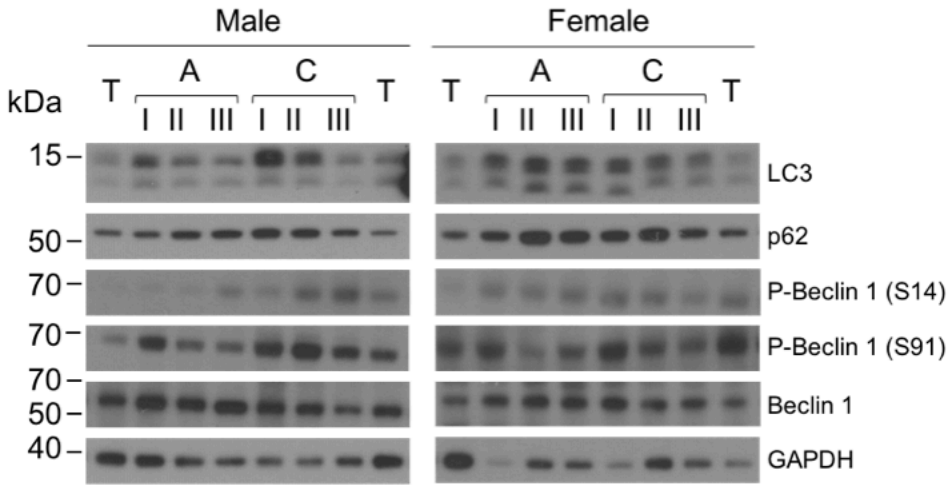
Male
Female
kDa
T
A
C
T
I II III I II III
15
50
70
70
70
50
40
LC3
p62
P-Beclin 1 (S14)
P-Beclin 1 (S91)
Beclin 1
GAPDH

Supplemental Figures

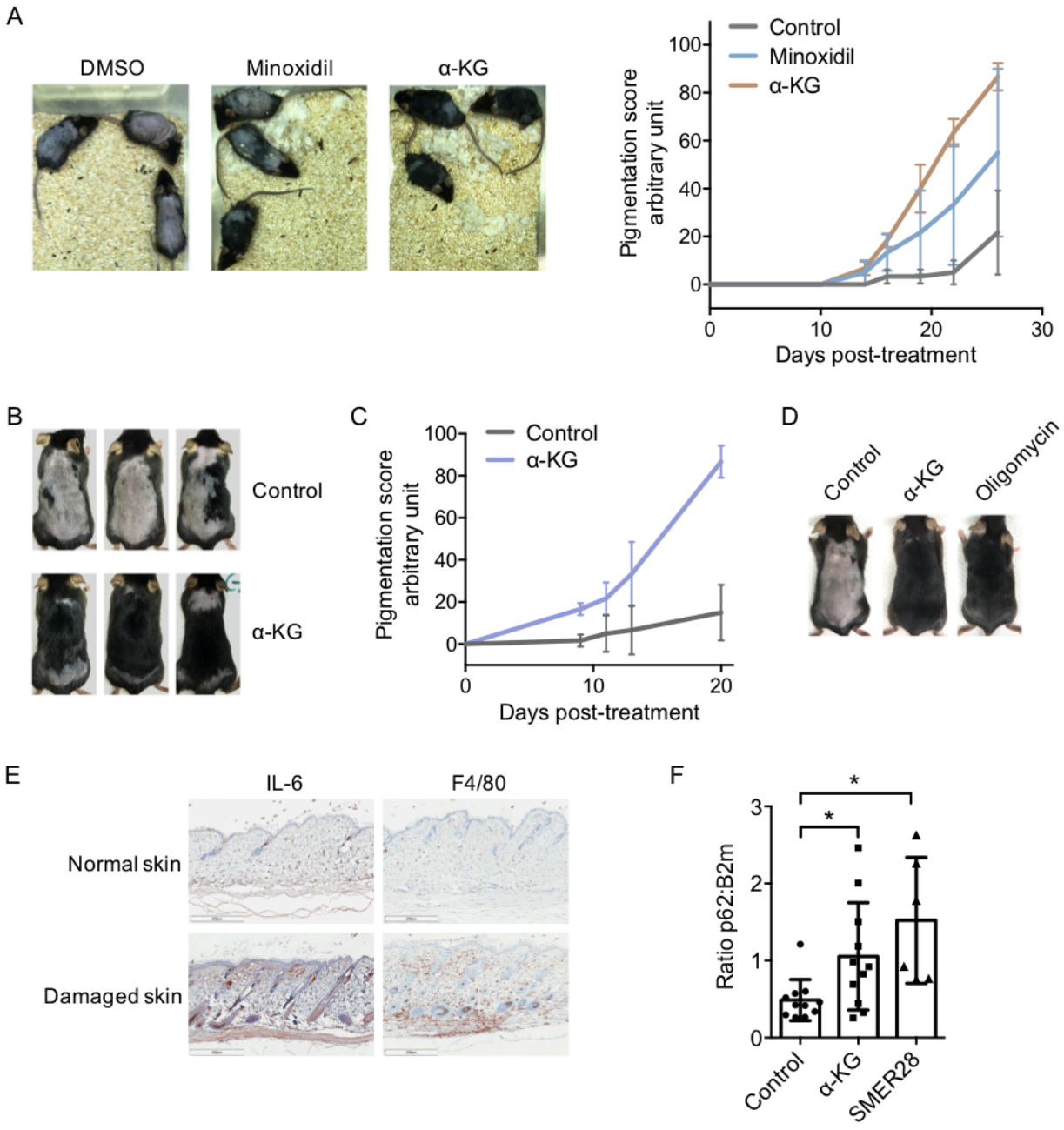

Figure S1. In both male and female mice, hair regeneration can be induced by α-KG or oligomycin treatment. Related to Figure 1.

(**A**) Minoxidil (5% in PLO base) as a positive control for hair regeneration. Photographs shown were taken on day 22 post-treatment. Number of animals: control (3), minoxidil (3), α-KG (3). Data are represented as mean ± s.d..

(**B**) Compared to 6.5-week old mice in Figure 1A, α-KG induces faster hair regeneration in 8-week old animals. Male mice were shaved on postnatal day 57 (telogen) and topically treated every other day with 32 mM α-KG. Photographs shown were taken on day 20 post-treatment. Number of animals: control (4), α-KG (3).

(**C**) Quantification for skin pigmentation in mice from (A). Pigmentation of α-KG treated animals became visible as early as on day 7, and full dorsal hair coverage was observed by day 20 post-treatment. Number of animals: control (3), α-KG (3). Data are represented as mean ± s.d..

(**D**) α-KG and oligomycin also stimulate hair regeneration in female animals. Female mice were shaved on postnatal day 58 (telogen) and topically treated with vehicle control (DMSO), α-KG (16 mM), or oligomycin (10 μM) every other day. Photographs shown were taken on day 26 post-treatment. Number of animals: control (9), α-KG (9), oligomycin (10).

(**E**) Positive controls showing IL-6 and F4/80 in damaged skin. 8-week old male mice with skin lesions, e.g., fight wounds or bite lesions, were employed. Scale bars, 400 μm.

(**F**) Quantitative RT-PCR showing increased p62 transcript levels in α-KG (**P* = 0.026; by *t*-test, two-tailed, two-sample unequal variance) and SMER28 (**P* = 0.017; by *t*-test, two-tailed, two-sample unequal variance) treated skin; *P* values were calculated using Microsoft Excel. The housekeeping gene B2m (beta-2-microglobulin) was used as an internal control. Mean ± s.d. is plotted.

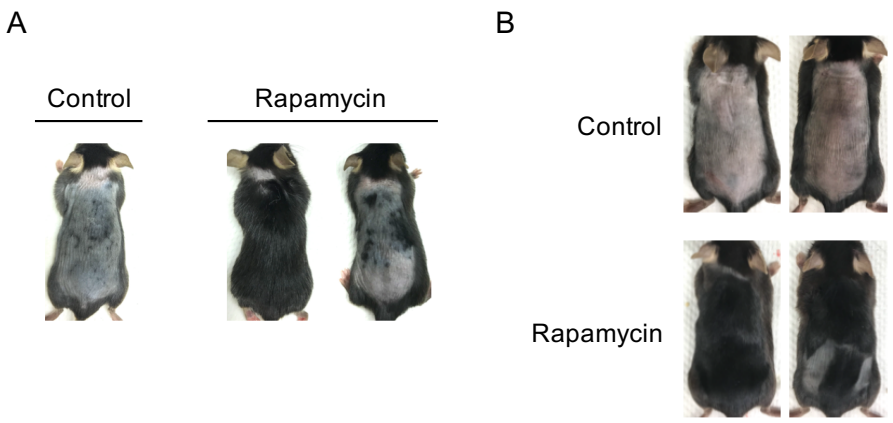

Figure S2. Effects of rapamycin on hair regeneration. Related to Figure 2.

(**A**) Rapamycin at 100 nM also promotes hair regeneration. Male mice were shaved on postnatal day 45 (telogen) and topically treated every other day with vehicle control (DMSO) or 100 nM rapamycin. Photographs shown were taken on day 23 post-treatment. Number of animals: control (7), rapamycin (7).

(**B**) Rapamycin also promotes hair regeneration in female animals. Female mice were shaved on postnatal day 58 (telogen) and topically treated every other day with vehicle control (DMSO) or rapamycin (1.6 μM). Number of animals: control (9), rapamycin (11).

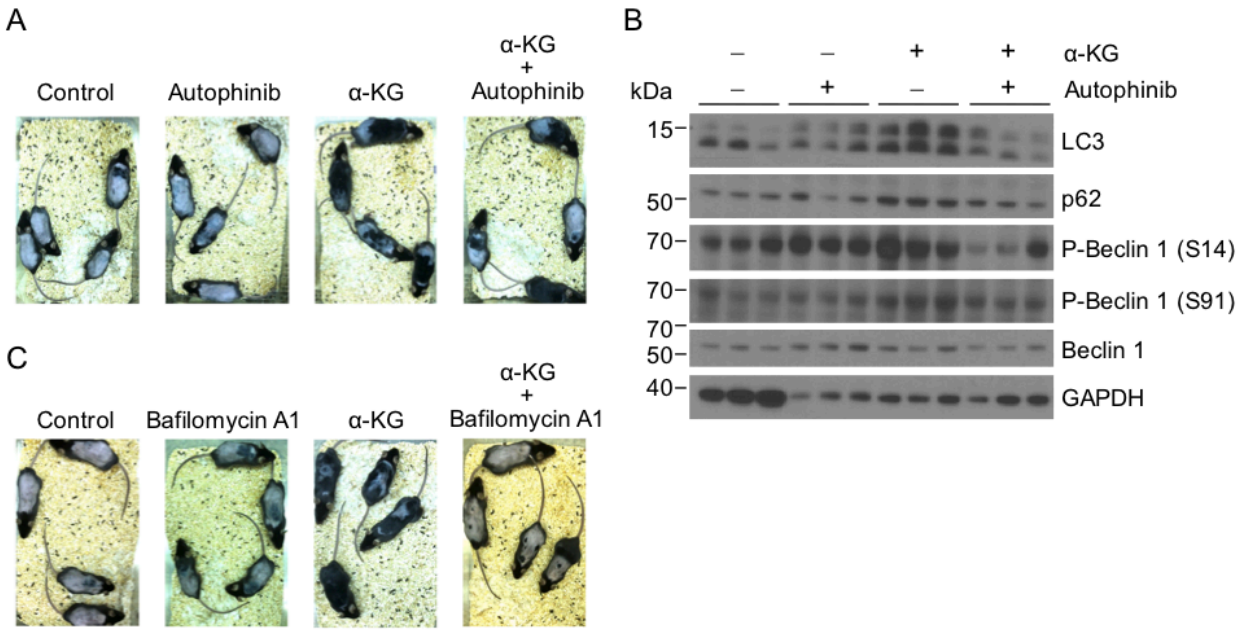

Figure S3. Autophagy is required for α-KG to induce hair regeneration. Related to Figure 4.

(**A**) Autophinib inhibits hair regeneration by α-KG. Male mice were shaved on postnatal day 53 (telogen) and topically treated with vehicle control (DMSO), autophinib (4 mM), α-KG (64 mM), or α-KG (64 mM) and autophinib (4 mM) together every other day. Photographs shown were taken on day 20 post-treatment. Number of animals: 4 for each treatment.

(**B**) Western blot analysis of autophagy related markers in mouse skin on day 5 post-treatment.

(**C**) Bafilomycin A1 also inhibits hair regeneration by α-KG. Male mice were shaved on postnatal day 52 (telogen) and topically treated with vehicle control (DMSO), bafilomycin (200 μM), α-KG (64 mM), or α-KG (64 mM) together with bafilomycin (200 μM) together

every other day. Photographs shown were taken on day 21 post-treatment. Number of animals: 4 for each treatment.

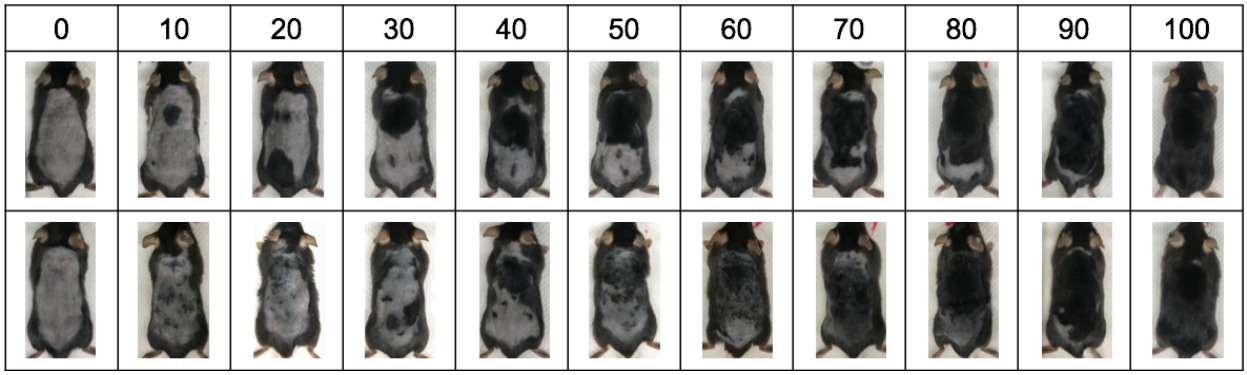

Figure S4. Images representing mouse hair cycle progression scores between 0 and 100. Related to Figures 1-3.

Mice were shaved and monitored for hair cycle progression. Arbitrary values from 0 to 100 were assigned based on skin pigmentation levels and hair shaft density, with 0 indicating no hair growth (and no pigmentation) and higher numbers corresponding to darker skin and larger areas of dense hair growth. For example, a score of 50 was assigned for full-length hair growth on 50% of dorsal skin area or pigmentation on 100% of dorsal skin area without hair shafts yet. A score of 70 was assigned for full-length hair growth on 70% of dorsal skin or pigmentation on 100% of dorsal skin with ~30-40% hair shafts. A value of 100 indicates full-length hair growth on 100% of dorsal skin.

Supplemental Experimental Procedures

Assay for hair regeneration in mice.

All compounds were tested in both male and female mice. Every experiment was repeated independently at least 2 times. Some treatments with different agents were performed concurrently with shared control arms. C57BL/6J male mice were obtained at 6 or 8 weeks of age from Jackson Laboratories (Bar Harbor, ME). C57BL/6J female mice were obtained at 8 weeks of age from Jackson Laboratories (Bar Harbor, ME). Mice were fed a standard chow diet and provided ad libitum access to food and water throughout the study. Mice were shaved dorsally in telogen, i.e., postnatal day 43~45 for males (unless otherwise indicated) and day 58 for females, respectively. Vehicle control (25 μL DMSO, unless otherwise indicated) or test compounds (in 25 μL DMSO, unless otherwise indicated) were topically applied on the shaved skin every other day (unless otherwise described) for the duration of the experiments (3-6 weeks). Appearance of skin pigmentation and hair growth were monitored and documented by photos and videos. Progression was also assigned a value from 0 to 100 based on pigmentation levels and hair shaft density, with 0 indicating no hair growth (and no pigmentation) and higher number corresponding to darker skin and larger areas of dense hair growth. Images representing different scores are presented in Figure S4. α-KG (Sigma, 75890), oligomycin (Cell Signaling, 9996L), rapamycin (Selleckchem, S1039), AICAR (Selleckchem, S1802), metformin (Sigma, PHR1084), α-KB (Sigma, K401), SMER28 (Selleckchem, S8240), autophinib (Selleckchem, S8596), bafilomycin A1 (Selleckchem, S1413), or indicated combinations in ~250 μL Premium Lecithin Organogel (PLO) Base

(Transderma Pharmaceuticals Inc.) were used for each mouse. The vehicle DMSO was also mixed with PLO base for topical application. The timing of the hair cycle was not altered using PLO base +DMSO vs PLO base alone in our experiments.

Aged mice.

For oral α-KB treatment, aged male and female C57BL/6J mice were obtained at 87 weeks of age (NIA aged rodent colonies). Mice were housed in a controlled SPF facility (22 ± 2 °C, 6:00-18:00, 12 h/12 h light/dark cycle) at UCLA. Mice were fed a standard chow diet and provided ad libitum access to food and water throughout the study. Treatment with either water (vehicle control), or α-KB (90 mg/kg bodyweight) in drinking water, started when mice were at 101 weeks of age. For topical α-KB treatment, aged male C57BL/6J mice were obtained at 21 months of age (NIA aged rodent colonies), shaved the following week, and topically treated with α-KB (32 mM) every other day for one month. All experiments were approved by the UCLA Chancellor's Animal Research Committee.

Histology and microscopy.

Mouse dorsal skin was shaved before being collected for histological and molecular analyses. Full-thickness skin tissue was then fixed in 10% formalin solution (Sigma, HT501128) overnight and dehydrated for embedding in paraffin. 5 μm paraffin sections were subjected to hematoxylin/eosin staining and immunohistochemistry for Ki-67 (Cell Signaling, 12202), IL-6 (Abcam, ab6672) or F4/80 (Bio-Rad, MCA497G). Images were captured by Leica Aperio ScanScope AT brightfield system at X20 magnification.

Western blotting.

Male mice were shaved and treated every other day starting on postnatal day 43. After 5 days, telogen skin samples were harvested and stage confirmed. Mouse skin tissue lysate was prepared by homogenization in T-PER Tissue Protein Extraction Buffer (Thermo Scientific, 78510) with protease inhibitors (Roche, 11836153001) and phosphatase inhibitors (Sigma, P5726) by FastPrep-24 (MP Biomedicals). Tissue and cell debris was removed by centrifugation and the lysate was boiled for 5 min in 1 x SDS loading buffer containing 5% β-mercaptoethanol. Samples were then subjected to SDS–PAGE on NuPAGE Novex 12% Bis-Tris gels (Invitrogen, NP0343BOX), and western blotting was carried out with antibodies against LC3 (Novus, NB100-2220), p62 (Sigma, P0068), Phospho-Beclin-1 (Ser15) (corresponding to Ser14 in mouse) (Cell Signaling, 84966), Phospho-Beclin-1 (Ser93) (corresponding to Ser91 in mouse) (Cell Signaling, 14717), Beclin-1 (Abcam, ab207612), or GAPDH (Ambion, AM4300).

Quantitative reverse transcription PCR (RT-qPCR).

At 24 h post-treatment, telogen skin samples were harvested and total RNA was isolated using TRIzol reagent (Invitrogen) from whole thickness mouse skin tissue. cDNA was synthesized using iScript Reverse Transcription Supermix (Bio-Rad). iTaq Universal SYBR Green Supermix (Bio-Rad) and a Bio-Rad CFX Connect instrument were used for quantitative RT-PCR. The primer sequences used for RT-qPCR are as follows:

p62 forward: GAAGAATGTGGGGGAGAGTGTGG;

p62 reverse: TGCCTGTGCTGGAACTTTCTGG;

B2m forward: CAGCATGGCTCGCTCGGTGAC;

B2m reverse: CGTAGCAGTTCAGTATGTTCG.

Statistical Analysis.

All treatments were repeated at least two times. Data represent biological replicates. Appropriate statistical tests were used for every figure. Data meet the assumptions of the statistical tests described for each figure. Mean ± s.d. is plotted in all figures.

CHAPTER 4

Conclusions

My Ph.D. research projects presented in this dissertation include the beneficial effects that endogenous metabolites have in longevity and its related diseases/disorders, Alzheimer diseases/hair loss respectively. In the investigation of related mechanism on genetic, molecular, and metabolomic levels, we applied comprehensive assays in cultured cell lines, *C. elegans* and moue models, including DARTS, metabolomics (mass spectrometry), bioenergetics (Seahorse respirometry), and epistasis analysis in *C. elegans* and mammalian cell lines.

Firstly, we evaluated the anti-aging effect of an endogenous metabolite, α-KB, in CHARPTER 2. Similar to α-KG, α-KB can extend worms lifespan with unaltered food intake preference, forging behavior or body size[1]. More significantly, α-KB treated worms exhibit higher activity and healthier body shape when they are getting old (data not shown). α-KB also extended healthy lifespan in mouse by oral administration started in late age (~100 weeks old)[2]. In isolated mitochondria in the Seahorse respirometry assay, α-KB perturbs pyruvate driven respiration. Further DARTS[3] and enzymatic kinetics[4] assay demonstrated α-KB as a competitive alternative substrate of pyruvate dehydrogenase, which explained the inhibitory effect of α-KB on pyruvate dependent complex I respiration.

Moreover, metabolomics analysis from cultured cells elucidated rewired pyruvate oxidation, fatty acid oxidation and glutaminolysis by α-KB[5, 6, 7]. In order to investigate how metabolism regulatory pathways are affected by α-KB, we utilized RNAi mediated and genetically mutated *C. elegans* and found that AMPK[8] and its downstream effectors are required by α-KB to extend lifespan. Consistently, both α-KB treated *C. elegans* and cultured cells showed activated AMPK by western blot analysis. *pdhb-1* knockdown in *C. elegans* also activates AMPK and confers its longevity effect. In a *C. elegans* Alzheimer's disease model[9], age dependent paralysis progression was delayed by α-KB, which can be abolished by *aak-2* or *pdhb-1* knockdown by RNAi. Our data demonstrated that decreased mitochondrial complex I activity through PDH modulation can induce anti-aging responses in both lifespan and neurodegeneration models. Moreover, α-KB represents an example that endogenous alternative substrates can be utilized to regulate their target metabolic enzymes and therefore to rewire metabolism and energy balance.

CHAPTER 3 investigated anti-aging compounds in mouse model. Previously, aged mice fed with α-KB through drinking water exhibited healthier lifespan with younger hair coating. Hair regeneration rate decreases with age in response to dampened hair follicle stem cell population and activity. Therefore, delaying aging may maintain hair follicle regenerative ability and hair growth. Firstly, the well characterized mitochondrial complex V inhibitor and anti-aging metabolite, α-KG, was tested in shaved mouse telogen skin. Consistently, telogen-anagen transition was accelerated by α-KG and followed by natural hair growth cycle[10]. In α-KG treated telogen skin, we assessed the potential changes in metabolism and energy regulatory signaling pathways. One of the anti-aging effectors,

autophagy[11,12,13], was found to be dramatically upregulated in a time dependent manner. Another mitochondrial complex V inhibitor, oligomycin, also promoted autophagy induction and hair regeneration. Then we evaluated what's the role of downstream signaling of α-KG and oligomycin in initiating autophagy and hair follicle activation. Both TOR and AMPK modulators were found to have similar influence on autophagy levels and hair regeneration. Moreover, we utilized a TOR independent autophagy activator, SMER28[14], to show that autophagy induction was sufficient to regenerate hair. Autophagy was also proven to be necessary when autophagy inhibitor was co-treated with SMER28 or α-KG. Interestingly, autophagy level changes with hair growth cycle progresses, increasing during anagen phase and decreasing from catagen entry until telogen phase. Lowest autophagy level can be detected in telogen while autophagy reaches highest during late anagen/early catagen. Our observation established dynamic changes and regulation of autophagy during hair cycle for the first time, while the physiological significance needs more investigation. Recently, autophagy was found to be required for anagen maintenance in human hair follicle development[15], which also indicated the potential application of autophagy activators in promoting hair regeneration.

With the rapidly growing aged population all over the world, inevitable aging related diseases, especially cancer, heart disease, type 2 diabetes, arthritis, and kidney disease, will increase and cause magnificent burden for families and society[16]. Therefore, it is urgent to develop easily applicable anti-aging approaches to delay or treat aging and aging related diseases. Here we identified a new anti-aging druggable metabolite and demonstrated its function in both aging models and aging related disorder models.

References

1. Chin, R. M., Fu, X., Pai, M. Y., Vergnes, L., Hwang, H., Deng, G., ... & Hu, E. (2014). The metabolite α-ketoglutarate extends lifespan by inhibiting ATP synthase and TOR. *Nature*, *510*(7505), 397.

2. Huang, J., *et al.* Ketobutyrate compounds and compositions for treating age-related symptoms and diseases. Google Patents, Google Patents (2016).

3. Lomenick, B., Hao, R., Jonai, N., Chin, R. M., Aghajan, M., Warburton, S., ... & Wohlschlegel, J. A. (2009). Target identification using drug affinity responsive target stability (DARTS). *Proceedings of the National Academy of Sciences*, *106*(51), 21984-21989.

4. Bisswanger, H., & Henning, U. (1971). Regulatory Properties of the Pyruvate-Dehydrogenase Complex from Escherichia coli: Positive and Negative Cooperativity. *European journal of biochemistry*, *24*(2), 376-384.

5. Peters, S. J., & LeBlanc, P. J. (2004). Metabolic aspects of low carbohydrate diets and exercise. *Nutrition & metabolism*, *1*(1), 7.

6. Vacanti, N. M., Divakaruni, A. S., Green, C. R., Parker, S. J., Henry, R. R., Ciaraldi, T. P., ... & Metallo, C. M. (2014). Regulation of substrate utilization by the mitochondrial pyruvate carrier. *Molecular cell*, *56*(3), 425-435.

7. Kim, J. W., Tchernyshyov, I., Semenza, G. L., & Dang, C. V. (2006). HIF-1-mediated expression of pyruvate dehydrogenase kinase: a metabolic switch required for cellular adaptation to hypoxia. *Cell metabolism*, *3*(3), 177-185.

8. Greer, E. L., Banko, M. R., & Brunet, A. (2009). AMP-activated Protein Kinase and FoxO Transcription Factors in Dietary Restriction–induced Longevity. *Annals of the New York Academy of Sciences*, *1170*(1), 688-692.

9. McColl, G., Roberts, B. R., Pukala, T. L., Kenche, V. B., Roberts, C. M., Link, C. D., ... & Cherny, R. A. (2012). Utility of an improved model of amyloid-beta (Aβ 1-42) toxicity in Caenorhabditis elegans for drug screening for Alzheimer's disease. *Molecular neurodegeneration*, *7*(1), 57.

10. MuÈller-RoÈver, S., Foitzik, K., Paus, R., Handjiski, B., van der Veen, C., Eichmüller, S., ... & Stenn, K. S. (2001). A comprehensive guide for the accurate classification of murine hair follicles in distinct hair cycle stages. *Journal of Investigative Dermatology*, *117*(1), 3-15.

11. Jia, K., & Levine, B. (2007). Autophagy is required for dietary restriction-mediated life span extension in C. elegans. *Autophagy*, *3*(6), 597-599.

12. Hansen, M., Chandra, A., Mitic, L. L., Onken, B., Driscoll, M., & Kenyon, C. (2008). A role for autophagy in the extension of lifespan by dietary restriction in C. elegans. *PLoS genetics*, *4*(2), e24.

13. Fernández, Á. F., Sebti, S., Wei, Y., Zou, Z., Shi, M., McMillan, K. L., ... & Marciano, D. K. (2018). Disruption of the beclin 1–BCL2 autophagy regulatory complex promotes longevity in mice. *Nature*, *558*(7708), 136.

14. Sarkar, S., Perlstein, E. O., Imarisio, S., Pineau, S., Cordenier, A., Maglathlin, R. L., ... & Rubinsztein, D. C. (2007). Small molecules enhance autophagy and reduce toxicity in Huntington's disease models. *Nature chemical biology*, *3*(6), 331.

15. Parodi, C., Hardman, J. A., Allavena, G., Marotta, R., Catelani, T., Bertolini, M., ... & Grimaldi, B. (2018). Autophagy is essential for maintaining the growth of a human (mini-) organ: Evidence from scalp hair follicle organ culture. *PLoS biology*, *16*(3), e2002864.

16. US Department of Health and Human Services (2008), A. o. A. Projected future growth of the older population, retrieved from http://www.aoa.gov/Aging_Statistics/future_growth/future_growth.aspx#age